Dissertation

Dominik Fröhlich

2013

# OLIGODENDROGLIAL EXOSOMES IN GLIA TO NEURON SIGNALING

Dissertation

zur Erlangung des Grades

Doktor der Naturwissenschaften

am Fachbereich Biologie

der Johannes Gutenberg-Universität Mainz

von

**Dominik Fröhlich**

geboren am 20.07.1982 in Heidelberg

Mainz, 2013

# 1. TABLE OF CONTENTS

# 2. ABSTRACT

In the CNS, myelinating oligodendrocytes and axons form a functional unit based on intimate cell-cell interactions. In addition to axonal insulation serving to increase the conduction velocity of electrical impulses, oligodendrocytes provide trophic support to neurons essential for the long-term functional integrity of axons. The glial signals maintaining axonal functions are just at the beginning to become uncovered. Yet, their determination is highly relevant for all types of demyelinating diseases, where lack of glial support significantly contributes to pathology.

The present PhD thesis uncovers exosomes as a novel signaling entity in the CNS by which cargo can be transferred from oligodendrocytes to neurons. Exosomes are small membranous vesicles of endocytic origin, which are released by almost every cell type and have been implicated in intercellular communication. Oligodendrocytes secrete exosomes containing a distinct set of proteins as well as mRNA and microRNA. Intriguingly, oligodendroglial exosome release is stimulated by the neurotransmitter glutamate indicating that neuronal electrical activity controls glial exosome release. In this study, the role of exosomes in neuron-glia communication and their implications on glial support was examined. Cortical neurons internalized and accumulated oligodendroglial exosomes in the neuronal cell soma in a time-dependent manner. Moreover, uptake occurred likewise at the somatodendritic and axonal compartment of the neurons via dynamin and clathrin dependent endocytosis. Intriguingly, neuronal internalization of exosomes resulted in functional retrieval of exosomal cargo *in vitro* and *in vivo* upon stereotactic injection of Cre recombinase bearing exosomes. Functional recovery of Cre recombinase from transferred exosomes was indicated by acquired reporter recombination in the target cell. Electrophysiological analysis showed an increased firing rate in neurons exposed to oligodendroglial exosomes. Moreover, microarray analysis revealed differentially expressed genes after exosome treatment, indicating functional implications on neuronal gene expression and activity. Taken together, the results of this PhD thesis represent a proof of principle for exosome transmission from oligodendrocytes to neurons suggesting a new route of horizontal transfer in the CNS.

# 3. INTRODUCTION

## 3.1. OLIGODENDROCYTES – NOT ONLY MYELINATING CELLS

The mammalian central nervous system (CNS) consists of two major cell types – neurons and glia. While neurons are highly specialized cells responsible for impulse propagation and capable of integrating thousands of synaptic inputs into a single output, an action potential, the types and functions of glia are diversified. Glial cells can be subdivided into oligodendrocytes, astrocytes, and microglia (Fig. 1). Astrocytes, the most abundant glial cells in the human brain, contribute essentially to the maintenance of brain homeostasis. Together with endothelial cells and pericytes they build up the blood brain barrier (BBB), control the extracellular ion balance, provide trophic support to neurons, participate in repair and scarring processes after CNS injury, and are involved in local communication by the release of gliotransmitters (Volterra and Meldolesi, 2005). Microglia, the resident macrophages of the brain migrate into the CNS during early embryogenesis and comprise around 10-12% of brain population (Ransohoff and Cardona, 2010). Their primary function is to maintain brain tissue homeostasis, to provide the first line of defense during infection and brain injury, and to promote tissue repair (Hanisch and Kettenmann, 2007).

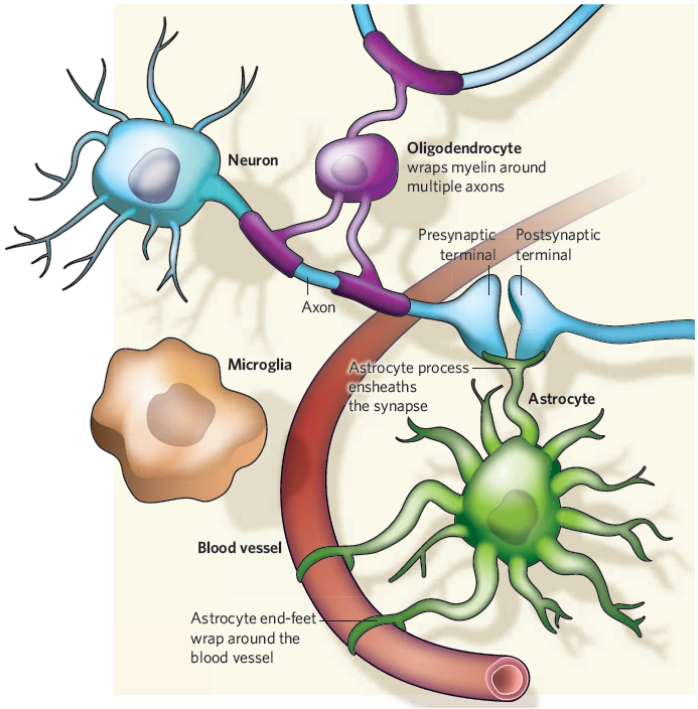


**FIGURE 1: CELL TYPES OF THE CNS.** The CNS comprises of neurons (blue), oligodendrocytes (purple), astrocytes (green), and microglial cells (brown). While microglia represent the resident macrophages of the brain, astrocytes contribute to the maintenance of brain homeostasis, and oligodendrocytes enwrap

axons with the myelin sheath enabling rapid saltatory impulse conduction. Adapted from (Allen and Barres, 2009).

Oligodendrocytes represent a highly specialized class of glia that - in a process termed myelination - spirally wrap long segments of axons with a multilayered sheath of extended cell membrane. They arise from a large pool of precursor cells, also termed NG2 cells due to the expression of the proteoglycan protein NG2 (Trotter et al., 2010). It has long been acknowledged that myelination increases the resistance of the axonal membrane and enables saltatory impulse propagation, boosting conduction velocity up to 100fold. Moreover, the myelin sheath helps to save energy. Normally, the $Na^+$, $K^+$-ATPase would consume a high number of ATP molecules to restore the ion gradients, but myelination restricts the area where action potentials are generated to less than 0.5% of the axon's surface (nodes of Ranvier) saving a high amount of energy (Nave, 2010a). On the downside, the covering of the axon by the myelin sheath limits access of the axon to the extracellular milieu and therefore to energetic metabolites necessitating trophic support by glia (Nave, 2010b). In the peripheral nervous system (PNS), the supporting function of glial cells can be independent from myelination. Functional perturbation of non-myelinating Schwann cells, also called Remak cells, by the expression of truncated ErbB4 receptor causes progressive degeneration of unmyelinated C-fibers and sensory neuropathy, indicating a role of these non-myelinating cells in preserving axonal functionality (Chen et al., 2003). Also in the CNS oligodendrocytes serve the vital function of preserving the integrity and survival of axons, independent of myelin formation (Fig. 2). The need for a supportive function of oligodendrocytes becomes evident considering the neuronal morphology. In long projecting neurons, e.g. corticospinal tract neurons, spinal motor neurons, and dorsal column sensory neurons, axons with a diameter of 1 µm can project up to 100 cm. In these neurons 99% of cytoplasm can be contained within the axon (Morrison et al., 2013). Regarding the speed of slow axonal transport by which proteins are transported (around 2 mm per day), it would need up to 500 days to transport proteins (e.g. structural proteins, ion channels, and synaptic vesicle proteins) from the place where they are synthesized to the distal end of the axon (Nave, 2010b), a timespan much longer than the halftime of most proteins making it impossible for a neuron to react on environmental changes. These unique characteristics, which on the one hand enable rapid impulse conduction over long distances, make neurons on the other hand extremely vulnerable. Recent studies could show that the transfer of energy metabolites like lactate via the monocarboxylate transporter 1 (MCT1) is essential for the survival of axons (Fig. 3) (Morrison et al., 2013). Down-regulation of MCT1 predominantly expressed by oligodendrocytes in the CNS resulted in axon injury and neurodegeneration *in vitro* and *in vivo* (Lee et al., 2012). In line with this, in mice where mitochondria function is selectively disturbed in oligodendrocytes due to a

mutation of cytochrome c oxidase (COX), brain lactate concentrations measured by magnetic resonance spectroscopy were increased under isoflurane anesthesia (Fünfschilling et al., 2012). This may be due to an increased non-oxidative metabolism in mutant oligodendrocytes. Intriguingly, lactate levels rapidly returned to normal after anesthesia, most likely because of fast axonal uptake (Fünfschilling et al., 2012). Both studies together provide evidence that oligodendrocytes directly support axons with energy metabolites. Since MCT1 can also transport pyruvate and ketone bodies, these metabolites may be involved in energy supply, too. The metabolites may also be produced by highly glycolytic astrocytes and passed to oligodendrocytes via gap junctions before being provided to the axon. In this case the oligodendrocytes would function as intermediaries (Morrison et al., 2013). The uptake of lactate, and maybe other metabolites, at the axonal side probably occurs via MCT2 transporters, which are primarily expressed by neurons (Fig. 3) (Bergersen et al., 2002; Rafiki et al., 2003).

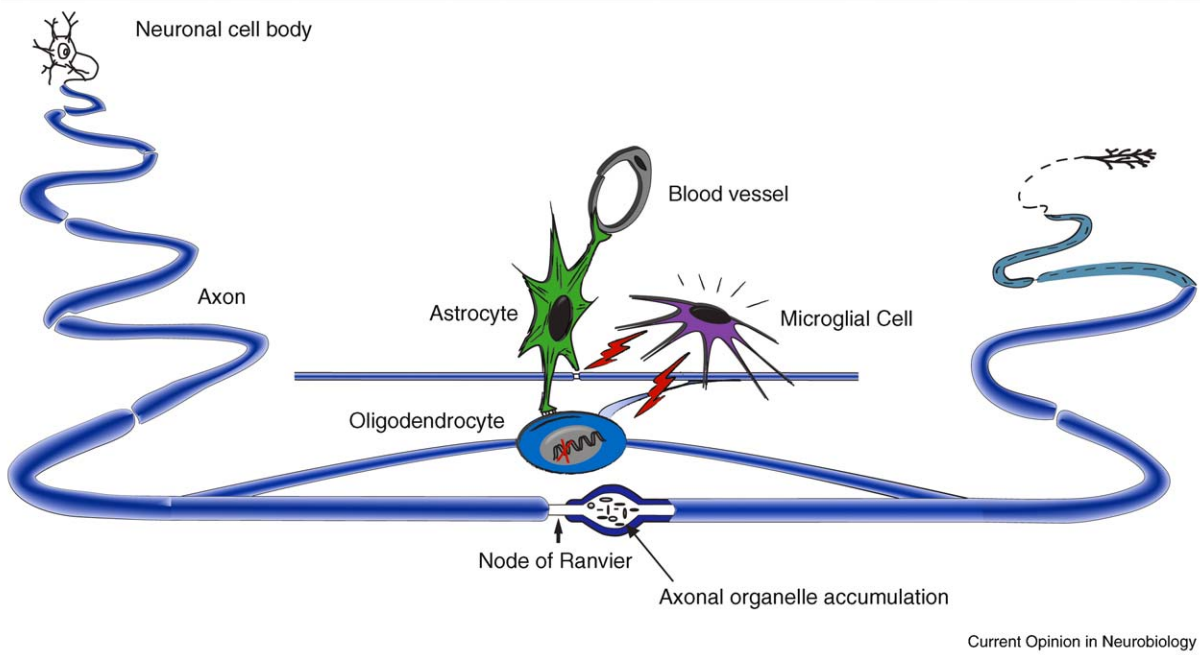


**FIGURE 2: AXONAL SUPPORT.** Oligodendrocytes (blue) not only enwrap axons with the myelin sheath enabling rapid saltatory impulse propagation, but also provide trophic support to axons, in particular important for long axons. The failure of this support becomes evident in different mouse models lacking important myelin proteins like PLP and CNP, or by loss of proper peroxisome function (PEX5 mutants). Interference with the supportive function results in axonal swelling due to impaired axonal transport followed by Wallerian degeneration starting typically at distal sides (displayed by the dashed line). Supportive molecules can also originate from astrocytes (green) and be passed onto oligodendrocytes via gap junctions. Adapted from (Edgar and Nave, 2009).

The supportive role of oligodendrocytes has been detected initially in mouse strains that carry mutations impairing glial support function. *Plp1*-null mice, which lack expression of the tetraspan membrane protein PLP (proteolipid protein), the most abundant CNS myelin protein, represent a model of hereditary spastic paraplegia type 2. They assemble almost regular myelin

except of minor ultrastructural abnormalities (Rosenbluth et al., 2006). However, at the age of three month these mice develop so called axonal swellings, enlargements of the axon filled with organelles and phosphorylated neurofilaments (Griffiths et al., 1998). The swellings lead to an impairment of fast anterograde and retrograde transport (Edgar et al., 2004) followed by distal Wallerian degenerations, progressive ataxia, and finally premature death of the neurons without obvious myelin loss (Griffiths et al., 1998). A similar pathology can be observed in *Cnp1*-null mice lacking the 2',3'-cyclic nucleotide 3'-phosphodiesterase (CNP). CNP is located in the non-compact myelin and has been suggested to bind to RNA and tubulin (Lee et al., 2005; Gravel et al., 2009). Also in CNP-KO mice, myelination is not markedly affected, but mice show axonal swellings followed by severe neurodegeneration and premature death (Lappe-Siefke et al., 2003). Swellings and neurodegeneration occur even earlier than in *Plp1*-null mice already at a few weeks of age (Edgar et al., 2009). Although the pathology of PLP- and CNP-KO mice is similar, they do not act in the same pathway downstream of each other, since double-KO mice show an increased axonal degeneration compared to the single mutants (Edgar et al., 2009). These mouse models are in contrast to *shiverer* mice, which lack myelin basic protein (MBP). In spite of strong dysmyelination, *shiverer* mice develop phenotypically inconspicuous axons (Griffiths et al., 1998). Conditional KO of the protein import factor PEX5 in oligodendroglial peroxisomes, organelles involved in fatty-acid β-oxidation, led to the absence of functional peroxisomes in oligodendrocytes and resulted in widespread axonal degeneration and neuroinflammation without influencing glial survival (Kassmann et al., 2007). In myelin forming Schwann cells peroxisomes are associated with myelin membranes. Perturbation of peroxisome biogenesis in PEX5 mutants resulted in paranodal swellings and symptoms of a demyelinating neuropathy, indicating that also in the PNS peroxisomes are required for long-term axonal integrity (Kassmann et al., 2011). Finally, targeted ablation of oligodendrocytes by diphtheria toxin treatment of mice selectively expressing diphtheria toxin receptors in oligodendrocytes resulted in severe axonal injury (Ghosh et al., 2011; Oluich et al., 2012). Overall myelination was not affected at the onset of symptoms indicating that oligodendrocytes themselves and not myelin are critical for the maintenance of axonal integrity. Taken together, the mouse models show that the vital function of oligodendrocytes in preserving integrity and survival of axons can be uncoupled from the myelination process itself (Lappe-Siefke et al., 2003). This concept was further confirmed by the observation of secondary axonal degeneration being the cause of persistent clinical impairment in human myelin diseases such as multiple sclerosis (Trapp et al., 1998).

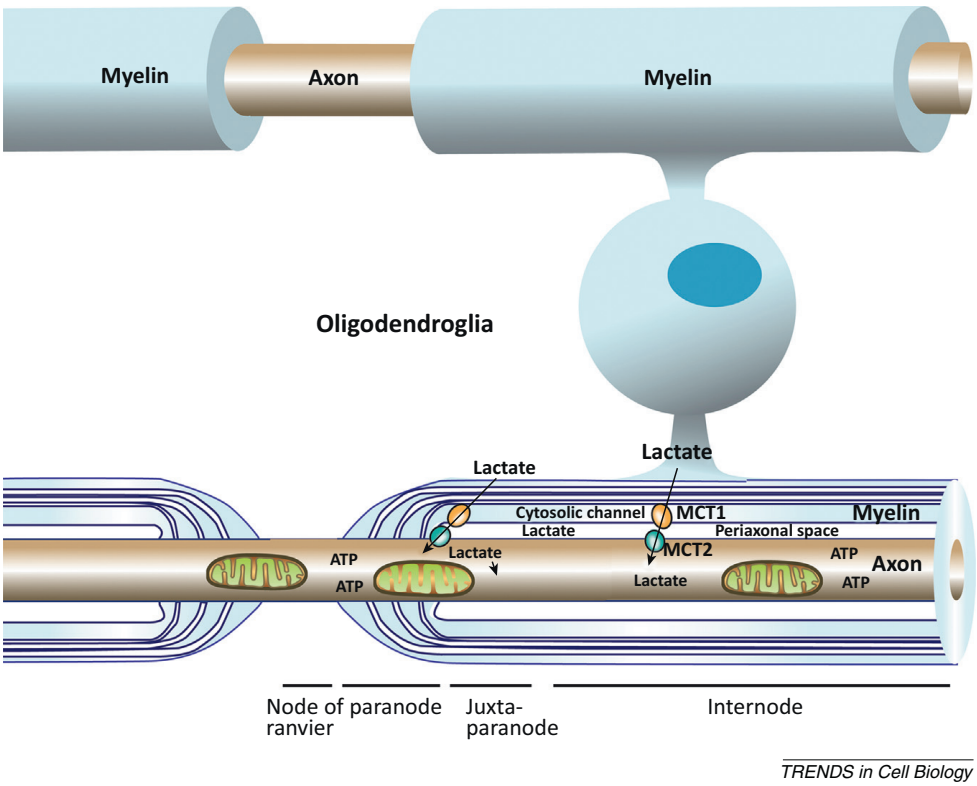


**FIGURE 3: METABOLIC SUPPORT OF THE AXON.** Oligodendrocytes metabolically support axons by the release of monocarboxylates like lactate or pyruvate to the periaxonal space via the monocarboxylate transporter 1 (MCT1). The metabolites can be internalized into the axon via MCT2 and used in mitochondria for the generation of ATP. Adapted from (Morrison et al., 2013).

## 3.2. INTERCELLULAR COMMUNICATION

The ability of cells to communicate with each other provided the basis for the development of multicellular organisms and is evolutionary conserved among species. Classical ways of intercellular communication are mediated by direct cell-cell contact via gap junctions and adhesion molecules, or by secreted molecules including paracrine factors and neurotransmitters. In recent years non-conventional routes of intercellular communication have been discovered by which whole sets of proteins, RNAs and even organelles can be transferred. The most prominent are tunneling nanotubes, shedding microvesicles, and exosomes, described in detail in the following.

### *3.2.1. TUNNELING NANOTUBES*

Tunneling nanotubes (TNTs) are exceedingly thin membrane protrusions up to several micrometers long, which can interconnect distant cells (Fig. 4) (for review see (Gurke et al.,

2008; Abounit and Zurzolo, 2012; Marzo et al., 2012)). TNTs were first discovered in cultures of PC12 (Rustom et al., 2004) and immune cells (Onfelt et al., 2004). Their composition is similar to that of filopodia, but in contrast they link two cells and do not contact the substrate (Rustom et al., 2004). Also functionally, TNTs can be distinguished from filopodia. While filopodia function as environmental sensors and are important for cell motility, the primary function of TNTs is the exchange of material between the cells they connect. They can mediate intercellular transfer of plasma membrane components, cytoplasmic molecules, intracellular microorganisms, and even whole organelles (Gerdes and Carvalho, 2008). Most TNTs form via directed actin-driven protrusions, but alternatively, they can also arise during detachment of previously connected cells (Abounit and Zurzolo, 2012). TNTs consist of a cytoskeletal core surrounded by the cell membrane. The core can either be composed of polarized actin filaments alone or can additionally contain microtubules enabling bi-directional transfer (Gerdes and Carvalho, 2008).

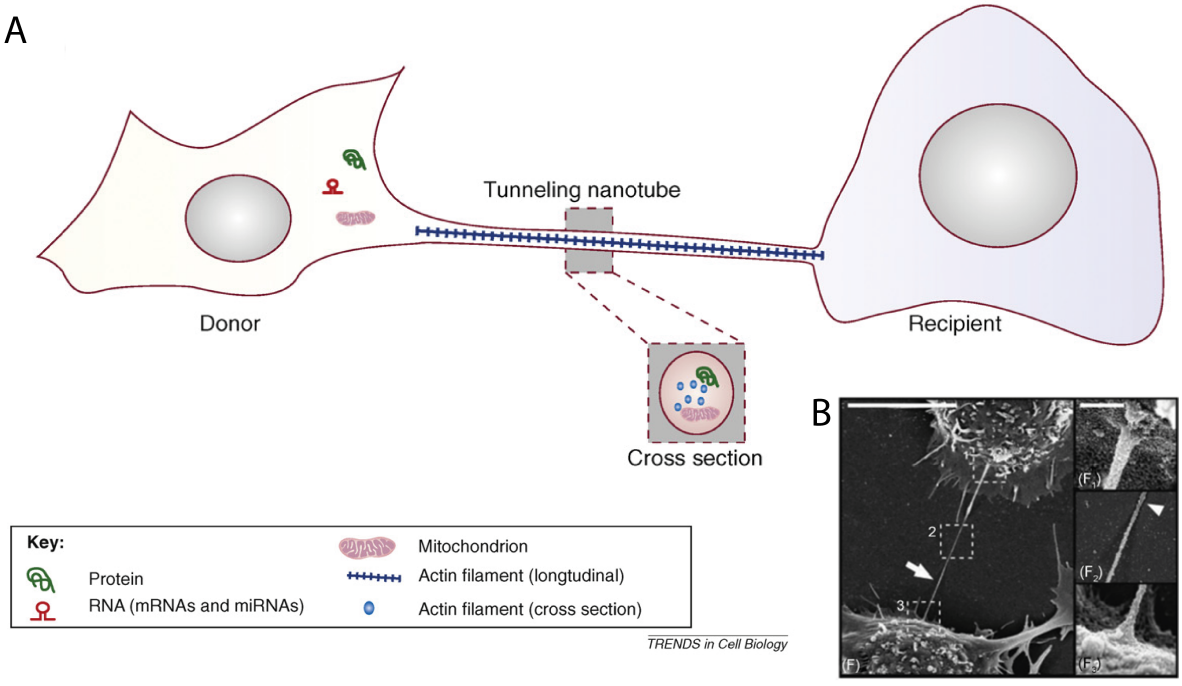


**FIGURE 4: TUNNELING NANOTUBES.** (A) Schematic of a tunneling nanotube (TNT) connecting a donor and a recipient cell. Cargo like proteins, RNA, and organelles (e.g. mitochondria) can be transferred along polarized actin filaments. Adapted from (Twiss and Fainzilber, 2009). (B) Scanning electron micrograph of a TNT connecting two PC12 cells. Adapted from (Rustom et al., 2004).

In the CNS, TNT-like structures have so far been described between neuronal cells and primary rat astrocytes, respectively (Zhu et al., 2005; Gousset et al., 2009). Interestingly, stress induced by hydrogen peroxide led to increased TNT formation in neurons and astrocytes resulting in an increased transfer of material (Zhu et al., 2005; Wang et al., 2011b). Moreover, TNTs in the CNS

can also be involved in the spread of pathogens, for instance the transfer of infectious prion proteins between neuronal cells (Gousset et al., 2009). However, until now TNTs have only been identified *in vitro* between cultured cells and it is unclear if they really exist *in vivo*.

### 3.2.2. *Extracellular Vesicles: Shedding Microvesicles vs. Exosomes*

Extracellular vesicles (EVs) can be subclassified into apoptotic bodies, shedding microvesicles and exosomes. In contrast to apoptotic bodies, which are bigger and originate from cells undergoing apoptosis, microvesicles and exosomes can be released from intact cells, both, in physiological and pathological conditions (Fig. 5).

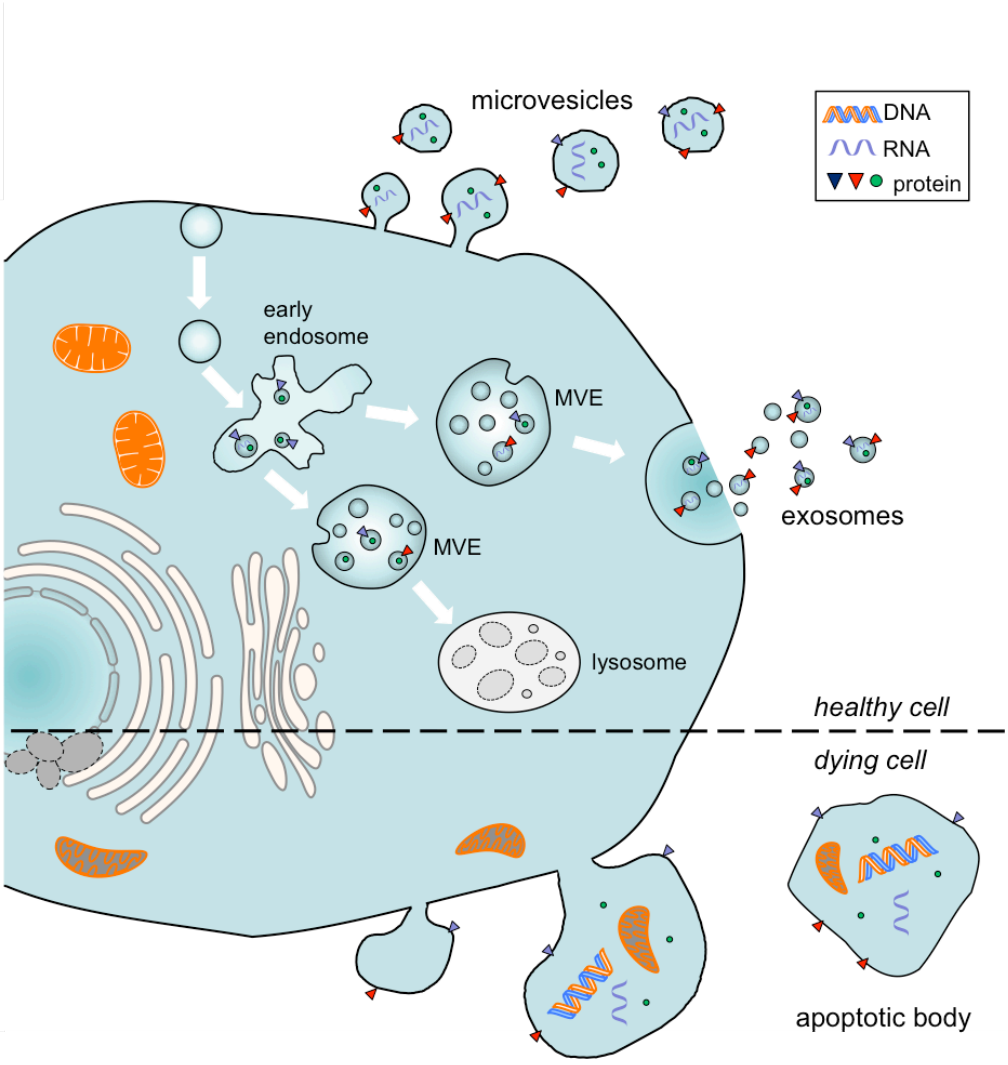


**Figure 5: Different Types of Extracellular Vesicles.** Schematic diagram of the different types of extracellular vesicles released either by healthy (above the dashed line) or by dying (beneath the dashed line) cells. Healthy cells secrete microvesicles and exosomes; cells undergoing apoptosis release apoptotic bodies. The distinct routes of biogenesis are depicted. Adapted from (Krämer-Albers and Frühbeis, 2013).

Shedding microvesicles (MVs), also termed ectosomes to underscore the distinct origin compared to exosomes, are small vesicles (0.1-1 μm in diameter) that directly bud from the plasma membrane. The budding of MVs is preceded by bleb formation at the cell surface and selective packaging of cellular constituents, already at this stage, into these blebs (Cocucci et al., 2009). MVs contain a selection of cell surface receptors, intracellular signaling molecules, and genetic material reflecting the cell of origin (Turola et al., 2012). The composition as well as potential function do not only reflect the cell type from where the MVs originate, but can further depend on the activation state, e.g. resting versus stimulated, and moreover on the type of stimulus (Bernimoulin et al., 2009). Although resting cells release MVs constitutively at a low rate, stimulation, for instance mediated by the second messenger $Ca^{2+}$, dramatically increases the release of MVs. Time-lapse imaging showed an explosive discharge of vesicles upon $Ca^{2+}$-dependent stimulation of microglia and dendritic cells, respectively (Bianco et al., 2005; Pizzirani et al., 2007). After extensive release of MVs, cells have to compensate the loss of membrane material from internal storage sites by regulated exocytosis of non-secretory vesicles (Fig. 6) (Chieregatti and Meldolesi, 2005; Cocucci et al., 2009). The mechanisms involved in MV formation and shedding seem to include the ESCRT (Endosomal Sorting Complex Required for Transport) machinery and the small GTP-binding protein ARF6, respectively (Muralidharan-Chari et al., 2009; Gan and Gould, 2011). Additionally, cholesterol-rich microdomains, called lipid rafts, are involved in sorting and formation of MVs (Del Conde et al., 2005). MVs exhibit the same topology compared to their donor cells, but have externalized the phospholipid phosphatidylserine on their surface, which may be responsible for target cell recognition and uptake (Al-Nedawi et al., 2009). In contrast to exosomes, MVs are highly heterogeneous in composition and size. Although there are some cell type specific MV-markers like integrins, selectins, and metalloproteinases, no unique marker has been identified so far (Mathivanan et al., 2010; Turola et al., 2012).

Initially, MVs as well as exosomes have been considered as *in vitro* artifacts or at best as a way for the removal of obsolete material. In the meanwhile, a multitude of functions has been ascribed to MVs. Similar to exosomes, MVs can affect the physiology of neighboring cells by transferring proteins, lipids, and genetic material (Thery et al., 2009) and may influence many physiological (e.g. development, immune reaction, coagulation) and pathological (e.g. cancer progression, proteopathies, viral infections) processes (Cocucci et al., 2009; Turola et al., 2012). Moreover, MVs and exosomes are secreted into body fluids like blood, urine or cerebrospinal fluid (CSF) and can serve as valuable clinical markers or therapeutic targets (Colombo et al., 2012; Verderio et al., 2012).

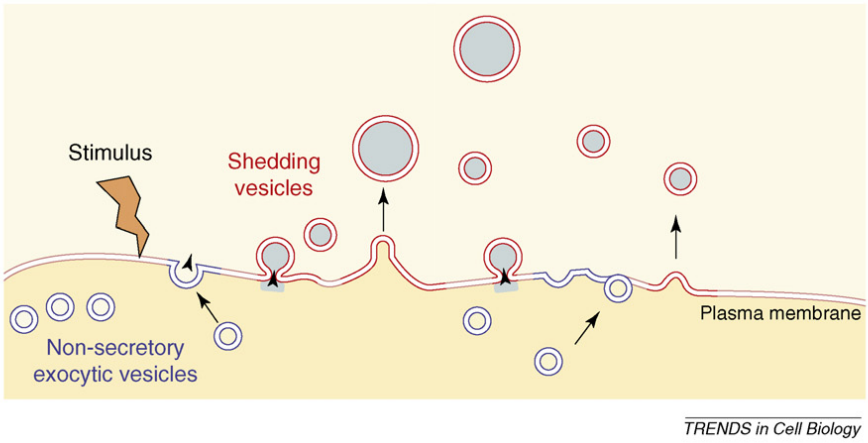


**FIGURE 6: RELEASE OF SHEDDING MICROVESICLES.** Shedding microvesicles (MVs) bud directly from the plasma membrane. Stimulation of the donor cell increases release of MVs. To compensate the loss of membrane material during extensive MV-release, non-secretory exocytic vesicles fuse with the plasma membrane. Adapted from (Cocucci et al., 2009).

## 3.3. EXOSOMES

### *3.3.1. HISTORY*

Exosomes have first been described in the maturation process of mammalian and avian reticulocytes. During differentiation, these cells use exosome release for the removal of obsolete transferrin receptors and for plasma membrane remodeling (Johnstone et al., 1991). Later on, it has been discovered that exosomes do not only serve to get rid of obsolete material but rather function as important signaling entities. For instance, in the immune system exosomes released by antigen presenting cells (APCs) like B lymphocytes and dendritic cells carry MHC molecules on their surface and are able to stimulate T cell proliferation and anti tumor responses (Raposo et al., 1996; Zitvogel et al., 1998; Thery et al., 2002). To date, the release of exosomes has been ascribed to a multitude of cells and plenty of functions, especially in intercellular communication, have been suggested so far.

### *3.3.2. BIOGENESIS AND COMPOSITION*

Exosomes are small EVs released to the extracellular space by fusion of multivesicular bodies (MVBs) with the plasma membrane. They are around 40-100 nm in diameter and appear to have a cup-shaped morphology as observed by transmission-electron microscopy. However, this may be a fixation artifact since they appear as round and well-delimited vesicles using cryo-electron microscopy (Conde-Vancells et al., 2008). Exosomes can be purified from tissue culture

supernatants and body fluids by differential centrifugation and sucrose density gradient centrifugation (see also 4.11.). Alternative purification methods are filtration and immunoprecipitation using antibody-coupled beads. On a sucrose gradient, exosomes float at a characteristic density around 1.13 – 1.19 g/ml (Thery et al., 2006). Besides their typical morphology, exosomes can be further discriminated from other EVs by a characteristic pattern of properties like size, density, protein, and lipid composition. Exosomes are enriched in raft-lipids like cholesterol, sphingolipids, ceramide, and glycerophospholipids with long and saturated fatty acid chains (Subra et al., 2007; Trajkovic et al., 2008). Independent from the cell type by which they are released, exosomes contain a common set of proteins reflecting their endosomal origin. Exosomes carry proteins involved in membrane transport and fusion (e.g. Rab GTPases, annexins, flotillin), in MVB biogenesis (ESCRT and ESCRT-associated proteins like Alix and Tsg101), heat shock proteins (Hsc/Hsp 70 and 90), integrins, and tetraspanins (e.g. CD9, CD63, CD81, CD82) (Simons and Raposo, 2009). Some of them are specifically enriched in exosomes and are therefore commonly used as exosomal markers (e.g. Alix, Tsg101, flotillin, and tetraspanins).

The biogenesis of exosomes requires in first place the formation of MVBs (Fig. 7). MVBs are generated by inward budding of the limiting membrane of late endosomes forming intraluminal vesicles (ILVs). Proteins internalized from the cell surface or derived from the trans Golgi network are sorted into the ILVs and can undergo two different fates. MVBs can either fuse with existing lysosomes resulting in cargo-degradation (Futter et al., 1996) or fuse with the plasma membrane releasing the ILVs as exosomes into the extracellular space (Fevrier and Raposo, 2004). Sorting of proteins to exosomes occurs at the endosomal membrane and probably requires the ESCRT machinery. While ESCRT-0, -I, and II complexes recognize and sort ubiquitinated proteins to the ILVs, ESCRT-III plays a role in membrane budding (Hurley, 2008). However, also ESCRT-independent sorting mechanisms exist, involving formation of membrane subdomains. For example, the lipid ceramide triggers budding of ILVs into MVBs probably due to its cone-shaped structure facilitating membrane curvature (Trajkovic et al., 2008). Also tetraspanins have been implicated in exosome formation and sorting of exosomal cargo by interacting with each other forming a so-called tetraspanin web. Interaction of tetraspanins with other transmembrane and cytosolic proteins results in their sorting to exosomes (Rana and Zoller, 2011). These sorting mechanisms may be independent from each other and lead to distinct exosome subpopulations (Simons and Raposo, 2009). Apart from lipids and proteins, exosomes also contain genetic material like mRNAs and microRNAs (miRNAs), which are probably specifically sorted to exosomes. Loading of exosomes with RNA may also involve ESCRT-II since this complex can specifically bind mRNA (Irion and St Johnston, 2007).

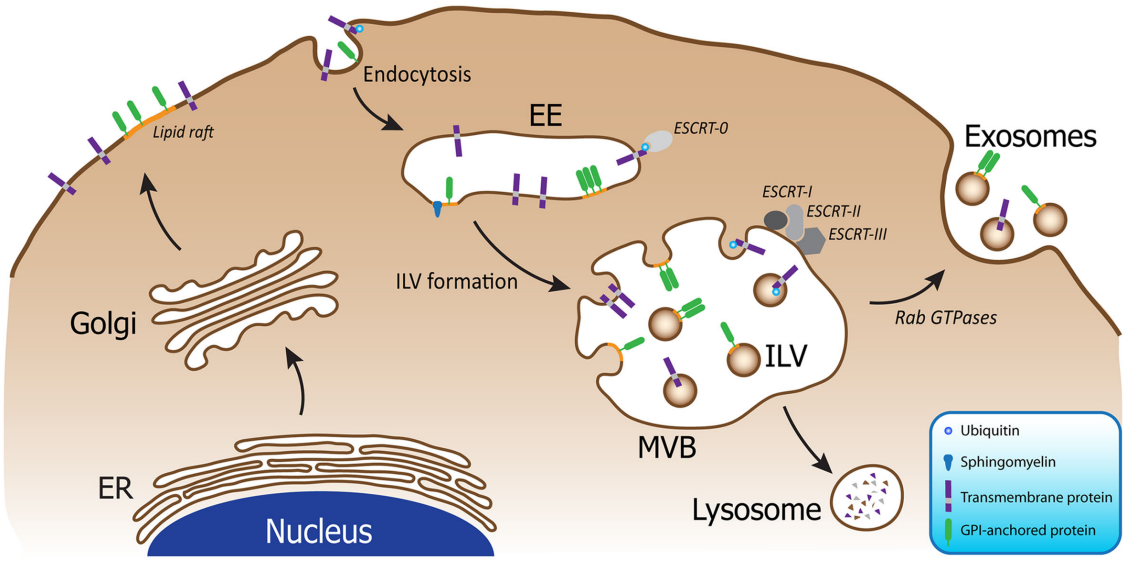


**FIGURE 7: BIOGENESIS OF EXOSOMES.** Exosomes are generated by inward budding of the limiting membrane of a late endosome resulting in formation of multivesicular bodies (MVBs). MVBs can either fuse with lysosomes resulting in cargo degradation or with the plasma membrane leading to the release of the intraluminal vesicles (ILVs) into the extracellular space. These vesicles are then termed exosomes. The release can either be constitutive or regulated by different stimuli. The ESCRT complexes 0-III are involved in exosome biogenesis and protein sorting. Docking of MVBs to the plasma membrane and release of exosomes requires the function of distinct Rab GTPases. Adapted from (Bellingham et al., 2012).

Exosome release from MVBs to the extracellular space is tightly controlled and seems to involve different Rab GTPases (Fig. 7). Rab proteins control intracellular vesicular trafficking by regulating budding, motility, docking, and fusion (Zerial and McBride, 2001). It has been shown that different Rab proteins regulate exosome release from different cell types. In HeLA cells Rab27a and Rab27b control docking of MVBs to the plasma membrane, a prerequisite for exosome release (Ostrowski et al., 2010). In oligodendrocytes the same process is controlled by Rab35 (Hsu et al., 2010), while in the erythroleukemic cell line K562 Rab11 promotes the docking of MVBs (Savina et al., 2005). Exosomes are secreted constitutively by resting cells, however, stimulation can dramatically increase exosome secretion. Stimulation is mediated by intracellular $Ca^{2+}$ levels, which regulate the release of exosomes (Savina et al., 2003; Faure et al., 2006; Krämer-Albers et al., 2007).

**TABLE 1: COMPARISON OF SHEDDING MICROVESICLES AND EXOSOMES.** *The morphology of exosomes has for a long time been considered as cup-shaped. Recent cryo-electron microscopic studies showed that they are round and well-delimited vesicles. Modified from (Cocucci et al., 2009; Mathivanan et al., 2010).

| | Shedding Microvesicles | Exosomes |
|---|---|---|
| Size | 100 – 1000 nm | 30 – 100 nm |
| Morphology | Various shapes / heterogeneous | Regular / homogeneous (cup-shaped*) |

| Site of generation | Plasma membrane | Late endosomes / MVBs |
|---|---|---|
| Mechanism of generation | Budding from plasma membrane | Inward budding of the endosomal membrane |
| Lipid composition | High phosphatidylserine exposure, cholesterol | Low phosphatidylserine exposure, raft-lipids like cholesterol, sphingolipids, ceramide, and glycerophospholipids |
| Protein markers | Selectins, integrins, CD40, metalloproteinases | Alix, Tsg101, Hsc/Hsp70, CD63, CD81, CD9 |
| Genetic material | mRNA, miRNA | mRNA, miRNA |
| Mechanism of sorting | ESCRT, lipid rafts | ESCRT, ceramide, tetraspanins, lipid rafts |
| Intracellular storage | No | Yes |
| Mechanism of discharge | Budding from plasma membrane | Exocytosis of MVBs |
| Type of discharge | Constitutive and regulated | Constitutive and regulated |

### *3.3.3. FUNCTIONS*

The first described function of exosomes was the disposal of obsolete proteins like the transferrin receptor during reticulocyte maturation. This displays an alternative route to lysosomal protein degradation and is ideally suited for cells with poor degradative capacities or for those, which are located close to the body's circulation and drainage systems (bloodstream or tubules of kidney and gut) (Johnstone et al., 1991; Johnstone, 2006). To date, multiple physiological and pathological functions have been ascribed to exosomes, the most prominent being their role in intercellular communication. In this process, target cell specificity may be achieved by exposure of specific adhesion molecules like integrins and tetraspanins on the exosome surface (Raposo and Stoorvogel, 2013). It has been suggested that tetraspanin- or tetraspanin-integrin-complexes are responsible for target cell selection and uptake of exosomes (Rana and Zoller, 2011; Rana et al., 2012). After docking to the target cell, different exosome fates are possible (Fig. 8). Exosomes may just attach to the cell surface and remain stably bound without the cargo being internalized, inducing signal transduction pathways or altering target cell surface properties. For instance, follicular dendritic cells carry exosomes containing MHC class II and other surface proteins that they do not express themselves attached to their surface enabling T cell interaction (Denzer et al., 2000). Alternatively, exosomes either fuse with the plasma membrane of the target cell releasing their cargo directly into the cytosol or are internalized by distinct endocytosis routes (Raposo and Stoorvogel, 2013). In the latter case,

exosomes have to back-fuse with the limiting endosomal membrane to release their intraluminal cargo into the cytosol of the recipient cell (Simons and Raposo, 2009).

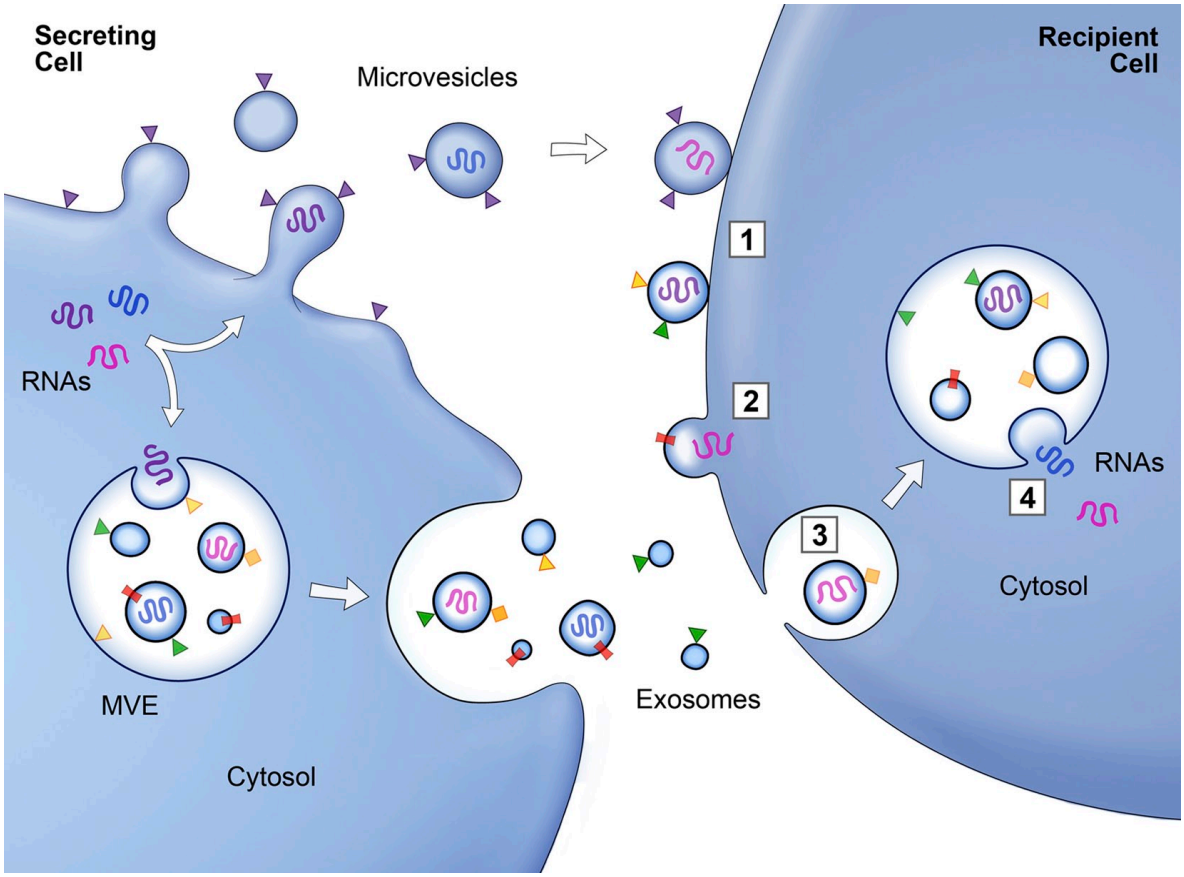


**FIGURE 8: INTERCELLULAR TRANSFER OF PROTEINS AND RNAS.** Proteins and RNAs (mRNA and miRNA) can be transferred to a recipient cell via shedding microvesicles (MVs) or exosomes. There are different ways of target cell interaction: (1) Vesicles stably attach to the surface of the recipient cell, either altering target cell surface properties or inducing signal transduction pathways. This docking process can be followed by either fusion (2) or endocytosis (3) of the vesicles. In the case of endocytosis the vesicles can back-fuse with the endosomal membrane and release their cargo into the cytosol (4). Adapted from (Raposo and Stoorvogel, 2013).

In recent years, the exchange of genetic material between cells by the means of exosomes has gained particular interest. For instance, mRNAs from murine mast cells are transferred to human mast cells via exosomes and afterwards translated, as indicated by newly synthesized mouse proteins in the recipient cells (Valadi et al., 2007). Moreover, small RNAs including miRNAs are functionally transferred between cells and mediate gene silencing in the target cell (Pegtel et al., 2010).

In the immune system, exosomes released by APCs like B-lymphocytes and dendritic cells carry MHC and T-cell co-stimulatory molecules and are able to stimulate T-cell activation. The activation can either be direct as shown for B-cell-derived exosomes (Raposo et al., 1996) or indirect as shown for dendritic cell-derived exosomes *in vivo* (Thery et al., 2002). Exosomes also

carry membrane-bound morphogens like Wnt proteins. Active Wnt proteins are secreted on exosomes from human cells as well as during Drosophila development and can induce Wnt signaling in target cells, indicating that the transfer of morphogens via exosomes is an evolutionary conserved mechanism (Gross et al., 2012). At the Drosophila larval neuromuscular junction (NMJ) presynaptic release of exosomes carrying the Wnt-binding protein Evi (Evenness interrupted) is required for Wnt transmission (Korkut et al., 2009).

In the nervous system, all major cell types release exosomes. The functions of these exosomes (and microvesicles) are described in detail in paragraph 3.4..

On the downside, exosomes play a role in multiple pathological processes. Exosomes released by tumor cells as well as other cells in the tumor microenvironment contain immunosuppressive molecules and modulate the tumor environment to facilitate tumor progression, angiogenesis, and metastasis (Skog et al., 2008; Rak, 2010; Zhang and Grizzle, 2011). Furthermore, exosomes are involved in spreading of viruses and other pathogens. For instance, retroviruses like the human immunodeficiency virus (HIV) use the intracellular machinery of exosome biogenesis for their budding, which has led to the "Trojan exosome" hypothesis (Gould et al., 2003; Nguyen et al., 2003). In the CNS, exosomes can transfer toxic proteins that are involved in neurodegenerative disorders (Bellingham et al., 2012).

### *3.3.4. APPLICATIONS*

Exosomes are present in various body fluids making them valuable biomarkers and therapeutic targets for different diseases. Cells in a pathological state release exosomes altered in quantity and composition, and some of them are drained to accessible body fluids like blood, urine, or CSF, where they can be detected for diagnostic reasons. For instance, exosomes present in the CSF have been suggested as biomarkers for multiple neurodegenerative disorders (Bellingham et al., 2012; Colombo et al., 2012). Moreover, dendritic cell-derived exosomes, also termed dexosomes (Dex), have been used as vaccines in cancer immunotherapy (for review see (Le Pecq, 2005; Viaud et al., 2010)). Compared to other vaccine vectors, Dex were able to stimulate the adaptive as well as the innate immune response (Viaud et al., 2010). Two phase I clinical trials were performed so far, successfully using Dex loaded with tumor-specific MHC class I and II peptides in melanoma and non-small cell lung cancer (NSCLC) patients (Escudier et al., 2005; Morse et al., 2005), and a phase II clinical trial with NSCLC patients is still ongoing (Viaud et al., 2010).

Additionally, exosomes have been used as vehicles for gene therapy. Since the commonly used gene delivery agents like viral vectors and synthetic liposomes have a variety of targeting

difficulties and unwanted side effects, exosomes as naturally derived vesicles could overcome these issues. Alvarez-Erviti et al. could show that the targeted delivery of GAPDH and BACE1 siRNA to the brain by systemic injection of exosomes led to knockdown of GAPDH and BACE1 in neurons, oligodendrocytes, and microglia. Targeting was achieved by expressing the RVG (rabies viral glycoprotein) peptide fused to the exosomal membrane protein Lamp2b (Alvarez-Erviti et al., 2011). RVG binds to the acetylcholine receptor, which is widely expressed in the brain, including the endothelial cells of brain capillaries, enabling the exosomes to cross the blood-brain-barrier and target neural cells (Kumar et al., 2007). In another study the anti-inflammatory drugs curcumin and JSI124 encapsulated in exosomes were delivered noninvasively and specifically to microglia via intranasal application (Zhuang et al., 2011). Mice treated with these exosomes were protected from LPS-induced brain inflammation, the progression of MOG induced experimental autoimmune encephalomyelitis (EAE), and had significantly delayed brain tumor growth in a GL26 tumor model.

## 3.4. EXTRACELLULAR VESICLES IN THE NERVOUS SYSTEM

### *3.4.1. NEURONAL EXTRACELLULAR VESICLES*

In neurons, endosomes are present in both pre- and postsynaptic compartments (Chivet et al., 2013). EM analysis of hippocampal neurons revealed the presence of MVBs in dendrites and sometimes even in dendritic spines, the postsynaptic parts of synapses (Chivet et al., 2012). MVBs can be observed 50 times more often in somatodendritic compared to axonal compartments of the neuron and enhanced synaptic activity increases the number of MVBs present in dendrites thus linking the localization of MVBs to the process of synaptic plasticity (Von Bartheld and Altick, 2011).

Cortical neurons in culture release exosomes that contain, besides classical exosomal marker proteins like Alix, Tsg101, and HSC70, the GluR2/3 AMPA receptor subunits as well as the neuronal cell adhesion molecule L1 (Faure et al., 2006). The release of exosomes from neurons is regulated by electrical activity since depolarization with high potassium resulted in an increased exosome release (Faure et al., 2006). Moreover, stimulation of synaptic glutamatergic activity by blocking inhibitory GABA (γ-aminobutyric acid) receptors with picrotoxin or bicucullin enhanced exosome release showing the involvement of NMDA and AMPA receptors (Lachenal et al., 2011). Furthermore, increasing cytosolic $Ca^{2+}$ levels by application of the calcium ionophore ionomycin also resulted in increased exosome secretion (Lachenal et al., 2011). Taken together, stimulation of ionotropic glutamate receptors leads to $Ca^{2+}$ influx into the postsynaptic terminal

and subsequently, to fusion of MVBs with the plasma membrane and release of exosomes. The enhanced release of exosomes containing AMPA receptor subunits from the postsynapse may result in local elimination of receptors from synapses undergoing plastic changes and could represent a mechanism of synaptic downscaling (Chivet et al., 2012). Additionally, neuronal exosomes contain miRNAs and transfer of these miRNAs may result in gene silencing in the recipient cell also contributing to synaptic plasticity (Chivet et al., 2012). Neuronal exosomes loaded with tetanus toxin become presynaptically internalized by hippocampal neurons (unpublished work by M. Chivet, C. Javalet and R. Sadoul), suggesting a retrograde transfer of tetanus toxin via exosomes (Lachenal et al., 2011; Chivet et al., 2013).

In Drosophila, neuronal exosomes are also involved in synaptic plasticity indicating that this may be an evolutionary conserved mechanism. Transfer of synaptotagmin 4 via exosomes from the presynaptic to the postsynaptic terminal enables retrograde back-signaling from the postsynaptic cell (Korkut et al., 2013). By this mechanism the presynaptic cell itself may influence retrograde signaling and synaptic plasticity.

Neuronal exosomes could also represent a route for the spreading of pathogens in the CNS. Exosomes carry and transfer α-synuclein, $PrP^{Sc}$ (the scrapie and disease specific form of the prion protein), APP and several APP cleavage products including the Aβ peptide, phosphorylated tau, and SOD, which are involved in Parkinson's disease, prion disease, Alzheimer's disease, and amyotrophic lateral sclerosis (ALS), respectively (Bellingham et al., 2012; Schneider and Simons, 2013).

### *3.4.2. MICROGLIAL EXTRACELLULAR VESICLES*

Activated microglia secrete a range of soluble factors such as cytokines and chemokines. Interestingly, microglia also release MVs of irregular shape and size (0.1-1 μm) characterized by high levels of externalized phosphatidylserine (PS). Upon ATP stimulation of $P2X_7$ receptors, reactive microglia release MVs carrying the inflammatory cytokine interleukin-1β (IL-1β), the IL-1β-processing enzyme caspase-1, and the $P2X_7$ receptor (Bianco et al., 2005). $P2X_7$ receptor activation in microglia induces translocation of acid sphingomyelinase to the outer leaflet of the plasma membrane and subsequently causes hydrolysis of sphingomyelin to the sphingolipid ceramide, which promotes membrane curvature resulting in increased MV formation (Bianco et al., 2009). It has been suggested that in MVs, which approach tissue areas with high ATP levels, the $P2X_7$ receptor becomes activated and IL-1β is processed and released from the vesicle to the external milieu. This pathway may induce and propagate inflammatory reactions throughout the brain (Prada et al., 2013).

Microglial MVs positive for the marker CD11b/c are detectable in the CSF of rodents and humans under physiological conditions. However, the amount of MVs increases dramatically during brain inflammation (e.g. MS in humans or EAE in mice) depending on disease severity and the extent of microglia activation (Verderio et al., 2012). Injection of MVs into the brain of mice with subclinical EAE recruits inflammatory cells to the injection site. However, acid sphingomyelinase deficient mice, which are impaired in MV production, are mainly protected from EAE. Intriguingly, FTY720, an oral drug for the treatment of MS reduces the amount of microglial MVs in the CSF of EAE mice (Verderio et al., 2012). Taken together, these data provide evidence that microglial MVs can enforce brain inflammation making them valuable diagnostic markers or even therapeutic targets of neuroinflammatory diseases (Colombo et al., 2012).

In addition, microglia-derived MVs can interact with neurons by stimulation of spontaneous and evoked excitatory transmission. Hippocampal neurons exposed to MVs show an increase in miniature excitatory postsynaptic current (mEPSC) frequency without changes in mEPSC amplitude. The lipid fraction of MVs affects the presynaptic site of the excitatory synapse by increasing the release probability of synaptic vesicles through induction of ceramide and sphingosine synthesis. Thus, microglial MVs may modulate synaptic activity and enhance neurotransmission by influencing the sphingolipid metabolism in neurons (Antonucci et al., 2012; Turola et al., 2012).

Besides MVs, microglia release exosomes with a protein content analogues to B cell- and dendritic cell-derived exosomes (Potolicchio et al., 2005). For instance, MHC class II is packed into exosomes and its amount is increasing upon stimulation with interferon-γ. Additionally, microglial exosomes contain the cell surface-bound aminopeptidase N (CD13), which can degrade the neuropeptides methionine- and leucine-enkephalin, thereby influencing the activity of the opioid receptor. Since microglial exosomes contain MCT1, responsible for lactate transport, and enzymes for anaerobic glycolysis and lactate production, they may deliver energy substrates to neurons (Potolicchio et al., 2005). Furthermore, microglia-derived exosomes carry the insulin-degrading enzyme (IDE), which can proteolize the Aβ peptide and may be involved in Aβ clearance (Tamboli et al., 2010). Finally, exosome release by rat microglia can be induced by the morphogen Wnt3a, which in turn is included and released via exosomes (Hooper et al., 2012).

### *3.4.3. ASTROGLIAL EXTRACELLULAR VESICLES*

Astrocytes secrete a heterogeneous population of EVs that can have supportive or pathological effects. As reported for microglia, MV shedding from astrocytes is evoked by the ATP-triggered

activation of the $P2X_7$ receptor and subsequent action of acid sphingomyelinase (Bianco et al., 2009). In culture, astrocytes and other BBB cells secrete MVs carrying nucleoside triphosphate diphosphohydrolases (NTDPases). The authors suggest that vesicular release of NTDPases increases the breakdown of toxic extracellular ATP levels derived from damaged BBB cells (Ceruti et al., 2011). Moreover, the angiogenic factors FGF-2 and VEGF are present in astroglial MVs (Proia et al., 2008). Intriguingly, MVs of astrocytic origin are detectable in the CSF of rodents indicating their existence *in vivo* (Verderio et al., 2012).

Astrocytes also secrete exosomes. Hsc/Hsp70 and Synapsin I are present in astrocyte-derived exosomes and rising amounts of these proteins associated with exosomes are released in response to heat or oxidative stress suggesting a signal-induced delivery of protective factors to neurons (Taylor et al., 2007; Wang et al., 2011a). In the mouse eye, retinal astrocyte-derived exosomes contain, in contrast to MVs, anti-angiogenic proteins such as endostatin and PEDF and can target macrophages and vascular endothelial cells, which are involved in angiogenic processes (Hajrasouliha et al., 2013). Moreover, it has been reported that astrocytes and glioblastoma cells secrete exosomes containing mitochondrial DNA (mtDNA), which may be transferred between cells (Guescini et al., 2010).

On the downside, astroglial exosomes could also be involved in the propagation of pathogenic proteins in neurodegenerative disorders. Cultured astrocytes expressing mutant SOD1 secrete increased amounts of exosomes, which carry mutant SOD1. The mutant SOD1 is transferred to cultured neurons and can induce motor neuron death, suggesting a role of astroglial exosomes in ALS (Basso et al., 2013). Exposure of amyloid peptide to astrocytes triggers the release of exosomes containing pro-apoptotic ceramide and PAR4 (prostate apoptosis response 4). In turn, they are internalized by other astrocytes and induce apoptosis, potentially promoting neurodegeneration in Alzheimer's disease (Wang et al., 2012). Treatment of cultured astrocytes with HIV Tat (trans-activator of transcription) protein and morphine activates shuttling of miR-29b via exosomes to neurons, which results in the decrease of neurotropic PDGF-B expression and neuronal cell death. Thus, spreading of miR-29b by astrocyte-derived exosomes may contribute to neurodegeneration in HIV-associated neurological disorders (Hu et al., 2012).

### *3.4.4. SCHWANN CELL EXTRACELLULAR VESICLES*

Schwann cells (SC) are the myelinating cells of the PNS and appear to be involved in the orchestration of axonal growth and regeneration (Lopez-Verrilli and Court, 2012). SCs release a variety of factors including NGF, BDNF, NT-3, and FGF-2, which are capable of promoting neuronal survival, axonal maturation, modulation of synaptic transmission, and repair (Madduri

and Gander, 2010). The lateral transfer of SC-derived vesicles to axons with potent neuroprotective cargo such as Hsp70 has been suggested earlier (Fevrier et al., 2004). Recently it has been shown that de-differentiated SCs release exosomes carrying classical exosomal markers like Tsg101 and CD63 as well as the p75-neurotrophin receptor ($p75^{NTR}$) (Lopez-Verrilli et al., 2013). Theses exosomes are selectively internalized by axons *in vitro* and increase axonal regeneration by inhibiting RhoA GTPase activity in growth cones. Inhibition of RhoA activity modulates growth cone dynamics to promote neurite extension. Intriguingly, also *in vivo* regeneration of injured sciatic nerves was enhanced by application of SC exosomes (Lopez-Verrilli et al., 2013). In addition to exosomes, SC-derived ribosomes are also transferred to axons by vesicular means after axonal injury, supplying the axons locally with components of the protein synthesis machinery (Court et al., 2008; Court et al., 2011). But SC-derived exosomes may also exert negative effects on target cells. SCs secrete exosomes carrying pathogenic prion proteins *in vitro* and these exosomes may contribute to the spreading of prions from the PNS to the CNS (Fevrier et al., 2004).

### *3.4.5. OLIGODENDROGLIAL EXTRACELLULAR VESICLES*

Exosomes released by oligodendrocytes carry characteristic exosomal marker proteins like Tsg101, Alix, the tetraspanins CD63 and CD81, and the heat shock proteins Hsp70 and Hsp90. Additionally, they contain the oligodendrocyte and myelin specific proteins PLP, CNP, MBP, MAG (myelin-associated glycoprotein), and MOG (myelin oligodendrocyte glycoprotein). Interestingly, they also include the NAD-dependent deacetylase sirtuin-2, stress alleviating proteins, and glycolytic enzymes (Fig. 9) (Krämer-Albers et al., 2007). Their membrane comprises the lipids galactocerebroside, sulfatide, and cholesterol, which are also enriched in the myelin sheath (Krämer-Albers et al., 2007). Moreover, oligodendroglial exosomes contain mRNAs and miRNAs (Frühbeis et al., 2013a).

Biogenesis of PLP-containing exosomes in the oligodendroglial cell line Oli-*neu* follows an ESCRT-independent pathway requiring activity of the neutral sphingomyelinase and subsequent formation of the sphingolipid ceramide (Trajkovic et al., 2008). However, there may also be ESCRT-dependent pathways present in oligodendrocytes eventually facilitating formation of distinct subpopulations of exosomes. The GTPase Rab35 and its activating proteins TBC1D10A-C regulate exosome release from oligodendroglial cells by controlling docking and fusion of secretory MVBs with the plasma membrane (Hsu et al., 2010). As described for other cell types, the release of exosomes from oligodendrocytes is mediated by elevation of cytosolic $Ca^{2+}$ levels (Savina et al., 2003; Lachenal et al., 2011). Treatment of primary mouse oligodendrocytes (pOL)

with the $Ca^{2+}$ ionophore ionmycin caused excessive $Ca^{2+}$ influx and triggered the release of exosomes (Krämer-Albers et al., 2007). Recent work in our group demonstrated that stimulation of cultured oligodendrocytes with the neurotransmitter glutamate significantly increased exosome release (Frühbeis et al., 2013a). Functional glutamate receptors are present on mature oligodendrocytes as well as their precursors (Karadottir and Attwell, 2007; Frühbeis et al., 2013a) and stimulation with NMDA and AMPA likewise resulted in enhanced exosome secretion. Moreover, we could show that stimulation of oligodendroglial exosome release is coupled to neuronal electrical activity, since stimulation of neuronal electrical activity by high potassium (KCl) or bicuculline markedly increased the release of oligodendroglial exosomes. Taken together, the neurotransmitter glutamate released by electrically active neurons evokes a rise in cytosolic $Ca^{2+}$ levels by acting on oligodendroglial ionotropic glutamate receptors of the NMDA and AMPA subtype and triggers secretion of exosomes (Frühbeis et al., 2013a).

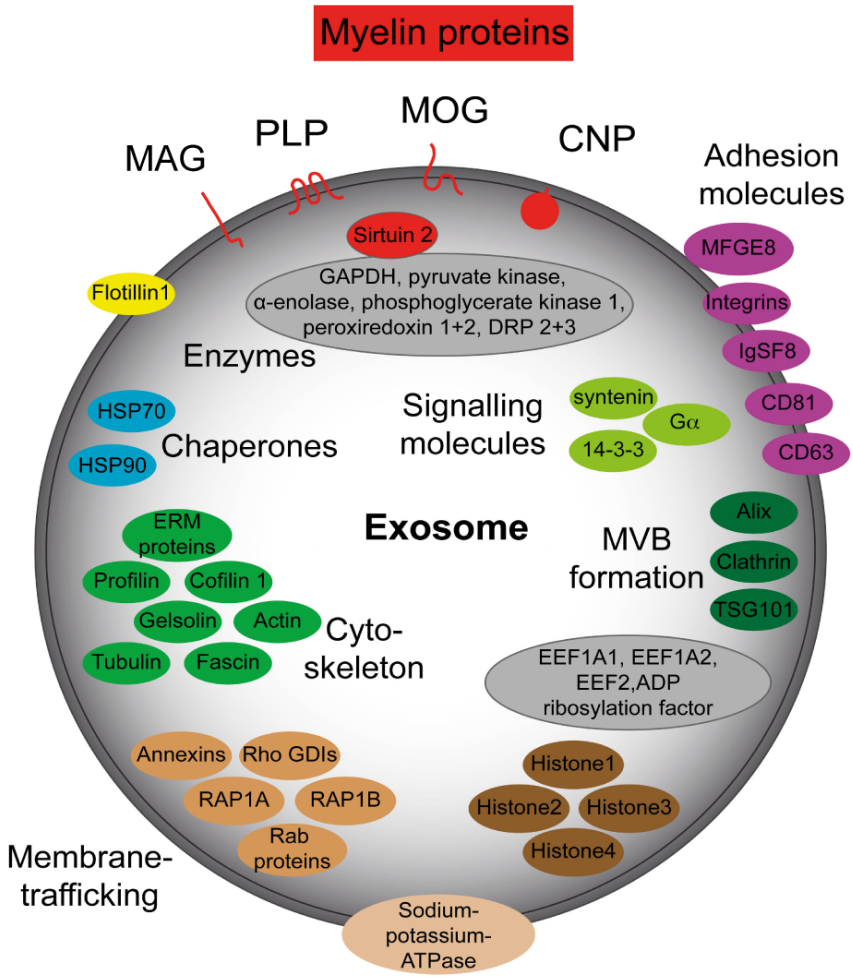


**FIGURE 9: PROTEIN COMPOSITION OF A TYPICAL OLIGODENDROCYTE-DERIVED EXOSOME.** This illustration is based on a proteomic analysis of oligodendroglial exosomes (Krämer-Albers et al., 2007). Adapted from (Frühbeis et al., 2012).

These findings raise the question whether oligodendrocyte derived exosomes can interact with distinct target cells in the CNS. So far, it has only been suggested that oligodendroglial exosomes may exert an inhibitory effect on oligodendrocyte differentiation and myelin membrane formation *in vitro* mediated by signal transduction pathways involving RhoA, Fyn, and Fak (Bakhti et al., 2011). Since neuronal conditioned medium decreased oligodendroglial exosome release, neurons may coordinate myelin membrane biogenesis by regulating the secretion of autoinhibitory exosomes from oligodendrocytes (Bakhti et al., 2011). Efficient internalization of oligodendroglial exosomes occurs by microglia in an immunological silent manner (Fitzner et al., 2011; Frühbeis et al., 2013a). A subset of MHC class II negative microglia with no antigen presenting capacity preferentially takes up oligodendroglial exosomes by macropinocytosis, which may represent a mechanism for the clearance of excess myelin membranes. However, it remains unclear whether stressed or pathogen-infected oligodendrocytes release exosomes with pro-inflammatory properties that may trigger autoimmune responses (Fitzner et al., 2011).

## 3.5. WORKING HYPOTHESIS

Exosome release from oligodendrocytes is triggered by the neurotransmitter glutamate (Frühbeis et al., 2013a). However, the fate of these vesicles upon release remained enigmatic so far. Up to now, it has only been suggested that oligodendroglial exosomes may act in an autoinhibitory fashion on other oligodendrocytes inhibiting myelin formation (Bakhti et al., 2011) or alternatively, can be cleared from the extracellular space by microglia in an immunologically silent manner (Fitzner et al., 2011).

Therefore, it is highly relevant to answer the question whether oligodendroglial exosomes can participate in intercellular communication in the CNS, potentially contributing to the trophic support function of oligodendrocytes. This study aims at the identification of potential target cells of oligodendroglial exosomes in the CNS, in particular focusing on the interaction with neurons. We ask if oligodendrocyte derived exosomes are internalized by neurons, and subsequently, if exosomal cargo is delivered to the neurons. Furthermore, the molecular mechanisms of exosome uptake will be investigated and the question whether exosomal cargo is degraded or functionally retrieved by the recipient cell will be addressed. Finally, functional implications on neuronal electrical activity as well as neuronal gene expression will be investigated.

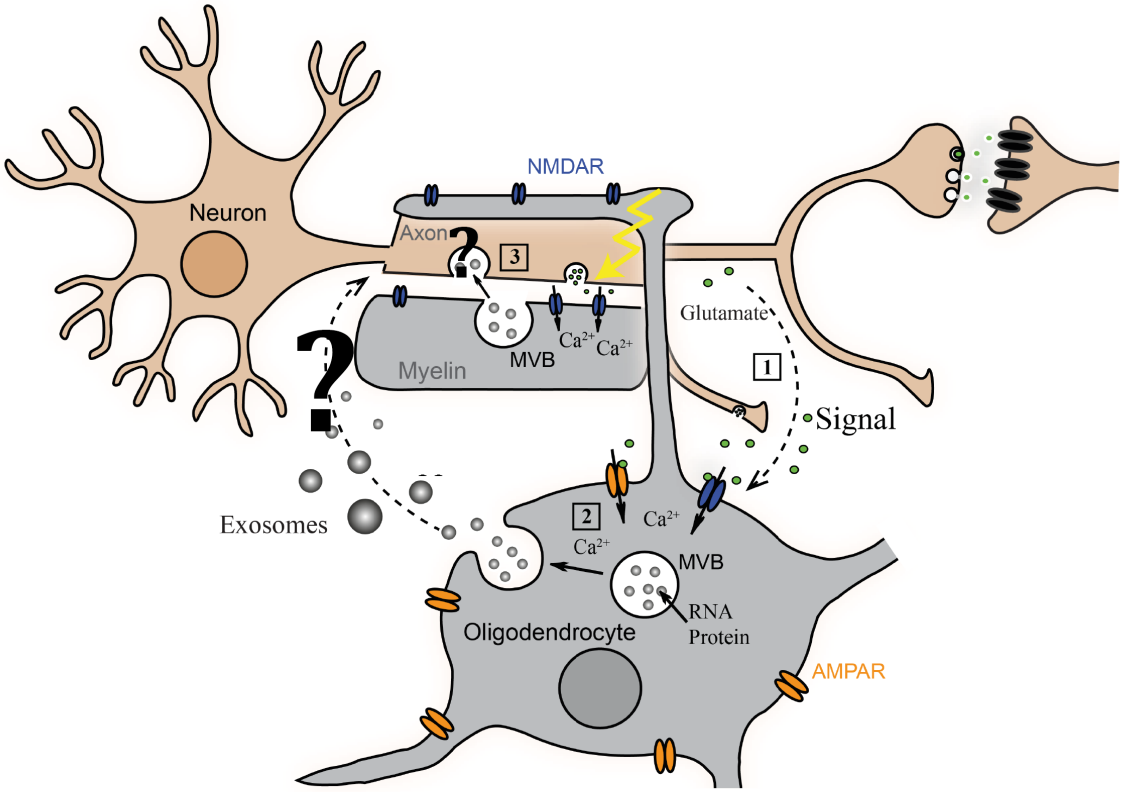


**FIGURE 10: WORKING HYPOTHESIS.** Electrically active neurons release glutamate, which in turn activates oligodendroglial NMDA and AMPA receptors. This leads to a rise in intracellular $Ca^{2+}$ that forces MVBs to fuse with the plasma membrane. The released exosomes could then shuttle back to neurons and may provide trophic support to axons. This PhD thesis tries to answer the questions, if, how, and where oligodendroglial exosomes are internalized by neurons, if the exosomal cargo can be functionally retrieved by the recipient neurons, and finally if exosomal cargo may influence neuronal electrical activity or gene expression. Adapted from (Frühbeis et al., 2013b).

# 4. MATERIALS AND METHODS

## 4.1. EQUIPMENT, MATERIALS, BUFFERS AND MEDIA

### *4.1.1. EQUIPMENT*

**TABLE 2: CENTRIFUGES**

| Centrifuges | |
|---|---|
| **3K20** | Sigma-Aldrich, München |
| **Biofuge 17RS** | Heraeus, Hanau |
| **Megafuge 1.0R** | Heraeus, Hanau |
| **Z383K** | Hermle, Wehingen |
| **Optima Ultracentrifuge Max-E** | Beckman, München |
| **Optima L-90 K Ultracentrifuge** | Beckman, München |
| **Optima XL-100 K Ultracentrifuge** | Beckman, München |
| **Rotors: TLA-55, TLS-55, SW28-Ti, SW40-Ti, SW41-Ti** | Beckman, München |

**TABLE 3: MICROSCOPES**

| Microscopes | |
|---|---|
| **DMLB** | Leica, Wetzlar |
| **DM6000** | Leica, Wetzlar |
| **TCS SP5** | Leica, Wetzlar |
| **Axiovert LSM 710** | Zeiss, Jena |

**TABLE 4: TRANSFECTION DEVICES**

| Transfection devices | |
|---|---|
| **GenePulser Xcell** | Bio-Rad, München |
| **Nucleofector II** | Lonza, Köln |

**TABLE 5: OTHER EQUIPMENT**

| Other equipment | |
|---|---|
| **T3 Thermocycler** | Biometra, Göttingen |
| **NanoDrop 1000 Spectrophotometer** | Peqlab, Erlangen |
| **Photospectrometer Ultrospect 2100 pro** | GE Healthcare, München |
| **Mini PROTEAN Electrophoresis System** | Bio-Rad, München |
| **Mini Trans-Blot Electrophoretic Transfer Cell System** | Bio-Rad, München |
| **Electrophoresis chamber NuPAGE** | Invitrogen, Karlsruhe |
| **Optimax Type TR X-Ray Film Processor** | MS Laborgeräte, Wiesloch |
| **StepOne Real-time PCR System** | Applied Biosystems, Darmstadt |

| | |
|---|---|
| **C200 Incubator** | Labotect, Göttingen |
| **SterilGARD III Advance Class II Bio-logical Safety Cabinet** | The Baker Company, Sanford, USA |

### *4.1.2. MATERIALS*

**TABLE 6: CHEMICALS**

| **Chemicals** | |
|---|---|
| **Dibutyryl-cAMP (dbcAMP)** | #D0627 Sigma-Aldrich, München |
| **Sodiumbutyrate** | #30341-0 Sigma-Aldrich, München |
| **GW4869** | #D1682 Sigma-Aldrich, München |
| **Glutamate** | Sigma-Aldrich, München |
| **Dynasore** | #D7693 Sigma-Aldrich, München |
| **Pitstop2** | #Asc-687 Ascent scientific, Bristol, UK |
| **CytochalasinD** | #C8273 Sigma-Aldrich, München |
| **Methyl-β-Cyclodextrin** | #C-4555 Sigma-Aldrich, München |
| **Hydrogen peroxide** | #8070.2 Roth, Karlsruhe |
| **Dextran biotin, 70000 MW** | #D1956 Molecular Probes, Eugene, USA |
| **Streptavidin-HRP** | #43-4323 Invitrogen, Karlsruhe |
| **Complete Protease Inhibitor Cocktail Tablets** | #11697498001 Roche, Mannheim |

**TABLE 7: KITS**

| **Kits** | |
|---|---|
| **PureLink HiPure Plasmid Miniprep Kit** | #K210011 Invitrogen, Karlsruhe |
| **PureLink HiPure Plasmid Maxiprep Kit** | #K2100-07 Invitrogen, Karlsruhe |
| **QIAquick Gel Extraction Kit** | #28706 Qiagen, Hilden |
| **QIAquick PCR Purification Kit** | #28106 Qiagen, Hilden |
| **Transcriptor High Fidelity cDNA Synthesis Kit** | #05091284001 Roche, Mannheim |
| **Quiagen miRNeasy mini Kit** | #217004 Qiagen, Hilden |
| **Illumina TotalPrep RNA Amplification Kit** | #AMIL1791 Illumina, San Diego, USA |
| **QuantiTect Rev. Transcription Kit** | #205311 Qiagen, Hilden |
| **AMAXA Basic Nucleofector Kit for Primary Neurons** | #VPI-1003 Lonza, Köln |
| **PKH67 Green Fluorescent Cell Linker Kit** | #MIDI67-1KT Sigma-Aldrich, München |
| **PKH26 Red Fluorescent Cell Linker Kit** | #MINI26-1KT Sigma-Aldrich, München |

**TABLE 8: MARKER**

| **Marker** | |
|---|---|
| **Lambda/HindIII DNA-Marker** | #SM0101 Fermentas, St. Leon-Rot |
| **PhiX 174 DNA/BsuRI (HaeIII) DNA-Marker** | #SM0251 Fermentas, St. Leon-Rot |
| **Precision Plus Protein Standards Dual Color** | #161-0374 Bio-Rad, München |

**TABLE 9: OTHER MATERIALS**

| Other materials | |
|---|---|
| **Amersham Hyperfilm ECL** | #28906837 GE Healthcare, München |
| **Luminata Crescendo ECL** | #WBLUR0100 Millipore, Billerica, USA |
| **Immobilon-P transfer membrane** | # IPVH00010 Millipore, Billerica, USA |
| **Glassware** | VWR, Darmstadt |
| **Plastic ware** | Nunc, Langenselbold; BD Falcon, Heidelberg; Sarstedt, Nümbrecht |
| **Six-well Companion Plates** | #353502 BD Falcon, Heidelberg |
| **Six-well Cell Culture Inserts** | #353102 BD Falcon, Heidelberg |
| **Microfluidic Chambers (Standard neuron device 150 µm)** | #SND150 Xona, Temecula, USA |

### *4.1.3. SOFTWARE*

**TABLE 10: SOFTWARE**

| Software | |
|---|---|
| **Word 2011** | Microsoft |
| **Excel 2011** | Microsoft |
| **Powerpoint 2011** | Microsoft |
| **Endnote X6** | Thomson Reuters |
| **SPSS Statistics 19** | SPSS Inc. |
| **Photoshop CS6** | Adobe |
| **Illustrator CS6** | Adobe |
| **ImageJ** | NIH |
| **Clone Manager 9, Professional Edition** | Scientific & Educational Software |
| **ApE plasmid editor** | M. Wayne Davis |

### *4.1.4. BUFFERS AND MEDIA*

If not stated otherwise, all chemicals are obtained from Roth, Karlsruhe.

**TABLE 11: BUFFERS AND MEDIA - GENERAL**

| General | |
|---|---|
| **PBS** | 150 mM NaCl; 8 mM $Na_2HPO_4$; 1.7 mM $NaH_2PO_4$; adjust pH to 7.2 |
| **PBST** | PBS; 0,1% Tween 20 |
| **TBS** | 50 mM Tris; 150 mM NaCl; adjust pH to 7.2 |

**TABLE 12: BUFFERS AND MEDIA – MOLECULAR BIOLOGY**

| Molecular Biology | |
|---|---|
| **TAE** | 40 mM Tris; 1 mM EDTA; adjust pH to 8.0 with acetic acid |
| **LB medium** | 10 g/l NaCl; 10 g/l trypton; 5 g/l yeast extract |
| **LB agar** | 2,25 g agar; 150 ml LB medium |

**TABLE 13: BUFFERS AND MEDIA - CELL CULTURE**

| Cell culture | |
|---|---|
| **Poly-L-Lysine (PLL)** | 0.1 g/l Poly-L-Lysine hydrobromide (degree of polymerization: 70000-150000) |
| **Trypsin/EDTA** | HBSS; 0.01% trypsin; 0.02% EDTA |
| **PBS 10% HS** | PBS; 10% horse serum |
| **Sato 1% HS** | 13.4 g/l DMEM (#52100-039 Invitrogen); 2 g/l $NaHCO_3$; 0.01 g/l Transferrin; 100 µg/l Insulin (Stock 10 µg/ml); 100 µM Putrescine; 200 nM Progesterone; 500 nM TIT; 220 nM Na-Selenite; 520 mM L-Thyroxine; 1% horse serum |
| **Cryoprotective medium** | RPMI 1640 70%; FCS 20%; DMSO 10% |
| **Sato/B27 1% HS** | 13.4 g/l DMEM (#52100-039 Invitrogen); 2 g/l $NaHCO_3$; 20 ml/l B27 (#17504044 Invitrogen); 0.011 % Pyruvate; 500 nM TIT; 520 mM L-Thyroxine; 0.05% Gentamycin; 1% horse serum |
| **HBSS** | 5.33 mM KCl; 0.441 mM $KH_2PO_4$; 4.17 mM $NaHCO_3$; 137.93 mM NaCl; 0,338 mM $Na_2HPO_4$; 5.56 mM D-glucose; 0.0266 mM Phenol Red |
| **HBSS$^+$** | HBSS; 0.15% $MgSO_4$ |
| **Neurobasal plating medium** | Neurobasal (#1309101 Gibco); 20 ml/l B27 (#17504044 Invitrogen); 0.5 mM L-glutamine; 10 ml/l 100x Pen-Strep (63.2 µg/ml Penicillin G K-salt; 135 µg/ml Streptomycin sulfate); 12.5 µM Glutamate |
| **Neurobasal feeding medium** | Neurobasal (#1309101 Gibco); 20 ml/l B27 (#17504044 Invitrogen); 0.5 mM L-glutamine; 10 ml/l 100x Pen-Strep (63.2 µg/ml Penicillin G K-salt; 135 µg/ml Streptomycin sulfate) |
| **DMEM 10% FCS** | 13.4 g/l DMEM (#52100-039 Invitrogen); 2 g/l $NaHCO_3$; 10 ml/l 100x Pen-Strep (63.2 µg/ml Penicillin G K-salt; 135 µg/ml Streptomycin sulfate); 100 ml/l fetal calf serum |
| **DMEM 10% HS** | 13.4 g/l DMEM (#52100-039 Invitrogen); 2 g/l $NaHCO_3$; 10 ml/l 100x Pen-Strep (63.2 µg/ml Penicillin G K-salt; 135 µg/ml Streptomycin sulfate); 100 ml/l horse serum |

**TABLE 14: BUFFERS AND MEDIA - PROTEIN BIOCHEMISTRY**

| Protein Biochemistry | |
|---|---|
| **Triton lysis buffer** | 50 mM Tris/HCl (pH 7,2); 150 mM NaCl; 1% Triton X-100; Roche® Complete protease inhibitor cocktail was added prior to use |
| **4x Sample Buffer** | 200 mM Tris-HCL (pH=6.8); 8% SDS; 0.4% bromphenol blue; 40% glycerol; 400mM DTT |

| | |
|---|---|
| | (if reducing conditions are desired) |
| **Stacking gel buffer** | 1 M Tris (pH 6,8) |
| **Separation gel buffer** | 1.5 M Tris (pH 8,8) |
| **Stacking/ Separation gel for SDS PAGE** | Gels were prepared according to Tables A8-9 and A8-10 (Volume 3, A8.43) „Molecular Cloning – A Laboratory Manual", Sambrook und Russell, 2001, Cold Spring Harbour Press, New York, USA |
| **5x SDS electrophoresis buffer** | 125 mM Tris; 1.25 M glycine; 0.5% SDS; adjust pH to 8.3 |
| **Western Blot Transfer buffer** | 24 mM Tris; 192 mM glycine; 20% ethanol |
| **Blocking solution** | PBST; 4% milk powder |
| **ECL solution** | Solution A: 0.1 M Tris-HCl (pH 8.6), luminol 0,25 g/l<br>Solution B: 1.1 g/l para-hydroxy coumaric acid<br>Development: Combine 1ml solution A + 100 µl solution B + 0.3 µl $H_2O_2$ |

**TABLE 15: BUFFERS AND MEDIA - IMMUNOCYTOCHEMISTRY**

| **Immunocytochemistry** | |
|---|---|
| **Fixation solution** | PBS; 4% paraformaldehyde |
| **Permeabilization solution** | PBS; 0.1% Triton X-100 |
| **Blocking solution** | PBS; 10% horse serum |
| **Mounting medium** | 2.4 g Moviol 4-88; 6 g glycerol; 6 ml dd$H_2O$; 12 ml 0.2 M Tris (pH 8.5) |

## 4.2. ANTIBODIES

### *4.2.1. PRIMARY ANTIBODIES*

**TABLE 16: PRIMARY ANTIBODIES**

| Antigen | Clone/# | Host species | Application | Manufacturer |
|---|---|---|---|---|
| **Acetylated-Lysine** | #9441L | rabbit | 1:1000 (WB) | Cell Signaling |
| **AIP-1/Alix** | #611621 | mouse | 1:250 (WB) | BD |
| **BIP/GRP78** | #610979 | mouse | 1:2000 (WB) | BD |
| **Calnexin** | #SPA-865 | rabbit | 1:2000 (WB) | Stressgen |
| **Calreticulin** | #SPA-600 | rabbit | 1:4000 (WB) | Stressgen |
| **Catalase** | #14276 | rabbit | 1:2000 (WB); 1:500 (IF) | Rockland |
| **Cre recombinase** | #PRB-106C | rabbit | 1:5000 (WB) | Covance |
| **Doublecortin** | #AB2253 | guinea pig | 1:5000 (WB) | Chemicon |
| **F4/80** | F4/80 D10 | rat | 1:100 (IF) | Hybridoma AG Kiewsky |

| | | | | |
|---|---|---|---|---|
| **GAPDH** | #A300-641A | rabbit | 1:2000 (WB) | Bethyl Lab. |
| **GFAP** | #Z0334 | rabbit | 1:5000 (WB); 1:1000 (IF) | Dako Cytomation |
| **GFP** | #ab6556 | rabbit | 1:5000 (WB); 1:2000 (IF) | Abcam |
| **GFP** | #ab13970 | chicken | 1:2000 (IF) | Abcam |
| **L1** | 324 | rat | undiluted (IF) | Hybridoma |
| **L1** | 555 | rat | 1:50 (WB) | Hybridoma |
| **Lamp1** | 1D4B/#553792 | rat | 1:50 (IF) | BD |
| **NF-H** | #SMI-32P | mouse | 1:1000 (WB); 1:1000 (IF) | Covance |
| **NF-H phosph.** | #SMI-31R | mouse | 1:1000 (WB); 1:1000 (IF) | Covance |
| **O4** | 81 | mouse | undiluted (IF) | Hybridoma |
| **PLP** | aa3 | rat | 1:10 (WB); undiluted (IF) | Hybridoma |
| **Sirtuin-2** | #sc20966 | rabbit | 1:2000 (WB) | Santa Cruz |
| **Sirtuin-2** | #67299 | rabbit | 1:1000 (WB) | abcam |
| **Sirtuin-2** | #2313 | rabbit | 1:1000 (WB) | Cell Signaling |
| **Tsg101** | 4A10/#GTX70255 | mouse | 1:500 (WB) | Genetex/Acris |
| **Tubulin α** | DM1A/#T9026 | mouse | 1:10000 (WB); 1:5000 (IF) | Sigma |
| **Tubulin α, acetylated** | 6-11B-1/#T6793 | mouse | 1:10000 (WB) | Sigma |
| **Tubulin β III** | #MRB-435P | rabbit | 1:5000 (WB); 1:1000 (IF) | Covance |
| **VP1,2,3** | B1/#61058 | mouse | 1:1000 (WB) | Progen |

IF, immunofluorescence; WB, western blot

### *4.2.2. SECONDARY ANTIBODIES*

**TABLE 17: SECONDARY ANTIBODIES**

| Host species | Target species | Conjugation | Application | Cat. No. | Manufacturer |
|---|---|---|---|---|---|
| goat | chicken | Alexa488 | 1:400 (IF) | A-11039 | Invitrogen |
| goat | guinea pig | HRP | 1:10000 (WB) | 106-035-003 | Dianova |
| goat | mouse | Cy2 | 1:200 (IF) | 115-225-003 | Dianova |
| goat | mouse | Cy3 | 1:800 (IF) | 115-165-166 | Dianova |
| goat | mouse | Cy5 | 1:100 (IF) | 115-175-003 | Dianova |
| goat | mouse | Alexa488 | 1:400 (IF) | A-11001 | Invitrogen |
| donkey | mouse | Alexa546 | 1:400 (IF) | A-10036 | Invitrogen |
| goat | mouse | Alexa647 | 1:400 (IF) | A-21236 | Invitrogen |
| goat | mouse | HRP | 1:10000 (WB) | 115-035-003 | Dianova |
| goat | rabbit | Cy2 | 1:200 (IF) | 111-225-144 | Dianova |
| goat | rabbit | Cy3 | 1:800 (IF) | 111-165-003 | Dianova |
| goat | rabbit | Cy5 | 1:100 (IF) | 111-175-003 | Dianova |
| goat | rabbit | Alexa488 | 1:400 (IF) | A-11008 | Invitrogen |
| goat | rabbit | Alexa647 | 1:400 (IF) | A-21244 | Invitrogen |
| goat | rabbit | HRP | 1:10000 (WB) | 111-035-003 | Dianova |
| goat | rat | Cy2 | 1:200 (IF) | 112-225-167 | Dianova |

| | | | | | |
|---|---|---|---|---|---|
| goat | rat | Cy3 | 1:800 (IF) | 112-165-003 | Dianova |
| goat | rat | Cy5 | 1:100 (IF) | 112-175-167 | Dianova |
| goat | rat | Alexa488 | 1:400 (IF) | A-11006 | Invitrogen |
| goat | rat | Alexa546 | 1:400 (IF) | A-11081 | Invitrogen |
| goat | rat | HRP | 1:10000 (WB) | 112-035-003 | Dianova |

IF, immunofluorescence; WB, western blot

## 4.3. DNA ANALYSIS AND MANIPULATION

### *4.3.1. POLYMERASE CHAIN REACTION (PCR)*

Template DNA was amplified by PCR according to the exemplary scheme below. Appropriate reaction conditions have been chosen suitable for the polymerase (Pfu) and the primers which were used. The conditions mainly varied in annealing temperature (depending on the melting temperature of the primers) and elongation time (depending on the length of the desired product).

**TABLE 18: PCR SETUP**

| **PCR setup** | |
|---|---|
| template DNA | ~ 50 ng |
| sense primer (10 µM) | 2 µl |
| antisense primer (10 µM) | 2 µl |
| dNTPs (2,5 mM each) | 4 µl |
| reaction buffer (10x) | 5 µl |
| Pfu polymerase | 1 µl |
| nuclease free dd$H_2O$ | fill to 50 µl |

**TABLE 19: PCR PROGRAM**

| **Step** | **Temp [°C]** | **Time [s]** | **Cycles** |
|---|---|---|---|
| 1. Initial denaturation | 95 | 120 | 1 |
| 2. Denaturation | 95 | 30 | 20-30 |
| 3. Annealing | ~ 60 | 30 | |
| 4. Elongation | 72 | 60 / kb | |
| 5. Final elongation | 72 | 600 | 1 |

### *4.3.2. REVERSE TRANSCRIPTION POLYMERASE CHAIN REACTION (RT-PCR)*

Total RNA was isolated from 6 days old primary oligodendrocytes using the *RNeasy Plus® Mini Kit* (Quiagen) according to the manufacturer´s protocol. RT-PCR was performed with the

*SuperScript™ III One Step RT-PCR System with Platinum® Taq High Fidelity* Kit (Invitrogen) according to the manufacturer´s instructions.

**TABLE 20: RT-PCR SETUP**

| RT-PCR setup | |
|---|---|
| template RNA | ~ 50 ng |
| sense primer (10 µM) | 1 µl |
| antisense primer (10 µM) | 1 µl |
| reaction mix (2x) | 25 µl |
| SuperScript™ III RT / Platinum® Taq High Fidelity Enzyme Mix | 1 µl |
| nuclease free dd$H_2O$ | fill to 50 µl |

**TABLE 21: RT-PCR PROGRAM**

| Step | Temp [°C] | Time [s] | Cycles |
|---|---|---|---|
| 1. cDNA synthesis | 50 | 1800 | 1 |
| 2. Initial denaturation | 94 | 120 | 1 |
| 3. Denaturation | 94 | 15 | 35 |
| 4. Annealing | ~ 60 | 30 | |
| 5. Elongation | 68 | 60 / kb | |
| 6. Final elongation | 68 | 300 | 1 |

### *4.3.3. DNA RESTRICTION DIGEST*

Restriction enzymes were purchased from New England Biolabs. All restriction enzymes and buffers were used according to the manufacturer´s instructions. Double digestions were performed as suggested by the manufacturer. For analytical digestions approximately 1 µg of DNA was used while for preparative purposes 10 µg of DNA were used.

### *4.3.4. AGAROSE GEL ELECTROPHORESIS*

Agarose gel electrophoresis was performed to separate DNA fragments according to their size. Agarose (1%) was dissolved in TAE buffer by boiling till the solution became clear. After cooling 0.6 µg/ml Ethidium bromide was added and the solution was poured into a horizontal gel chamber. The DNA was mixed with 6x loading dye (Fermentas) and loaded to the gel. The gel was run in TAE buffer at 80 V. Afterwards the separated DNA bands were visualized by UV light.

### 4.3.5. DNA EXTRACTION FROM AGAROSE GELS

The corresponding DNA fragments were excised from the gel with a clean razor blade and the DNA was isolated using the *QIAquick Gel Extraction* Kit (Quiagen) according to the manufacturer´s instructions.

### 4.3.6. DNA PURIFICATION FROM PCR REACTIONS

The amplified DNA was purified after PCR / RT-PCR reactions using the *PCR Purification* Kit (Quiagen) according to the manufacturer´s instructions. This step was performed to remove dNTPs, buffers, primers, etc, which may disturb further downstream applications.

### 4.3.7. DNA LIGATIONS

The digested vector backbone and insert were ligated using the *T4 DNA ligase* and corresponding buffer (Fermentas) according to the manufacturer´s protocol. To prevent self-ligation of the digested vector, it was dephosphorylated before ligation using *Antarctic phosphatase* and corresponding buffer (New England Biolabs) according to the manufacturer´s instructions. Ligations were carried out at a molecular ratio of 3:1 (insert : vector).

### 4.3.8. BLUNTING OF 5' OVERHANGS

5' overhangs were blunted using the *Klenow fragment (3' -> 5' exo$^-$)* (New England Biolabs) according to the manufacturer´s instructions. This Klenow fragment retains polymerase activity which allows the fill-in of 5' overhangs to form blunt ends, but lacks 3' -> 5' exonuclease activity (3' overhangs stay sticky).

### 4.3.9. TRANSFORMATION INTO COMPETENT BACTERIA

Chemically competent bacteria *E. coli* Top10 F' (Invitrogen) were thawed on ice and mixed with the ligation product or with the plasmid of choice. After incubation on ice for 30 minutes the bacteria were heat-shocked at 42 °C for 1 minute. Afterwards, 1 ml of antibiotic free LB medium

was added and the suspension was incubated at 37 °C for 30 minutes. Subsequently, the transformed bacteria were plated on agar plates containing adequate antibiotics for selection. The agar plates were incubated over night at 37 °C.

### *4.3.10. Plasmid Preparation from Bacteria (Mini-/ Maxiprep)*

Single colonies were picked from the agar plates and incubated in 4 ml LB medium containing selective antibiotics on a shaking device (225 rpm) at 37 °C over night. Plasmids were extracted using the *PureLink™ Hipure Plasmid Miniprep* Kit (Invitrogen) according to the manufacturer´s protocol. Pelleted plasmids were eluted with 30 µl of nuclease free dd$H_2O$.

For large scale isolation of plasmids 200 ml LB medium containing selective antibiotics were inoculated with bacteria carrying the plasmid of choice and incubated on a shaking device (225 rpm) at 37 °C over night. Plasmids were extracted using the *PureLink™ Hipure Plasmid Maxiprep* Kit (Invitrogen) according to the manufacturer´s instructions. Pelleted plasmids were eluted with 200 µl of nuclease free dd$H_2O$.

### *4.3.11. Generated and Used Plasmids*

#### 4.3.11.1. pCMV/EGFP-SIRT2

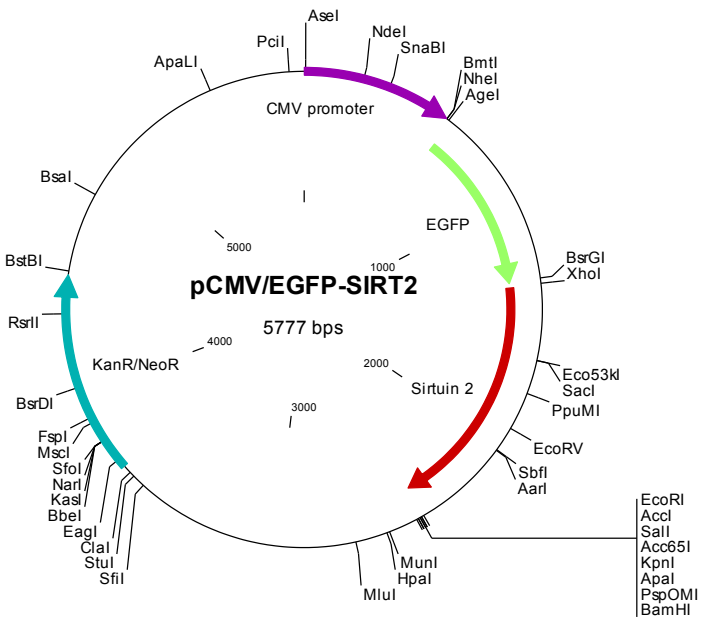


Used restriction sites:
XhoI and EcoRI

### 4.3.11.2. pCMV/SIRT2-EYFP

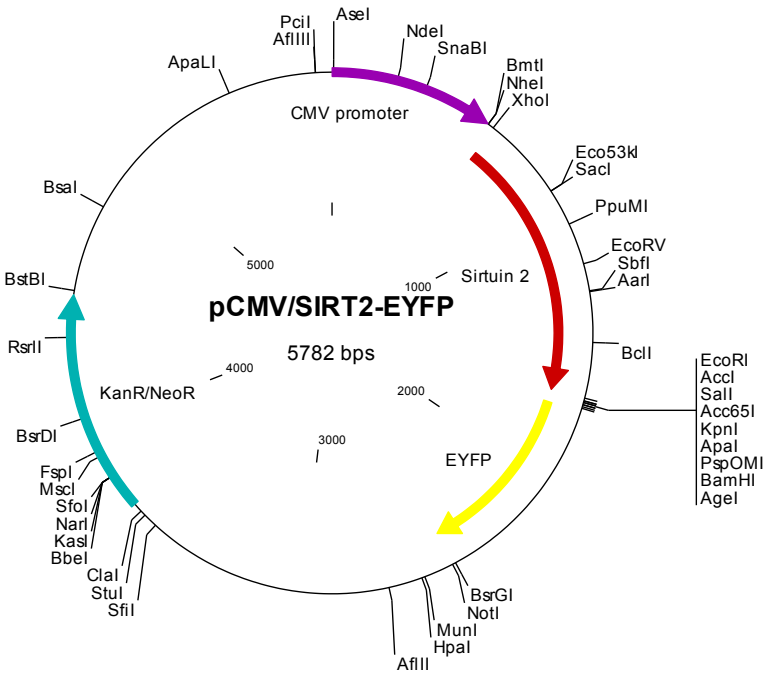


Used restriction sites:
XhoI and EcoRI

### 4.3.11.3. pCMV/SIRT2

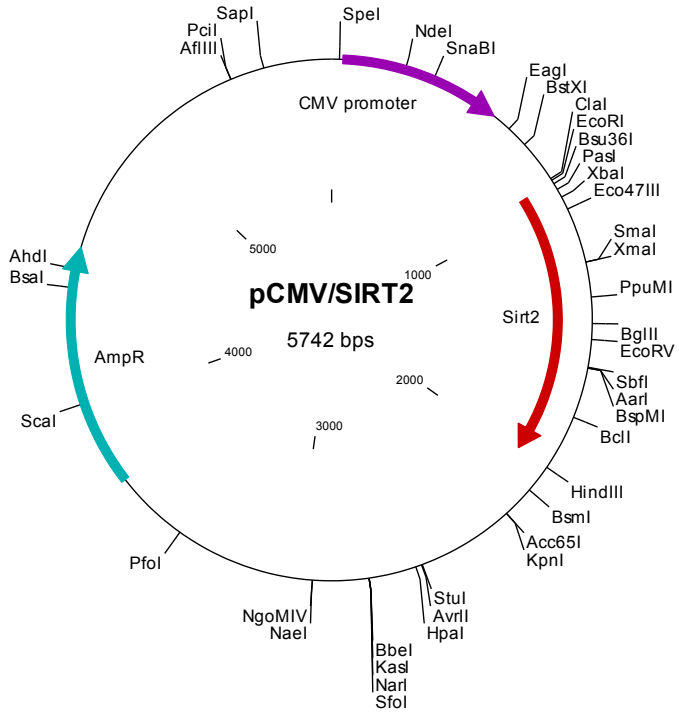


Used restriction sites:
EcoRI and HindIII

#### 4.3.11.4. pCMV/MYC-SIRT2

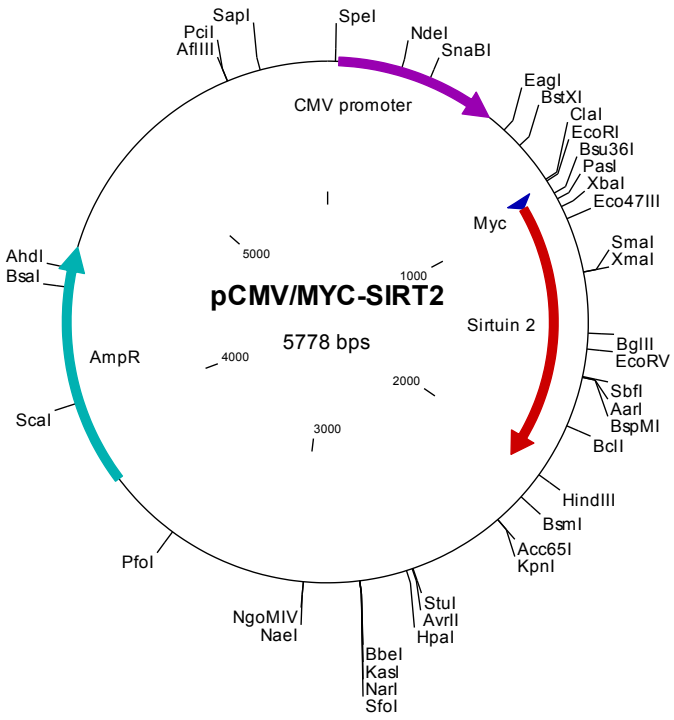


Used restriction sites:
EcoRI and HindIII

#### 4.3.11.5. pCMV/PLP-MYC-EGFP

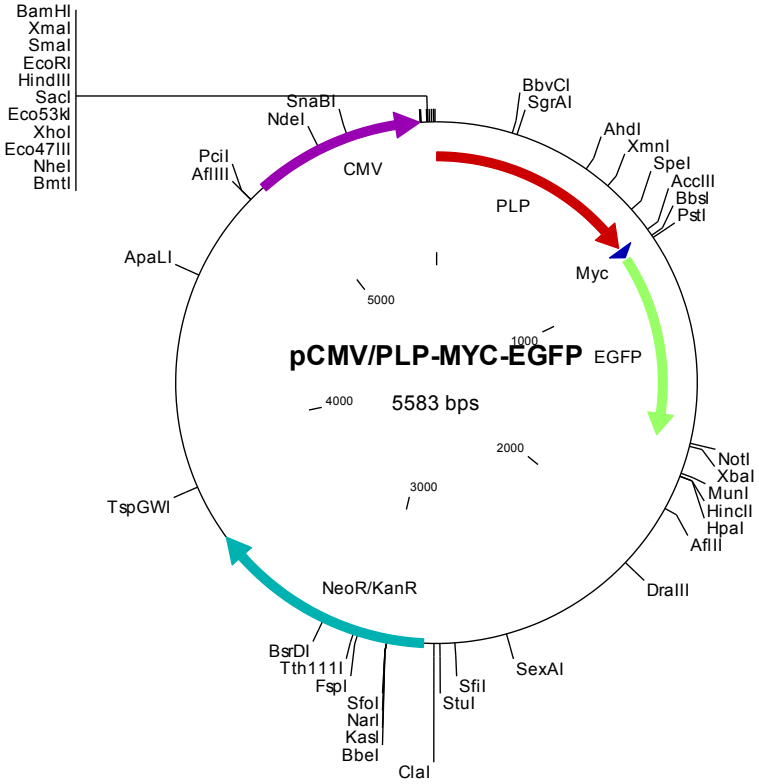

### 4.3.11.6. pAM/CBA-EGFP

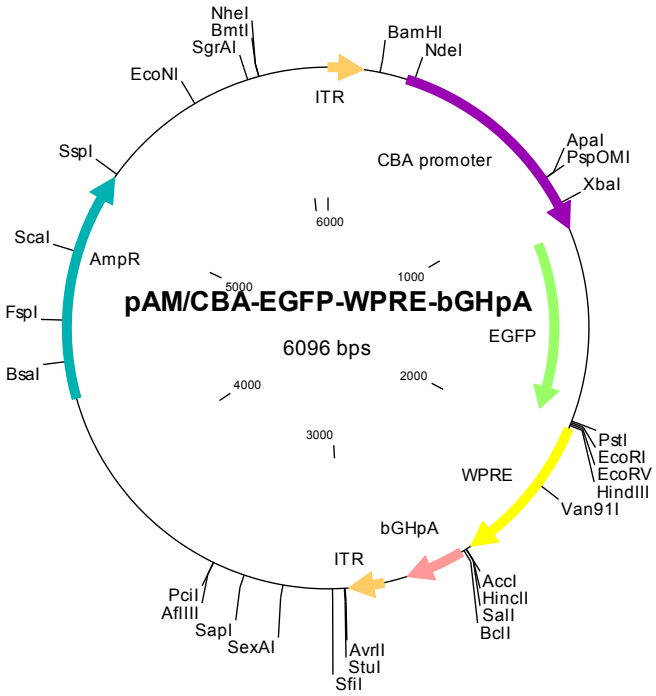


### 4.3.11.7. pAM/MBP-EGFP

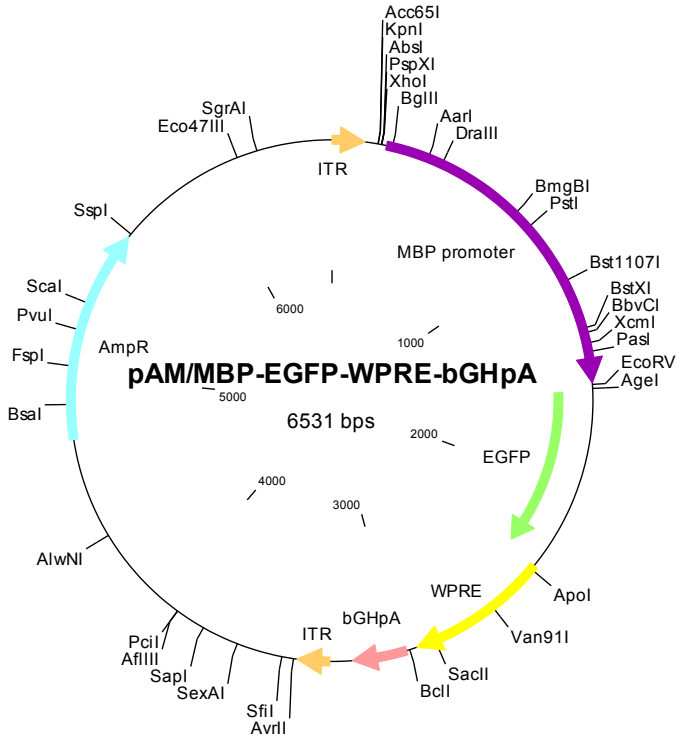

### 4.3.11.8. pAM/CBA-FLOXSTOP-hrGFP

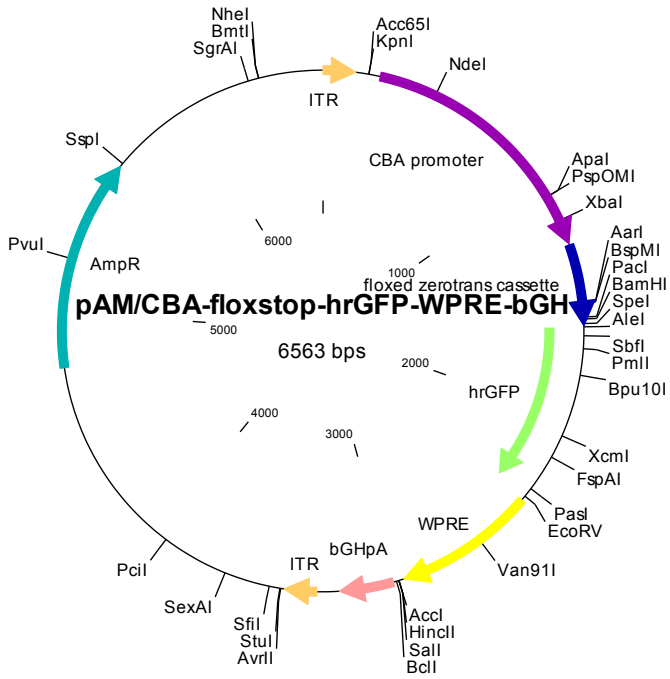


### 4.3.11.9. pAM/MBP-FLOXSTOP-EGFP

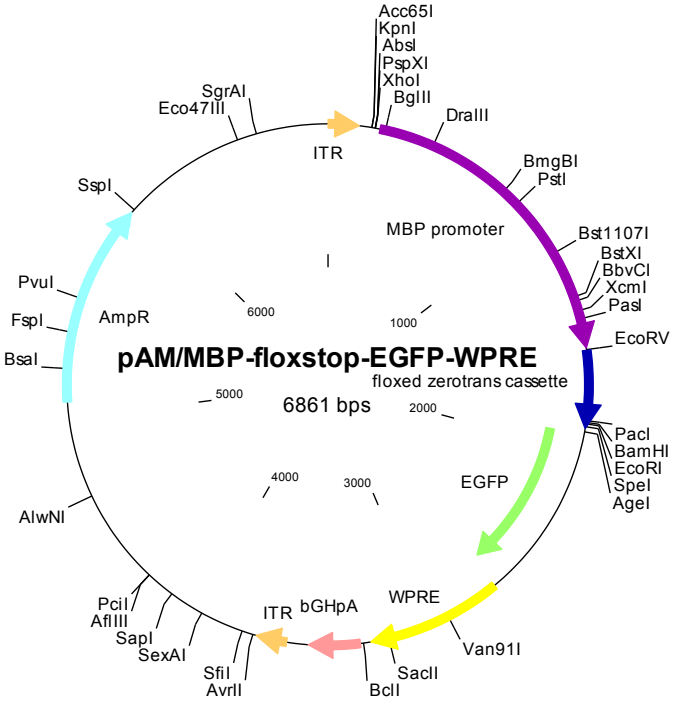


Floxstop cassette excised with EcoRV and HpaI (blunt); pAM/MBP-EGFP opened with EcoRV (blunt).

### 4.3.11.10. pAM/CBA-HA-CRE

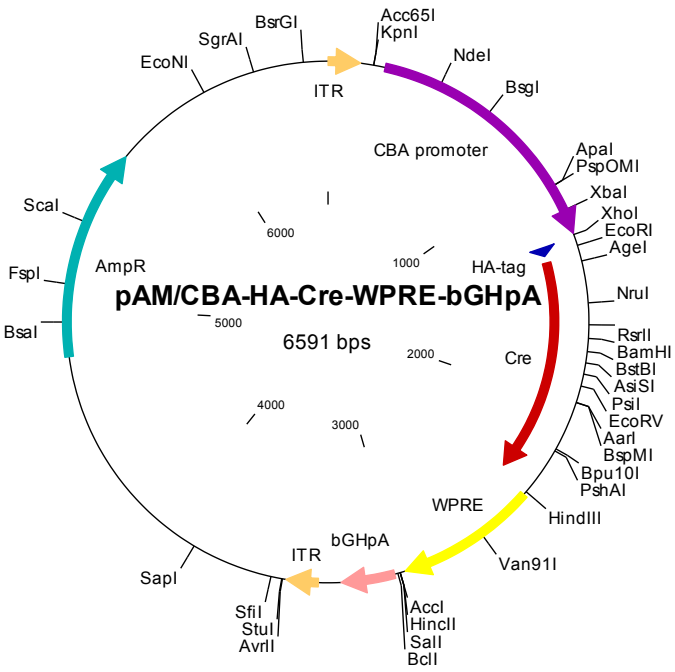


### 4.3.11.11. pAM/MBP-HA-CRE

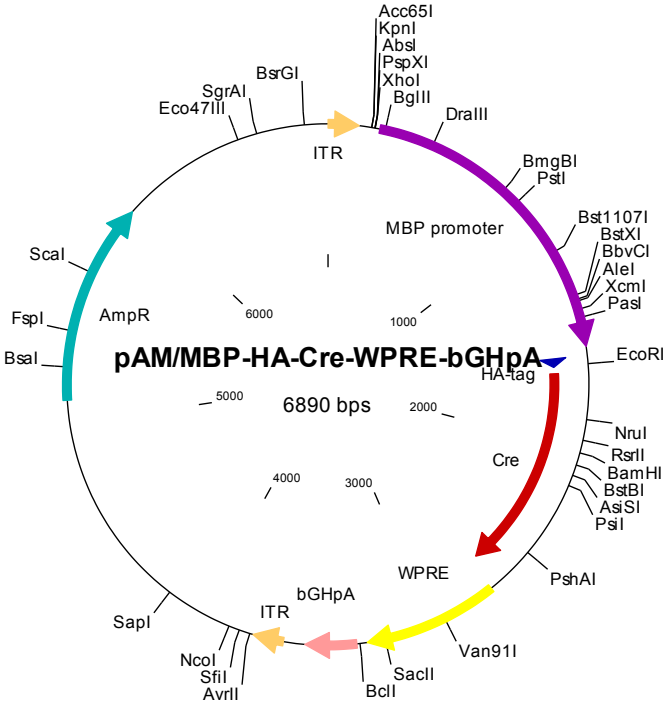


MBP-promoter excised from pAM/MBP-EGFP plasmid with KpnI and AgeI (blunt), pAM/CBA-HA-Cre opened with KpnI and XhoI (blunt).

### 4.3.11.12. pAM/CBA-HA-SIRT2

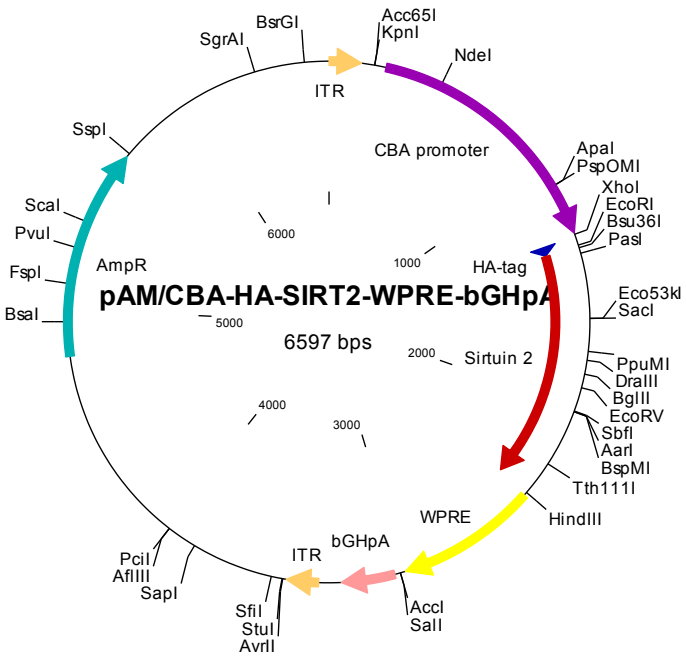


Used restriction sites: EcoRI and HindIII

### 4.3.11.13. pAM/MBP-HA-SIRT2

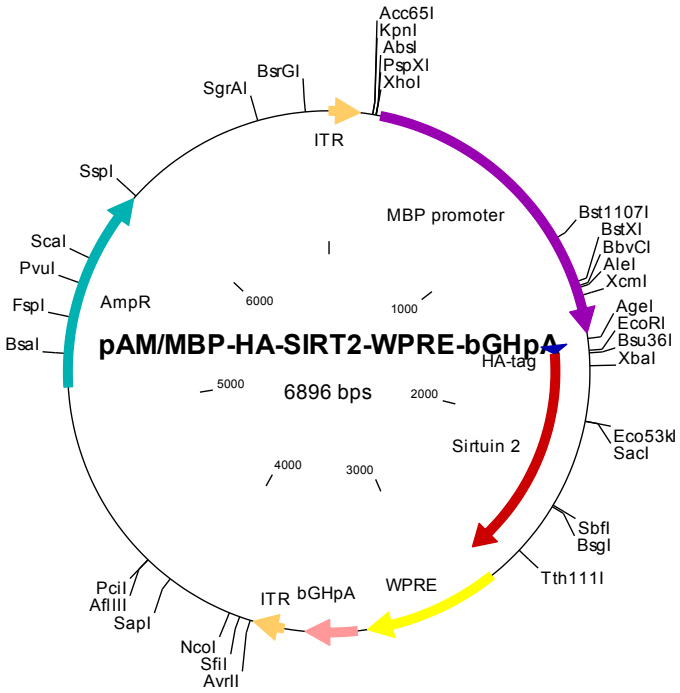


MBP-promoter excised from pAM/MBP-EGFP plasmid with KpnI and AgeI (blunt), pAM/CBA-HA-SIRT2 opened with KpnI and XhoI (blunt).

### 4.3.11.14. pAM/CBA-PLP-EGFP

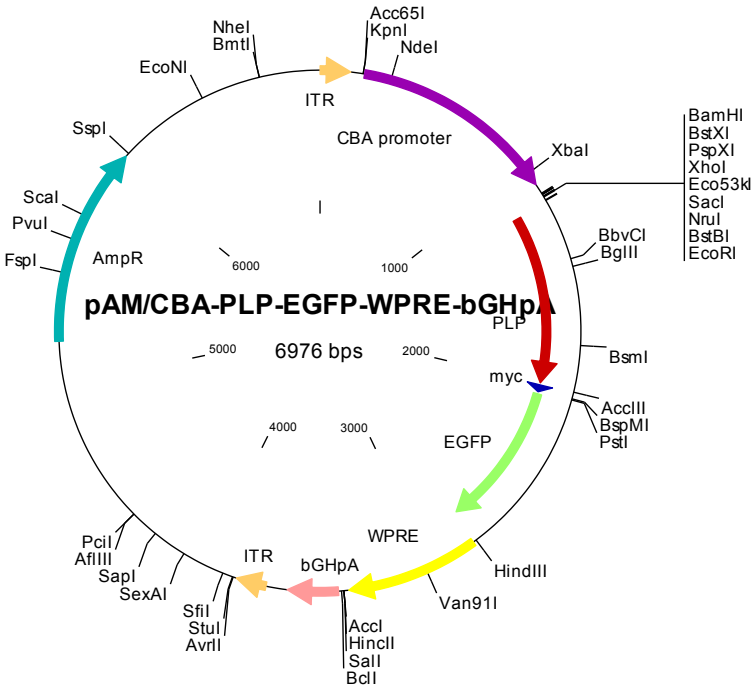


Used restriction sites: EcoRI and HindIII

### 4.3.11.15. pAM/MBP-PLP-EGFP

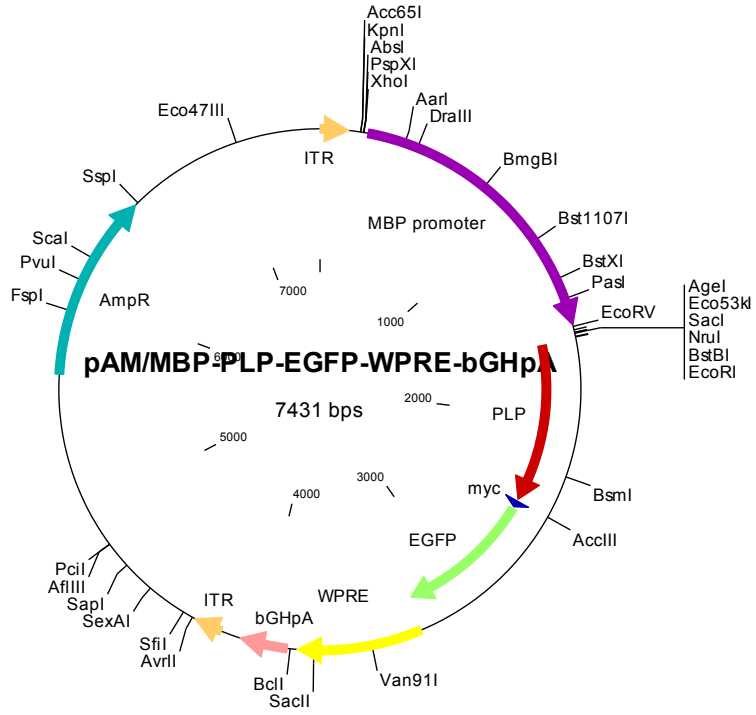


MBP-promoter excised from pAM/MBP-EGFP plasmid with KpnI and AgeI (blunt), pAM/CBA-PLP-EGFP opened with KpnI and XhoI (blunt).

### 4.3.11.16. pAM/MBP-FLOXSTOP-HA-SIRT2

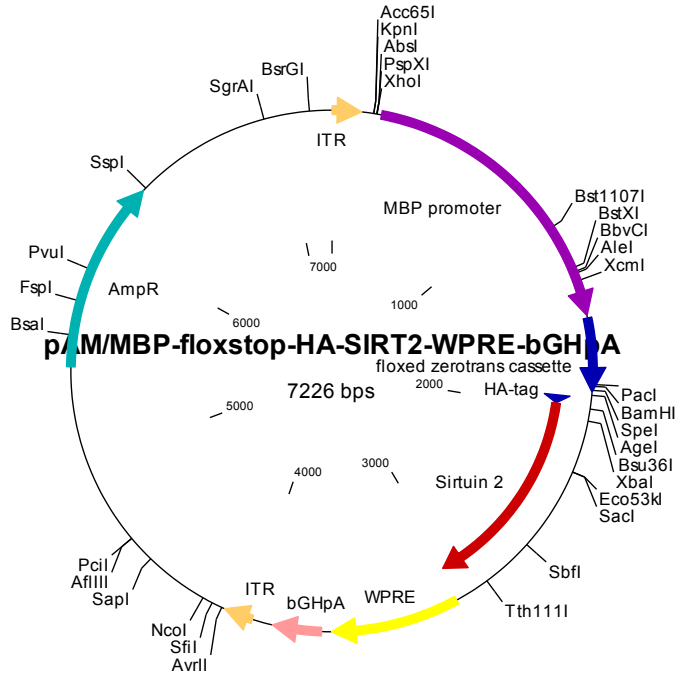


MBP-floxstop excised from pAM/MBP-floxstop-EGFP plasmid with KpnI and AgeI (blunt), pAM/CBA-HA-SIRT2 opened with KpnI and XhoI (blunt).

### 4.3.11.17. pAM/CBA-empty

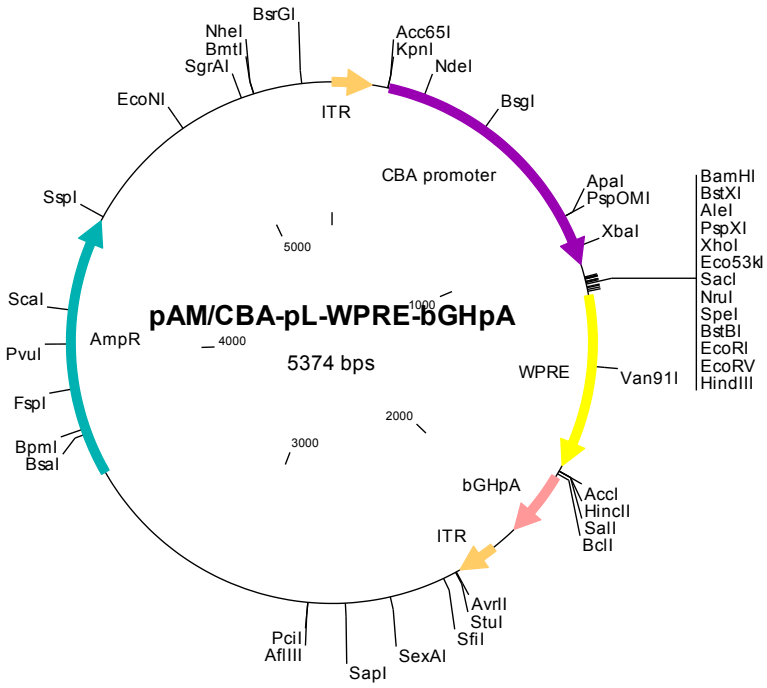

## 4.4. ADENO ASSOCIATED VIRUSES (AAVS)

Adeno-associated viruses (AAVs) were prepared, isolated, and used as described (During et al., 2003).

### *4.4.1. PREPARATION AND ISOLATION*

The cDNA encoding the particular transgene (see plasmid maps of pAM vectors listed above) was cloned into an AAV expression cassette containing the CBA (CMV immediate early enhancer/chicken β-actin) promoter or the MBP (Myelin basic protein) promoter, the woodchuck hepatitis virus post-transcriptional regulatory element (WPRE), and the bovine growth hormone polyadenylation sequence (bGHpA) flanked by AAV2 inverted terminal repeats (ITR). To enable targeted expression of the transgene in a subpopulation of cells (cells expressing Cre recombinase) a stop cassette flanked by loxP sites was integrated downstream of the CBA and MBP promoter, respectively (Guggenhuber et al., 2010). AAV1/2 mosaic viruses with equal ratios of AAV1 and AAV2 capsid proteins were generated as described previously (Hauck et al., 2003). Human embryonic kidney 293 (HEK293) cells were transfected with the AAV plasmid, the AAV1 (pH21) and AAV2 (pRV1) helper plasmids encoding AAV1 and AAV2 rep and cap genes, and the adenovirus helper plasmid (pFΔ6) by $CaPO_4$ transfection method (Klugmann et al., 2005). Cells were harvested 60 - 65 h post transfection and pelleted at 800 x g for 10 min. The pelleted cells were lysed and AAVs were purified by heparin affinity chromatography. Genomic titers were determined by quantitative real-time PCR using primers against WPRE (During et al., 2003).

### *4.4.2. TRANSDUCTION OF CELLS*

Primary cortical neurons and primary oligodendrocytes were infected with 2-5 x $10^9$ particles/ml (normally 1 µl AAVs per 6cm dish) on DIV 2. Virus titers were reproducible among different AAV preparations, so if the titer was not determined, generally 1 µl AAVs per 6cm dish was used. 3 d after infection, the complete medium was exchanged. Adequate transgene expression could be observed 7 d post transduction.

## 4.5. CELL CULTURE

All cells were cultured at 37 °C, 95% humidity and 8% $CO_2$.

### *4.5.1. PRIMARY CELLS*

#### 4.5.1.1. Mixed Neural Culture

Primary mixed neural cultures were prepared from embryonic day 15 C57/Bl6 mouse brains. First, embryos were taken out of the uterus, brains were extracted from the skull, and the meninges were removed. After digestion with 1% Trypsin in HBSS at 37 °C for 4 min and washing twice with $HBSS^+$, the brains were mechanically dissociated in 0.05% DNAse in HBSS using Pasteur pipettes with decreasing diameters. The obtained single cell suspension was washed two times with $HBSS^+$ and cells were pelleted at 130 x g and 4 °C for 10 min. Cells were seeded in DMEM 10% HS onto PLL coated culture flasks (3-3.5 x $10^7$ cells in 10 ml) or 6cm Petri dishes (1.5 x $10^7$ cells in 5 ml).

#### 4.5.1.2. Oligodendrocytes

Primary mouse oligodendrocytes (pOL) were prepared as described (Trotter and Schachner, 1989). In principal, the mixed neural cultures were prepared as described above and 5 days later the neurons were removed by a complement mediated immune cytolysis using M5 antibody (358 hybridoma supernatant, diluted 1:10) and guinea pig complement (diluted 1:15). Dead cells were washed off with DMEM 10% HS and cells were cultured in DMEM 10% HS. 2 days later the medium was changed and insulin was added (0.5 µg/ml). Another 4 days later microglia sitting on top of pOL were removed by gently shaking the culture flask and changing the medium. On day 14 after preparation microglia were removed again and pOL were shaken off the astrocyte layer by intensely shaking the culture flask. The detached pOL were spun down at 130 x g and 4 °C for 10 min and plated onto PLL coated culture dishes at a density of 1.4 – 2.1 x $10^5$ cells / $cm^2$ in Sato/B27 1% HS + PDGF (**P**latelet **D**erived **G**rowth **F**actor, 10 ng/ml) + FGF (**F**ibroblast **G**rowth **F**actor, 5 ng/ml).

#### 4.5.1.3. Cortical Neurons

Primary cortical neurons (pCN) were prepared from embryonic day 15 C57/Bl6 mouse brains. Embryos were taken out of the uterus, brains were extracted from the skull, and the meninges were removed. The cortices were dissected from the rest of the brain and the bulbi olfactorii were removed. The cortices were digested with 1% Trypsin in HBSS at 37 °C for 4 min and washed with $HBSS^{+}$. Afterwards the cortices were mechanically dissociated in 0.05% DNAse in HBSS using Pasteur pipettes with decreasing diameters. The obtained single cell suspension was washed two times with $HBSS^{+}$ and cells were pelleted at 130 x g and 4 °C for 10 min. Cells were plated onto PLL coated culture dishes in Neurobasal plating medium ($0.7 \times 10^6$ cells in 2 ml medium / 3cm dish or 6well, $2.8 \times 10^6$ cells in 5 ml medium / 6cm dish). The medium was exchanged on day 4 to Neurobasal feeding medium.

#### 4.5.1.4. Microglia

Primary mouse microglia were obtained as a side product during pOL preparation (see 4.5.1.2). The microglia containing medium was spun down at 130 x g and 4 °C for 10 min and the pelleted microglial cells were plated onto PLL coated culture dishes in DMEM 10% HS ($5 \times 10^5$ cells in 2 ml / 6well).

#### 4.5.1.5. Astrocytes

Primary mouse astrocytes were also obtained during pOL preparation (see 4.5.1.2). After oligodendrocytes had been shaken off the astrocyte layer, astrocytes were detached from the culture flask surface by incubating them for 3 min with warm (37 °C) Trypsin/EDTA and shaking them strongly off. The reaction was stopped by adding an equal amount of cold (4 °C) PBS 10% HS. Cells were pelleted at 130 x g and 4 °C for 10 min and plated onto PLL coated culture dishes in DMEM 10% HS ($3.5 \times 10^5$ cells in 2 ml / 6well).

### *4.5.2. CELL LINES*

#### *4.5.2.1.* Oli-*neu*

The oligodendroglial cell line Oli-*neu* was generated by transfer of the t-*neu* oncogene into oligodendroglial precursor cells using replication deficient retroviruses. The t-*neu* oncogene is a constitutive active form of the c-*neu* proto-oncogene, which is expressed in Oli-*neu* cells under control of the thymidine kinase promoter and keeps the Oli-*neu* cells in a proliferative state (Jung et al., 1995). Differentiation of precursor-like Oli-*neu* cells can be induced by daily treatment with 1 mM dbcAMP. Oli-*neu* cells were cultured on PLL coated culture dishes in Sato 1% HS. For passaging, cells were detached from the culture dish surface by incubation with warm (37 °C) Trypsin/EDTA. The reaction was stopped by adding an equal amount of cold (4 °C) PBS 10% HS and cells were pelleted at 130 x g and 4 °C for 10 min. For long term storage, cells were frozen in cryoprotective medium at -80 °C and stored in liquid nitrogen.

#### 4.5.2.2. HT22

HT22 is a widely used hippocampal neuronal cell line. It is a sub-line derived from parent HT4 cells that were originally immortalized from primary mouse hippocampal neuronal cultures (Liu et al., 2009). HT22 cells were cultured on PLL coated culture dishes in DMEM 10% HS. For passaging, cells were detached from the culture dish surface by incubating them with warm (37 °C) Trypsin/EDTA. The reaction was stopped by adding an equal amount of cold (4 °C) PBS 10% HS and cells were pelleted at 130 x g and 4 °C for 10 min. For long term storage, cells were frozen in cryoprotective medium at -80 °C and stored in liquid nitrogen.

#### 4.5.2.3. N2A

The mouse neuroblastoma cell line Neuro 2A (N2A) is a neural crest-derived cell line that has been extensively used to study neuronal differentiation, axonal growth and signaling pathways (Tremblay et al., 2010). N2A cells were cultured on PLL coated culture dishes in DMEM 10% HS. For passaging, the semi adherent cells were detached from the culture dish surface by flushing them with DMEM 10% HS. For long term storage, cells were frozen in cryoprotective medium at -80 °C and stored in liquid nitrogen.

## 4.6. TRANSFECTION

### *4.6.1. PLASMIDS*

Oli-*neu* or HT22 cells were transfected with plasmids by electroporation using the Bio-Rad GenePulser Xcell. 1 x $10^6$ cells in 600 µl warm (37 °C) Sato 1% HS were mixed with 10 µg plasmid DNA in a 4mm electroporation cuvette. After incubation for 5 min at room temperature the cell suspension was pulsed (exponential decay program; 220 V, 950 µF), incubated for another 5 min at room temperature, and plated onto PLL coated 6cm culture dishes. After 4 h medium was exchanged and dbcAMP (1 mM) and Sodiumbutyrate (2 mM) were added.

### *4.6.2. SIRNA*

Primary mouse oligodendrocytes were prepared according to section 4.5.1.2. 4 x $10^6$ cells in suspension were pelleted, resuspended in 100 µl nucleofector-solution and thoroughly mixed with 160 pmol siRNA. The cell-siRNA mix was transferred to an electroporation cuvette and nucleofected using program O-005 of the Lonza Nucleofector II. After nucleofection 500 µl warm (37°C) pre-equilibrated Sato/B27 1% HS + PDGF +FGF were added to the cuvette and the whole solution was plated on PLL coated 3cm culture dishes containing Sato/B27 1% HS + PDGF +FGF. 4 h post nucleofection the complete medium was exchanged with fresh Sato/B27 1% HS + PDGF +FGF.

## 4.7. IMMUNOCYTOCHEMISTRY

Cells designated for staining were cultured on PLL coated glass coverslips. All steps were performed at room temperature. First, coverslips were washed two times with PBS to remove residual medium and cell debris. Afterwards, cells were fixed for 15 min in 4% paraformaldehyde. After washing three times with PBS, cells were permeabilized with 0.1% Triton X100 in PBS for 2 min and washed again three times with PBS. Cells were then incubated in blocking solution for at least 15 min before applying the primary antibody diluted in blocking solution (dilution see table 15) for 1 h. After washing three times with PBS, the secondary antibody was added diluted in blocking solution (dilution see table 16) for 30 min. After three additional washing steps with PBS, sometimes nuclei were stained with 4'6-Diamidino-2-phenylindole (DAPI) for 2 min. Finally, the coverslips were washed three times with PBS and

briefly submerged in dd$H_2O$ to remove residual buffer salts before mounting them in moviol on object slides.

## 4.8. IMMUNOHISTOCHEMISTRY

For immunohistochemical analysis, adult mice were fixed by transcardial perfusion with 4% formaldehyde, and brains were cut into 30mm slices on a vibratome and stained according to standard protocols by our collaborators.

## 4.9. ELECTRON MICROSCOPY

Immunoelectron microscopy was performed by Wiebke Möbius (Max Planck Institute of Experimental Medicine, Göttingen, Germany) as described (Frühbeis et al., 2013a): Briefly, adult mice were fixed by perfusion with 4% formaldehyde and 0.2% glutaraldehyde (Science Services) in 0.1 M phosphate buffer containing 0.5% NaCl. Slices of spinal cord and gelatin-embedded pieces of optic nerves were infiltrated in 2.3 M sucrose in 0.1 M phosphate buffer overnight; pieces from the area of the dorsal column and optic nerve samples were mounted onto aluminum pins for ultramicrotomy and frozen in liquid nitrogen. Ultrathin cryosections were prepared using a cryo-ultramicrotome (UC6 equipped with a FC6 cryobox, Leica). Sections were incubated with primary antibodies followed by protein A-gold (15 nm) and analyzed with a LEO EM912 Omega (Zeiss). Digital micrographs were obtained with an on-axis 2048x2048-CCD camera (TRS). For quantitation of multivesicluar bodies, cryosections of optic nerves from three different animals were immunolabeled with anti-PLP and protein A-gold (10 nm). Ten large images were taken from every sample at 8000x magnification each covering an area of 11.5 µm x 11.5 µm, summing up to a total area of 1322.5 $\mu m^2$ per sample. On every image, the number, location, and labeling of MVBs were analyzed and the number of axons determined. The number of MVBs is expressed relative to the number of axons in the imaged field.
After differential centrifugation exosomes derived from 12 x $10^6$ cells were pelleted directly on a 75 meshes Ni-Grid, fixed with 4% PFA, and analyzed by electron microscopy after washes with dd$H_2O$ and embedding in 2% methylcellulose with 0.4% uranyl acetate.

## 4.10. PROTEIN BIOCHEMISTRY

### *4.10.1. CELL LYSIS*

Cells were scraped off on ice in cold (4 °C) triton lysis buffer containing Roche® Complete protease inhibitor cocktail. Lysates were incubated for 45 min at 4 °C on a rotating wheel and subsequently cleared of cellular debris and nuclei by a 300 x g centrifugation step for 10 minutes at 4 °C. Lysates were stored at –20 °C.

### *4.10.2. DETERMINATION OF PROTEIN CONCENTRATION*

If needed, protein concentrations were determined using the Bradford assay (Biorad) or BCA test (Pierce) according to the manufacturers' instructions.

### *4.10.3. SDS-PAGE*

Proteins were separated by **S**odium **D**odecyl **S**ulfate **P**olyacrylamide **G**el **E**lectrophoresis (SDS-PAGE). Stacking and separation gels with different polyacrylamide concentrations were prepared according to "Molecular Cloning – A Laboratory Manual" tables A8-9 and A8-10 (Sambrook and Russell, 2001). Preparing and running of the gels were carried out using the Bio-Rad Mini PROTEAN electrophoresis system. Alternatively, NuPAGE pre-cast gradient (4-12%) gels from Invitrogen with either MOPS or MES buffer were used according to the manufacturer's protocol. Samples were prepared by adding an appropriate amount of 4x sample buffer. To determine protein size the prestained marker Precision Plus from Bio-Rad was run on the same gels.

### *4.10.4. WESTERN BLOTTING*

After SDS-Page proteins were blotted from the gels on a **p**oly**v**inyli**d**ene **f**luoride (PVDF) membrane (Immobilon-P transfer membrane, 0,45 µm pore size, Millipore) using the Bio-Rad Mini Trans-Blot Electrophoretic Transfer Cell system for 3 hours at 300 mA or for 12 hours at 50 mA. Afterwards, the membrane was washed briefly in $dH_2O$ and incubated for at least 30 min in

blocking solution (4% milk powder in PBST) to block unspecific antibody binding to the membrane. First antibodies were applied in blocking solution overnight at 4 °C. After three washing steps (10 min each) with PBST, secondary antibodies coupled to horseradish peroxidase (HRP) were applied in blocking solution for 30 min at RT. After three additional washing steps with PBST proteins were visualized on X-Ray films (Amersham Hyperfilm ECL, GE Healthcare) by **e**nhanced **c**hemi**l**uminescence (ECL) reaction. Membranes were stored at - 20 °C to be re-blotted later on. To quantitatively analyze the detected signals hyperfilms developed with an appropriate exposure time were scanned and analyzed using the ImageJ software.

## 4.11. Isolation of Exosomes

Exosomes can be isolated from body fluids or tissue culture supernatants by differential centrifugation. The supernatants of pOL or Oli-neu cells were collected and subjected to several centrifugation steps. All steps were carried out at 4 °C. First dead cells and cell debris were removed by centrifugation for 10 min at 130 x g and for 20 min at 10000 x g, respectively. Afterwards, the supernatant was centrifuged for 1 h at 100000 x g to pellet the exosomes (crude exosomes). To better dissolve the exosome pellet from the ultracentrifugation tube, exosomes

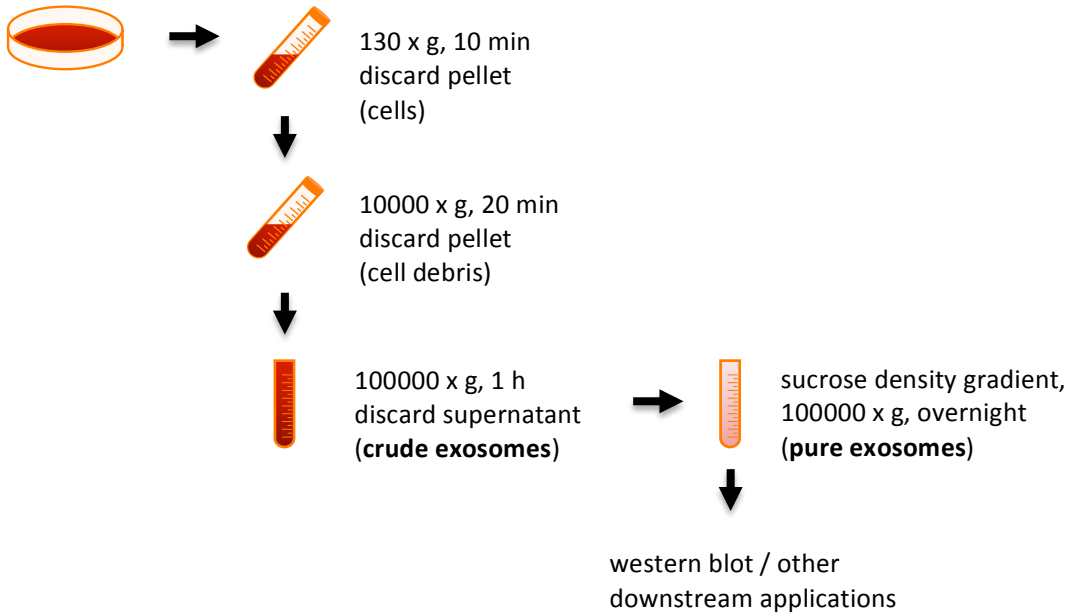


**Figure 11: Flow chart of exosome preparation.** Tissue culture supernatants of pOL and Oli-neu cells were centrifuged for 10 min at 130 x g and for 20 min at 10000 x g to get rid of dead cells and cell debris. Subsequently, exosomes were pelleted for 1h at 100000 x g. Further purification was achieved by sucrose density gradient centrifugation.

were pelleted onto a sucrose cushion (1.8 M sucrose in TBS). To further purify exosomes, the sucrose cushion containing the exosomes was loaded on top of a continuous sucrose gradient. The gradient was made by carefully overlaying equal amounts of 1.8 M sucrose with 0.3 M sucrose in an ultracentrifugation tube. After putting the tube horizontally at 4 °C the gradient was built up within 1 h by diffusion. After centrifugation overnight at 100000 x g, 12 fractions were collected from top to bottom carefully using a pipette. The density of each fraction was determined using a refractometer. Finally, the single fractions were centrifuged for 1 h at 100000 g to pellet the exosomes. Exosomes typically pellet from fractions with densities around 1.13-1.19 g/ml (pure exosomes).

## 4.12. Co-Culture Assay (Boyden Chambers)

To investigate transfer of exosomes in a more *in vivo* like situation, oligodendrocytes and neurons (or glial cultures) were co-cultured in Boyden-Chambers, which allow contact-free co-culture. While particles like exosomes can pass through the 1 µm pores of the filter membrane, whole cells cannot. Six-well companion plates (353502) and six-well cell culture inserts (353102) were obtained from BD Falcon. Either Oli-neu cells or pOL ($1.25 \times 10^6$ pOL per insert) were grown on the membrane of the inserts and subsequently co-cultured with pCN ($0.7 \times 10^6$ per well), pOL ($1.8 \times 10^6$ per well), Astrocytes ($3.5 \times 10^5$ per well), or Microglia ($5 \times 10^5$ per well). $1 \times 10^6$ Oli-neu cells were transfected with 10 µg PLP-EGFP and 10 µg Sirt2-EYFP plasmids or alternatively stained with PKH67- or PKH26-dye according to the manufacturer's protocol. 1 day post transfection/staining complete medium was exchanged and another day later co-culture with pCN (6 DIV) or HT22/N2A cells was started. After 1-2 days of co-culture, pCN were either immunocytochemically stained or lysed and analyzed by Western blotting.

pOL were either stained with PKH67- or PKH26-dye according to the manufacturer's instructions on DIV 4 or infected with AAV/MBP-HA-Cre on DIV 2 and afterwards extensively washed. In the latter case, pCN were infected with AAV/CBA-floxstop-hrGFP as reporter construct for the detection of Cre activity on DIV 2 (Guggenhuber et al., 2010). Co-culture was started when pOL and pCN were 6 DIV and lasted for 1-3 days. PKH67/PKH26 fluorescence or reporter gene expression in pCN was visualized by fluorescence microscopy or Western blotting and quantified using ImageJ.

To examine neuronal uptake of exosomes by endocytosis, pCN (6 DIV) or HT22 cells were pre-treated with inhibitors for 30 min (Dynasore, 50 or 100 µM; Pitstop2, 30 µM; CytochalasinD, 10 µM; Methyl-β-Cyclodextrin, 500 µM) and subsequently co-cultured for 24 h with pOL or Oli-neu cells as described above. HT22 transfected with the dominant negative Dynamin construct

pEGFP-DynK44A were co-cultured with Oli-neu cells ectopically expressing PLP-EGFP and Sirt2-EYFP or stained with PKH26 for 24 h. As positive control for endocytosis Alexa568-transferrin (Alexa568-Tf) was applied to HT22 cells expressing pEGFP-DynK44A and endocytosis was analyzed by fluorescence microscopy after 24 h.

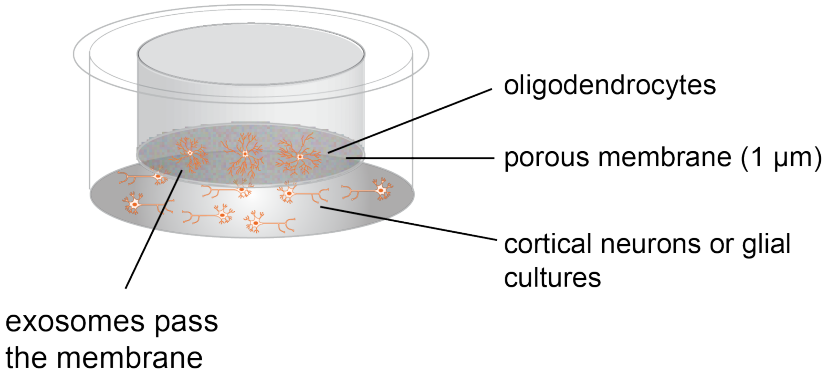


**FIGURE 12: BOYDEN CHAMBER CO-CULTURE ASSAY.** Primary oligodendrocytes or Oli-neu cells were grown on a porous membrane (1 µm pores) and co-cultured with primary cortical neurons or glial cultures (oligodendrocytes, astrocytes, microglia). Exosomes can pass the membrane while cells cannot. For analysis, the insert containing oligodendrocytes or Oli-neu cells can be removed and exosome uptake by neuronal or glial cultures can be visualized.

## 4.13. MICROFLUIDIC CHAMBERS

To discriminate between axonal or somatodendritic uptake of exosomes, microfluidic chambers with a microgroove length of 150 µm were used (Xona, standard neuron device 150 µm, Cat# SND150). pCN were plated into the device according to the manufacturer's protocol. Exosomes were prepared from pOL (7 DIV), which were either stained with PKH67 on DIV 4 or infected with AAV/MBP-HA-Cre on DIV 2. 7 days after plating pCN into microfluidic chambers, axons have grown through the microgrooves and exosomes were either applied to the somatodendritic or axonal compartment of the device. In each case the opposite compartment was filled with a larger volume creating a hydrostatic pressure, thereby fluidically isolating each chamber. In case of the addition of Cre exosomes, pCN were infected with AAV/CBA-floxstop-hrGFP as reporter construct for the detection of Cre activity 1 day after plating into the device. PKH67 fluorescence or reporter gene expression in pCN was visualized by fluorescence microscopy. For quantification of uptake efficiency, recombined hrGFP-positive pCN located with their cell bodies in an area of 100 µm above the microgrooves were counted.

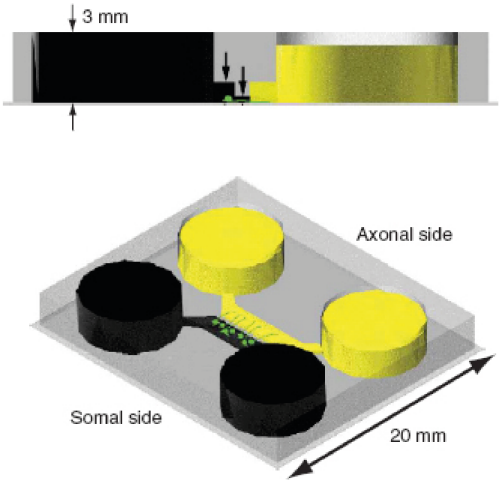


**FIGURE 13: MICROFLUIDIC CHAMBERS.** This scheme shows the principle of microfluidic isolation. The larger volume on the left side (black) creates a hydrostatic pressure between both chambers thereby fluidically isolating the right chamber (yellow). Modified after Xona Microfluidics LLC, Temecula, USA.

## 4.14. STEREOTACTIC INJECTION OF EXOSOMES

Stereotactic injection was performed in collaboration with Anja Schneider (Department of Psychiatry and Psychotherapy, University of Göttingen, Germany) and Mikael Simons (Max Planck Institute of Experimental Medicine, Göttingen, Germany) as described (Frühbeis et al., 2013a): 2-5 month old male and female ROSA26-lacZ reporter mice were anesthetized with ketamine and xylazin and placed in a stereotactic frame. Exosomes prepared from AAV/MBP-HA-Cre infected pOL (Infection: DIV 2; exosome preparation DIV 8 and 11) dissolved in PBS were injected in the right hippocampus (coordinates in relation to bregma: anteroposterior 1.8 mm, mediolateral 1.8 mm, dorsoventral 1.8 mm) and cerebellum (coordinates: anteroposterior 6.2 mm, mediolateral 2.0 mm, dorsoventral 2.0 mm). As a control, exosomes prepared from uninfected pOL were injected. A volume of 2 µl was injected using a glass microcapillar and a motorized injection pump (World Precision Instruments) at a constant flow rate of 250 nl/min starting 120 s after injection. To limit fluid reflux along the injection track, the needle was kept in place for additional 5 min after injection. Mice were sacrificed 14 d after injection and perfused with PFA. Brains were vibratome cut (30 µm slices). LacZ and immunofluorescence staining was performed according to standard protocols.

## 4.15. MULTI-ELECTRODE ARRAY

Multi-electrode arrays (MEA) were performed in collaboration with Jyh-Jang Sun and Heiko Luhmann (Institute of Physiology, Johannes Gutenberg-University, Mainz, Germany). Primary cortical neurons were prepared from embryonic day 15 C57/Bl6 mouse brains as described above and plated on 6-well MEA chips (2 x $10^5$ cells per well). Each well contained 9 electrodes at the bottom. Experiments were performed at DIV 14 to allow the cultures to differentiate and establish neuronal circuits and electrical activity. At DIV 14 exosomes derived from 6-10 x $10^6$ primary oligodendrocytes (7 DIV) were prepared as described above (crude exosomes), resuspended in 25 µl Neurobasal feeding medium, and applied to one well pCN. As a control, 25 µl Neurobasal feeding medium alone was applied. Recording of the electrical activity was started one hour before exosome treatment and lasted at least 12 hours. Results were only taken in account if 3 or more electrodes were active during recording. Firing rate, relative burst index, and spike amplitude were analyzed.

## 4.16. MICROARRAY

Microarrays were performed in collaboration with Sheena Pinto and Bruno Kyewski (Deutsches Krebsforschungszentrum (DKFZ), Heidelberg, Germany). pOL and pCN were prepared and co-cultured in Boyden chambers for 2 days as described above. 4 individually prepared primary neuronal cultures were either co-cultured with pOL or with empty inserts containing exosome depleted conditioned pOL medium as control (-> 8 different samples, n = 4). After co-culture, RNA was prepared from pCN using the Quiagen miRNeasy mini Kit according to the manufacturer's protocol including on column DNA digestion. Sample preparation for the microarrays was done using the Illumina® TotalPrep RNA Amplification Kit including oligo dT primers for cDNA synthesis. For measuring gene expression, the commercial BeadArray Mouse v2 microarray platform from Illumina was used. Data processing and analysis was performed by Jörn Tödling (Institute of Molecular Biology (IMB), Mainz, Germany).

# 5. RESULTS

## 5.1. PERIAXONAL LOCALIZATION AND FUSION OF MVBS

MVBs are endosomal structures generated by inward budding of the limiting membrane of late endosomes. Fusion of MVBs with the plasma membrane results in release of the intraluminal vesicles as exosomes. Immunoelectron analysis of cross-sections of myelinated fibers in the spinal cord and the optic nerve showed a predominant localization of MVBs in the adaxonal loop, the innermost uncompacted wrapping of the myelin sheath (Fig. 14 A-C). The adaxonal loop is in direct neighborhood to the axon, so fusion of MVBs with the plasma membrane results in release of the intraluminal vesicles (exosomes) into the periaxonal space, where they are available for

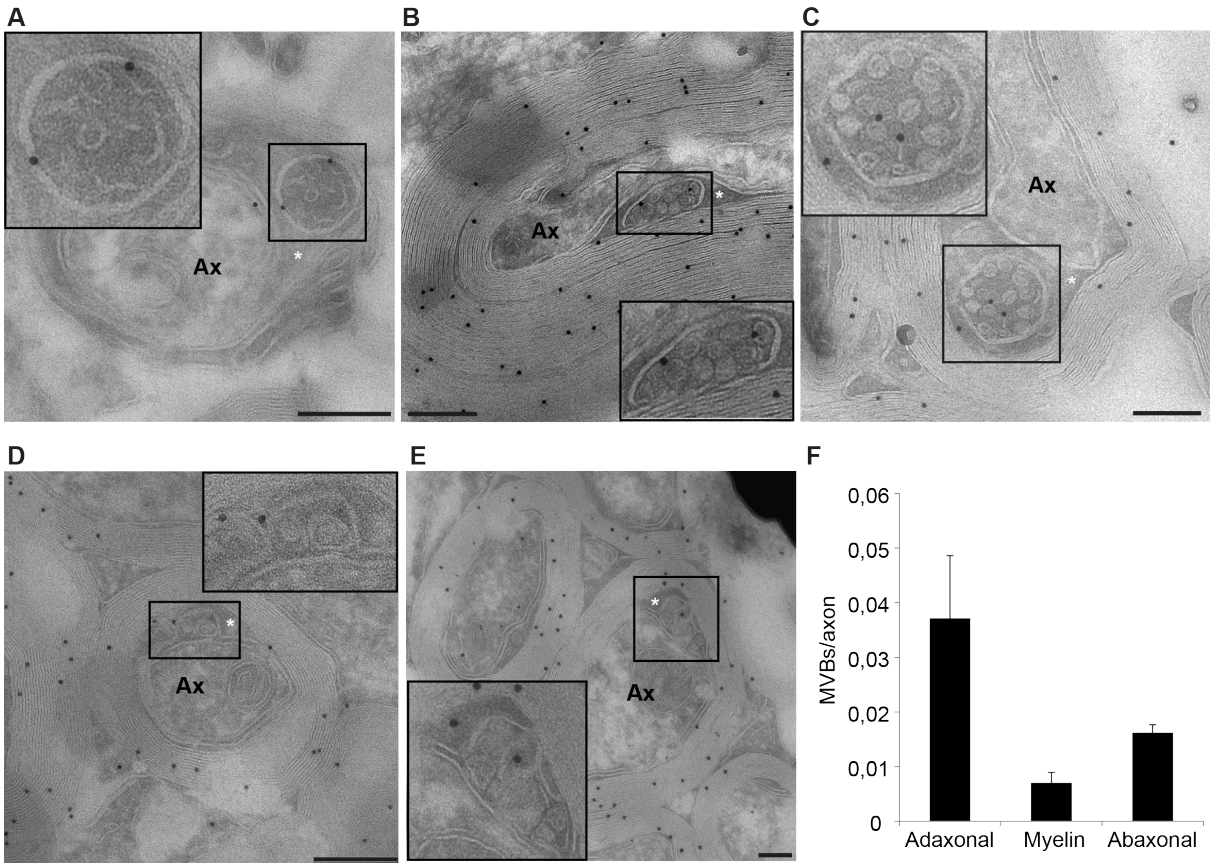


**FIGURE 14: ADAXONAL LOCALIZATION AND FUSION PROFILES OF MVBS.** (A-E) Immunoelectron microscopic analysis of spinal cord (A, D, and E) and optic nerve (B and C) cross-sections labeled with antibodies against Lamp1 (A), PLP (B-D), and Sirt2 (E). Pictures show the adaxonal localization of MVBs (A-C) and potential fusion profiles of MVBs with the plasma membrane resulting in release of vesicles with the typical size of exosomes (D and E) (scale bar: 200 nm; asterisk marks the adaxonal loop). (F) Quantification of MVBs located adaxonally, abaxonally, or within compact myelin in optic nerve cross-sections normalized to axon number. Analysis was performed by Wiebke Möbius (Max Planck Institute of Experimental Medicine, Göttingen, Germany).

axonal uptake (Fig. 14 D and E). Immunogold labeling of the cross-sections revealed that MVBs are positive for Lamp1 (Fig. 14 A; indicating their endosomal origin) and PLP (Fig. 14 B-D; indicating their oligodendroglial origin). The intraluminal vesicles carried immunolabeling of PLP (Fig. 14 B-D) and Sirt2 (Fig. 14 E). Quantification of MVBs in cross-sections of the optic nerve showed a prevalent localization within adaxonal loops compared to channels within the compact myelin or the outermost abaxonal loops (Fig. 14 F).

## 5.2. Uptake of Oligodendroglial Exosomes by Neural Cells

Since MVBs and fusion profiles can be observed *in vivo* (Fig. 14) and oligodendroglial exosome secretion is triggered by neuronal glutamate (Frühbeis et al., 2013a), we asked whether exosomes are internalized by neurons and other neural cells. To answer the question, primary oligodendrocytes (pOL) stained with the lipophilic dye PKH67 were co-cultured in Boyden chambers for 2 d either with mixed neural cultures (Fig. 15 A and B), or with cultures of primary cortical neurons (pCN, Fig. 15 C and 16), microglia, oligodendrocytes, or astrocytes (Fig. 16).

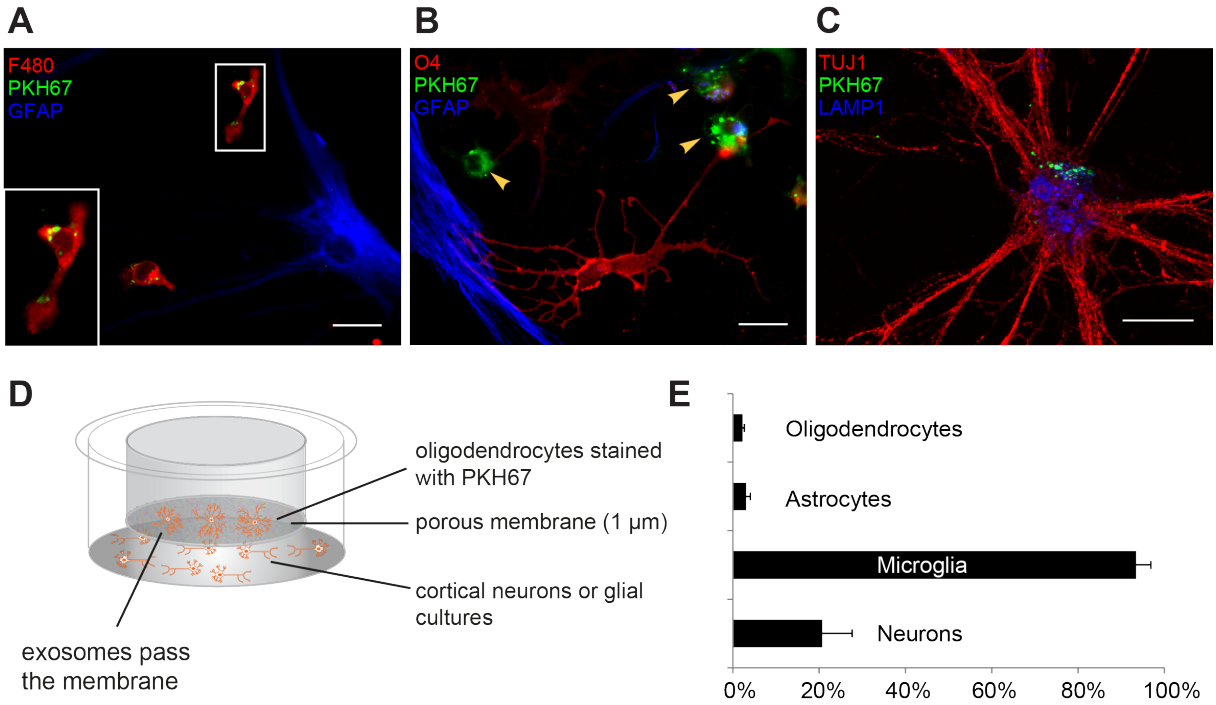


**Figure 15: Cell-Type Dependent Uptake of Oligodendroglial Exosomes.** (A-D) pOL stained with the lipophilic dye PKH67 were co-cultured in Boyden chambers for 2 d either with mixed neural cultures containing astrocytes (A and B, blue marker GFAP), oligodendrocytes (B, red marker O4), and microglia (A, red marker F480; B, arrowheads), or with pCN cultures (C, red marker Tuj1). PKH67 labeled oligodendroglial exosomes are displayed in green. Scale bar, 20 µm. (E) Quantification of exosome uptake by the different target cells normalized to total cell type number. Error bars, SEM, n = 3.

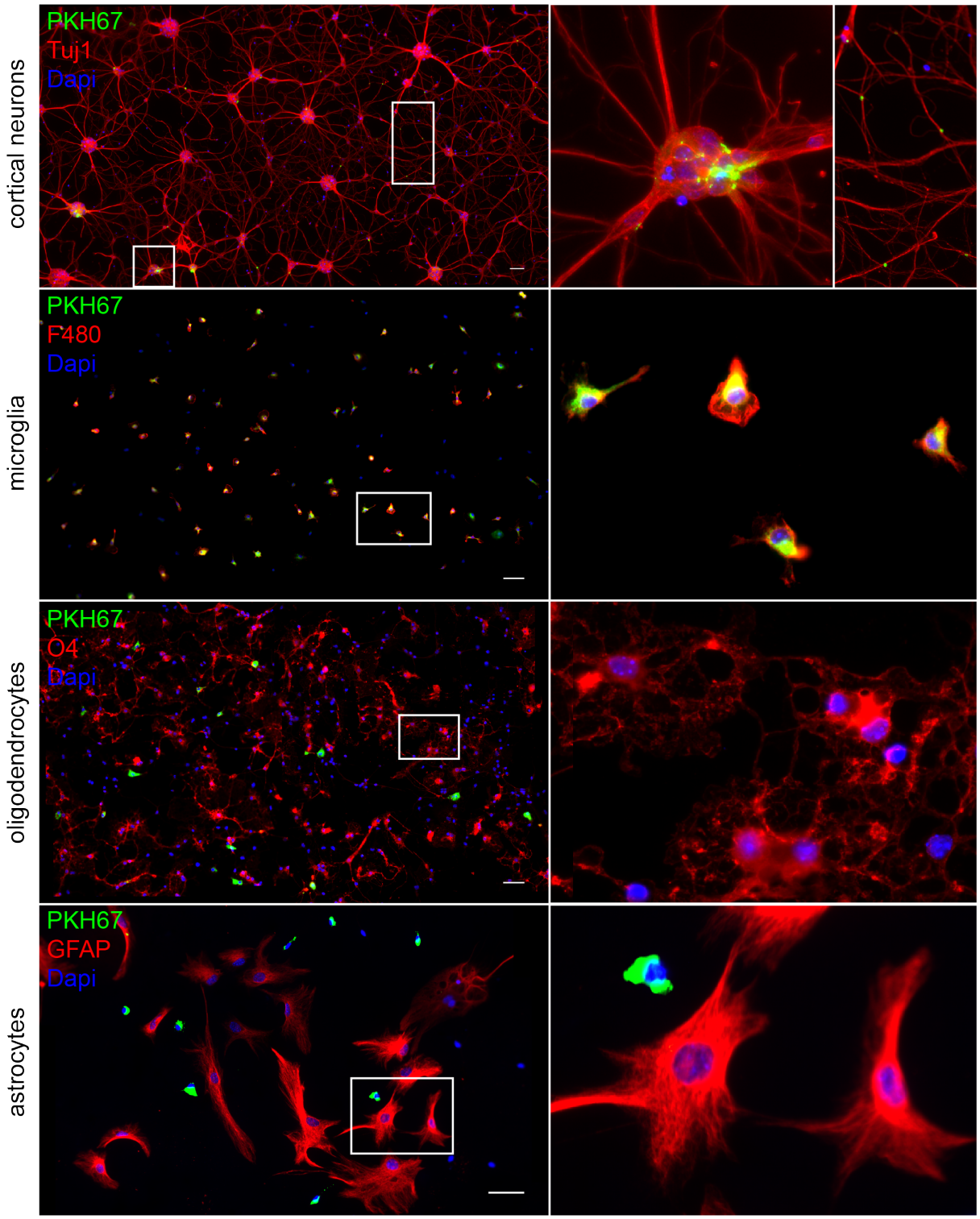


**Figure 16: Uptake of Oligodendroglial Exosomes by Neural Cells.** pOL stained with the lipophilic dye PKH67 were co-cultured in Boyden chambers for 2d with cortical neurons, microglia, oligodendrocytes, or astrocytes. Neurons were immunostained for Tuj1, microglia for F480, oligodendrocytes for O4, and astrocytes for GFAP (all markers are displayed in red). PKH67 labeled exosomes are shown in green. Nuclei were stained with Dapi (blue). Scale bar, 50 µm.

Boyden chambers allow contact free co-culture and subsequent, individual analysis of the co-cultured cells. PKH67 stained primary oligodendrocytes were grown in the top chamber on a membrane containing 1 µm pores that allow passage of exosomes. PKH67 is a lipophilic dye, which is incorporated into endosomes and released in association with exosomes (Fig. 19 B) (Pegtel et al., 2010). In order to visualize cell-type dependent uptake of fluorescently labeled exosomes, the cultures in the bottom chamber were immunocytochemically stained with cell-type specific markers and the frequency of uptake was quantified. Oligodendroglial exosomes were preferentially internalized by cortical neurons (20.7 ± 7%) and microglia (93.4 ± 3.5%), while uptake by astrocytes and oligodendrocytes was only marginal (3 ± 1% and 2.2 ± 0.4%, respectively), suggesting target cell selectivity of oligodendrocyte-derived exosomes in the CNS (Fig. 15 E).

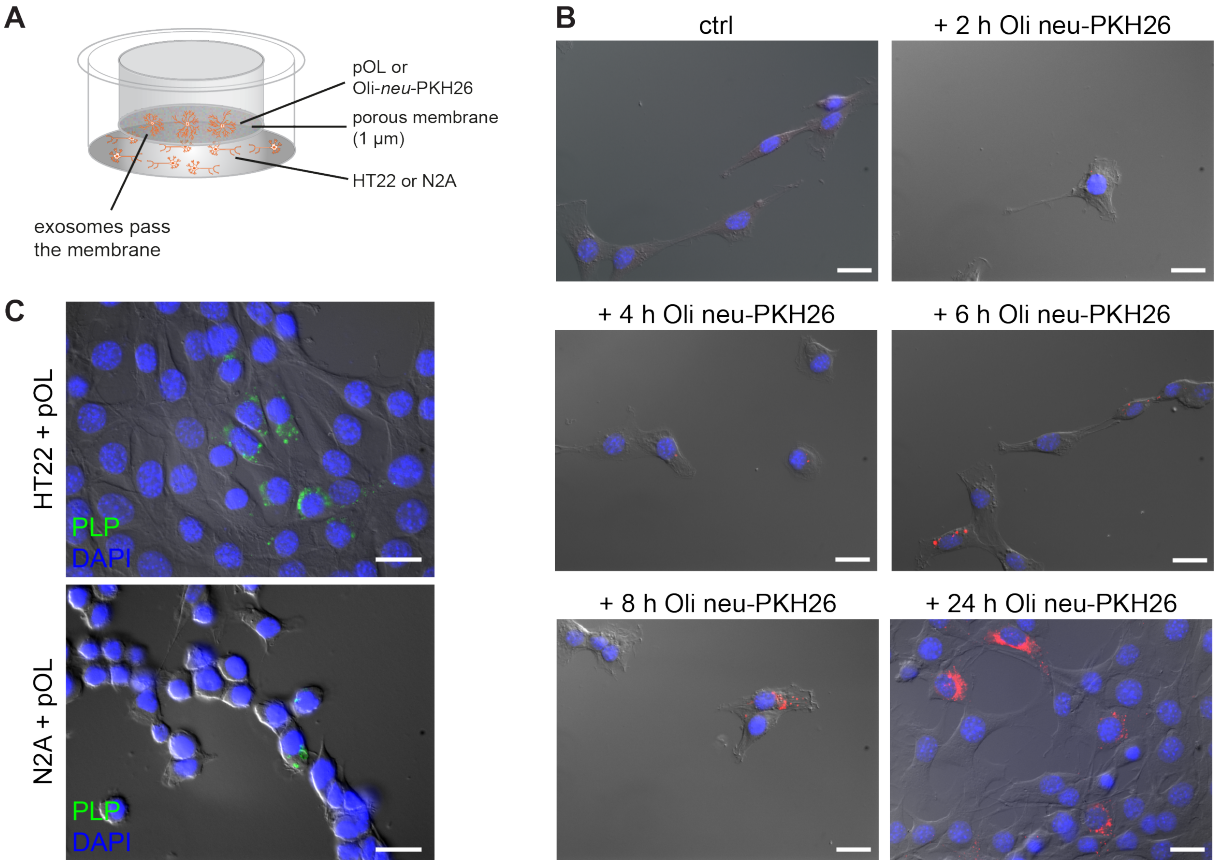


**FIGURE 17: UPTAKE OF OLIGODENDROGLIAL EXOSOMES BY THE NEURONAL CELL LINES HT22 AND N2A AFTER CO-CULTURE.** (A) Boyden chamber co-culture of HT22 or N2A cells with pOL or Oli-*neu* cells. (B) Co-culture of HT22 cells with PKH26-stained Oli-*neu* cells for 2, 4, 6, 8, or 24 h. DIC images are shown. PKH26-positive exosomes are displayed in red; nuclei were stained with DAPI (blue). Scale bar, 20 µm. (C) Co-culture of HT22 or N2A cells with pOL for 24 h. DIC images are displayed. Exosomal PLP is shown in green; nuclei were stained with DAPI (blue). Scale bar, 20 µm.

## 5.3. UPTAKE OF OLIGODENDROGLIAL EXOSOMES BY NEURONAL CELL LINES

Focusing on neuronal uptake, we tested whether other neuronal subtypes also internalize oligodendroglial exosomes. The hippocampal cell line HT22 and the neuroblastoma cell line N2A were used in the Boyden chamber co-culture assay (Fig. 17 A). HT22 as well as N2A cells internalized primary oligodendrocyte-derived exosomes after co-culture for 24 h (Fig. 17 C). The transfer of oligodendroglial exosomes was visualized by immunocytochemical staining of the oligodendrocyte specific protein PLP internalized by HT22 and N2A cells. Additionally, exosomes derived by PKH26-labeled Oli-*neu* cells were efficiently internalized by HT22 cells and accumulated in the neuronal cell body over time (Fig. 17 B). However, uptake of oligodendroglial exosomes by HT22 cells was more efficient than uptake by N2A cells (Fig 17 C).

## 5.4. UPTAKE OF OLIGODENDROGLIAL EXOSOMES BY NEURONS

To test whether the observed transfer can indeed be attributed to exosomes, primary cortical neurons were incubated with purified oligodendroglial exosomes. Oligodendrocytes release constitutively and after glutamate stimulation exosomes of characteristic size and morphology (Fig. 18 A). Moreover, these exosomes migrate on a sucrose density gradient at typical densities and are positive for exosomal marker proteins like Tsg101 (Fig. 18 B). Incubation of primary cortical neurons with purified exosomes from the oligodendroglial cell line Oli-*neu* ectopically expressing the fluorescently tagged proteins Sirt2-EYFP and PLP-EGFP resulted in uptake of fluorescent particles (Fig. 18 B). Both proteins are part of oligodendroglial exosomes (Fig. 18 B) (Krämer-Albers et al., 2007). While PLP is located in the exosomal membrane, the cytosolic protein Sirt2 is contained within the lumen of exosomes. The uptake of oligodendroglial exosomes by primary cortical neurons occurred in a time dependent manner, since longer incubation times resulted in an increased uptake of exosome-associated Sirt2-EYFP and PLP-EGFP (Fig. 18 C). Importantly, treatment of neurons with the protease Trypsin before lysis in order to remove surface bound exosomes did not alter the uptake pattern, indicating that exosomes were indeed internalized and not just sticking at the cell surface (Fig. 18 D).

As shown before (Fig. 15 C and 16), the transfer of oligodendroglial exosomes to neurons can be visualized after Boyden chamber co-culture. Primary oligodendrocytes stained with the lipophilic dye PKH67 incorporate the dye into endosomes (Fig. 19 B) and subsequently release PKH67-labeled exosomes, which are in turn internalized by primary cortical neurons (Fig. 19 C). To demonstrate that the observed neuronal uptake in this assay is dependent on exosomes and not due to other membrane fragments, we either interfered with or increased exosome secretion

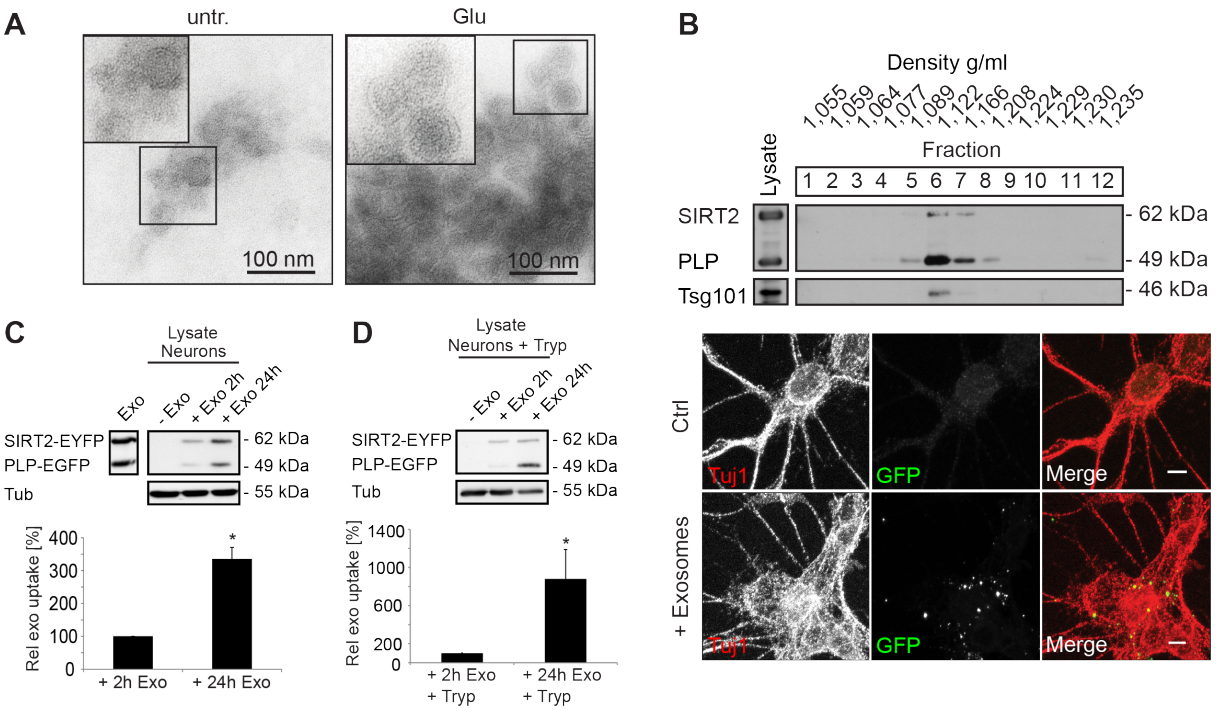


**FIGURE 18: UPTAKE OF PURIFIED OLIGODENDROGLIAL EXOSOMES BY PRIMARY CORTICAL NEURONS.** (A) Electron microscopic pictures of crude exosome preparations from culture supernatants of pOL collected over 5 h from either untreated (left) or glutamate stimulated (right) cells. Scale bar, 100 nm. (B) Fluorescent exosomes were purified by sucrose density gradient centrifugation from Oli-*neu* cells transiently expressing Sirt2-EYFP and PLP-EGFP. Western Blot indicates Sirt2-EYFP and PLP-EGFP together with the exosomal marker Tsg101 in the typical exosomal fractions. Images below show maximum projections of confocal Z-stacks after incubation with purified exosomes for 24 h (GFP, green). pCN were stained for Tuj1 (red). Scale bar, 5 µm. (C) Western blot of purified Oli-*neu* exosomes (left lane) and neuronal lysates after treatment with these exosomes for 2 and 24 h, respectively. Exosomes are loaded with Sirt2-EYFP and PLP-EGFP, Tubulin (Tub) is used as normalization standard. Relative exosome uptake is calculated as the Sirt2-EYFP/PLP-EGFP signal normalized to Tub (n=8). (D) Same experimental setting as in (C) but surface bound exosomes were removed by Trypsin (Tryp) treatment before lysis (n=5). Error bars, SEM (* $p<0.05$; Wilcoxon-test).

from oligodendrocytes. It has been shown previously that GW4869, an inhibitor of the neutral sphingomyelinase, interferes with exosome release in Oli-*neu* cells (Trajkovic et al., 2008). Application of GW4869 to Oli-*neu* cells significantly reduced the amount of released exosomes and thus the amount of exosomes internalized by primary cortical neurons (Fig. 19 D), validating that exosomes were indeed responsible for the horizontal transfer of oligodendroglial proteins to neurons. Consistently, stimulation of exosome release from primary oligodendrocytes with glutamate significantly increased the release and therefore the uptake of oligodendroglial exosomes by primary cortical neurons (Fig. 19 E). The proteins PLP/DM20 and Sirt2, endogenously expressed by oligodendrocytes, were transferred to primary cortical neurons after Boyden chamber co-culture. Intriguingly, the transfer of oligodendroglial proteins by the means of exosomes seems to be selective, since Hsc70-EGFP overexpressed in Oli-*neu* cells is delivered to neurons while untagged EGFP is not (Fig. 19 F).

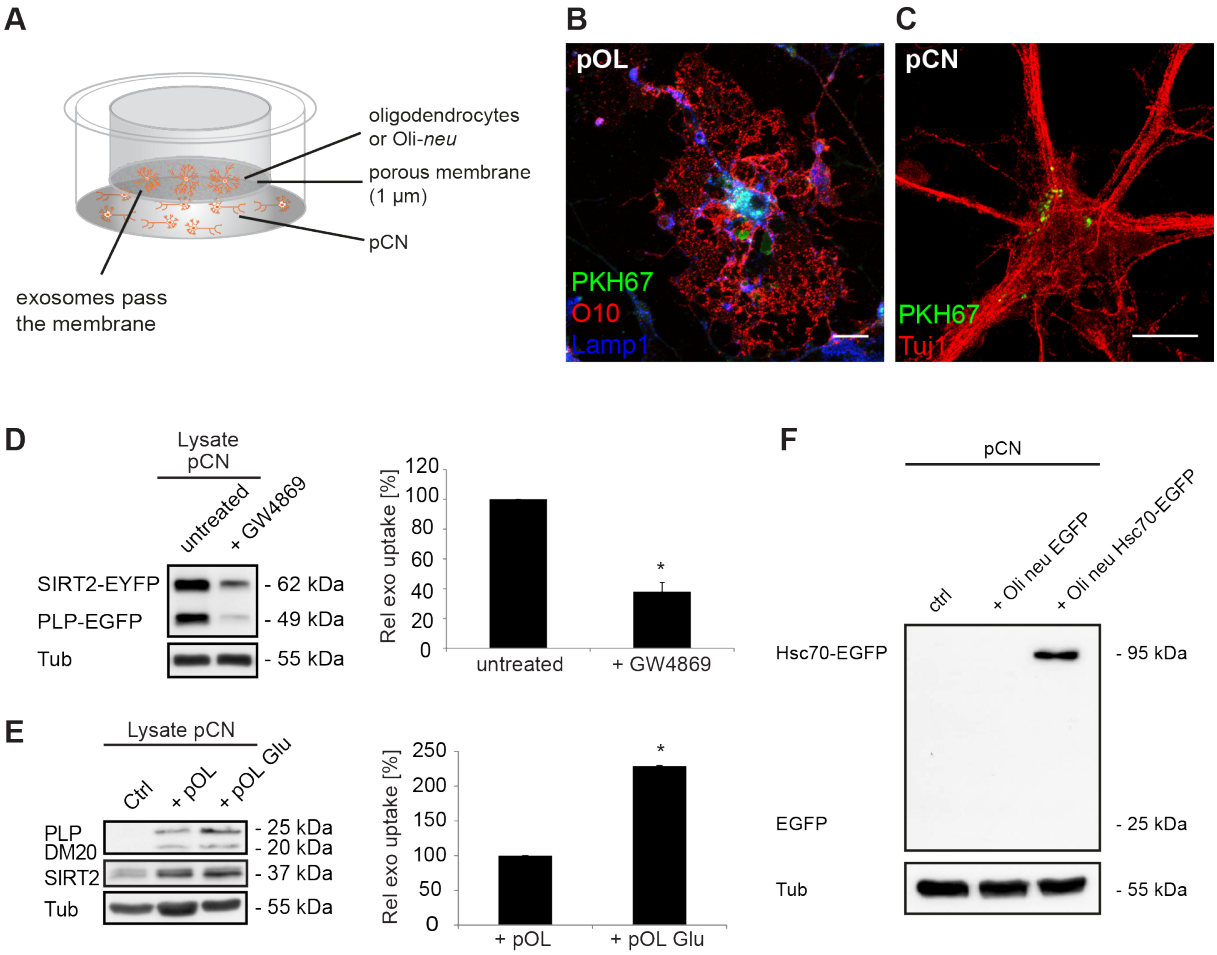


**FIGURE 19: NEURONAL UPTAKE OF OLIGODENDROGLIAL EXOSOMES AFTER CO-CULTURE.** (A) Illustration of Boyden chamber co-culture setup. (B) pOL stained with PKH67 (green), oligodendroglial marker O10 (red) and late endosomal/lysosomal marker Lamp1 (blue). Scale bar, 20 µm. (C) pCN after co-culture with PKH67-stained pOL for 2 d. Transferred exosomes are labeled with PKH67 (green), pCN were stained with Tuj1 (red). Scale bar, 20 µm. (D-E) Western blot analysis of the exosomal proteins Sirt2 and PLP in pCN lysates after co-culture with Oli-*neu* (D) or pOL (E) for 2 d. Tubulin (Tub) was used as normalization standard. Error bars, SEM (* $p<0.05$; Wilcoxon-test). (D) Sirt2-EYFP and PLP-EGFP expressing Oli-*neu* cells were treated or not with 5 µM GW4869 inhibiting exosome release (n=6). (E) pOL were treated with 100 µM glutamate stimulating exosome release (n=5). (F) Co-culture of pCN with Oli-*neu* cells expressing Hsc70-EGFP or EGFP for 2 d.

## 5.5. NEURONAL UPTAKE OF OLIGODENDROGLIAL EXOSOMES BY ENDOCYTOSIS

To determine the neuronal uptake mechanism and the subcellular destination of internalized exosomes, primary cortical neurons were stained for endocytic markers after Boyden chamber co-culture with PKH67-labeled primary oligodendrocytes. Exosomes accumulated in Lamp1-positive late endosomal/lysosomal compartments (Fig. 20 A) and 3D reconstruction of a confocal Z-stack indicated that exosomes were indeed located within these structures (Fig. 20 B).

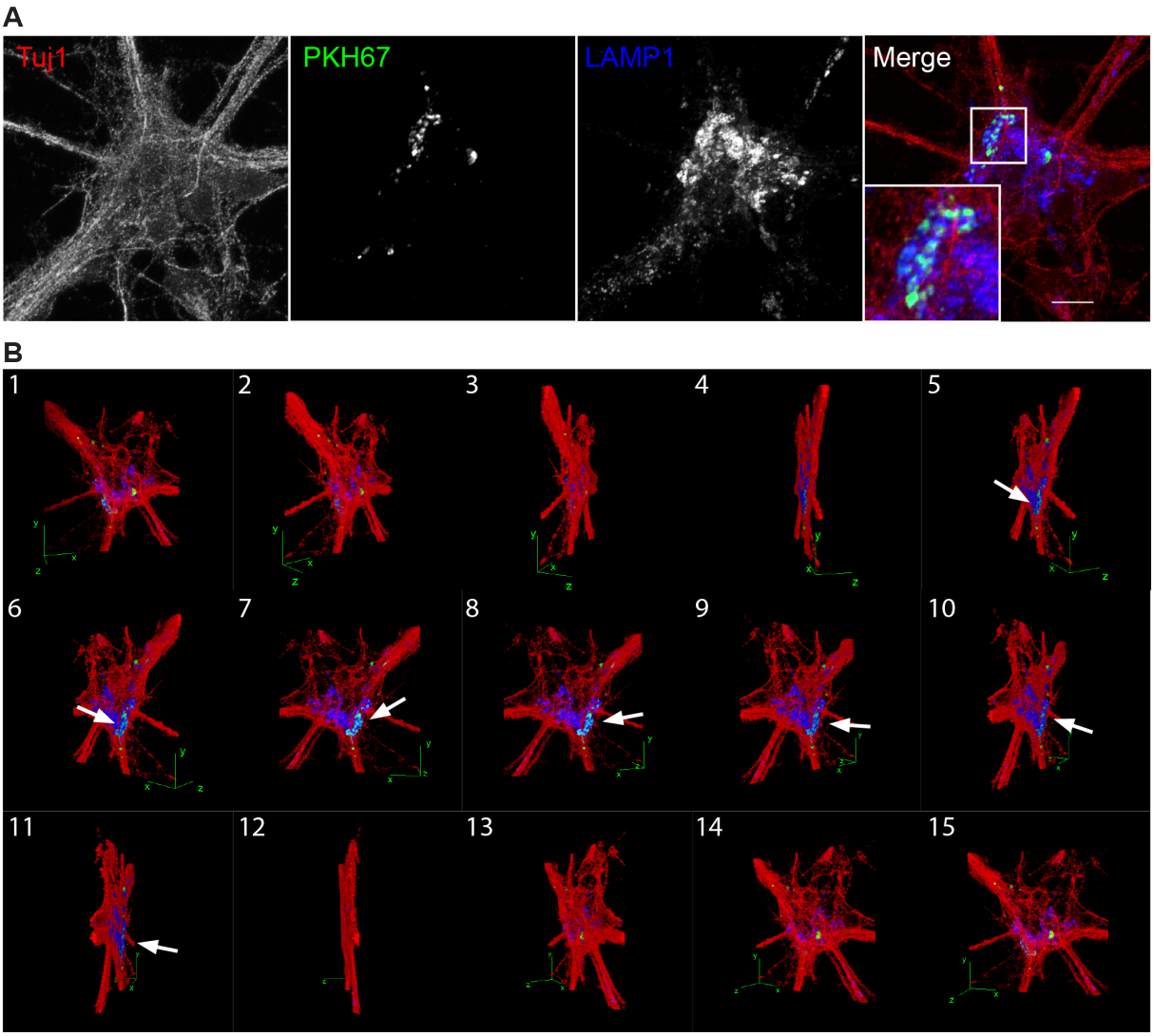


**FIGURE 20: OLIGODENDROGLIAL EXOSOMES ACCUMULATE IN LATE ENDOSOMAL STRUCTURES.** (A and B) Boyden chamber co-culture of pCN with PKH67-labeled pOL (green). pCN were immunostained for Tuj1 (red) and the late endosomal/lysosomal marker Lamp1 (blue). (A) Maximum projection of a confocal Z-stack. Scale bar: 10 µm. (B) 3D reconstruction of the same confocal Z-stack shown from different angles. Arrows indicate the localization of the exosomes in the late endosomal compartment.

To validate that neuronal exosome uptake occurs via endocytosis and furthermore, to identify the exact endocytosis mechanism, different endocytosis inhibitors were applied to HT22 cells in the Boyden chamber co-culture assay. While Dynasore is an inhibitor of dynamin dependent endocytosis (Macia et al., 2006), Pitstop2 selectively blocks clathrin mediated endocytosis (von Kleist et al., 2011). Pre-treatment of HT22 cells with both inhibitors strongly interfered with the uptake of Oli-*neu*-derived exosomes (Fig. 21 A-C). Dynasore reduced the amount of internalized exosomes by 82 ± 11% and Pitstop2 by 76 ± 5%. Furthermore, inhibition of actin polymerization by pre-treatment with CytochalasinD also resulted in a strong reduction of exosome uptake (96 ±1 %; Fig. 21 A-C). Contrary, interfering with cholesterol-dependent (clathrin-independent)

endocytosis by depriving cholesterol from the plasma membrane using Methyl-β-Cyclodextrin (MβCD) had no significant influence on neuronal exosomal uptake (Fig. 21 A-C). Notably, application of the inhibitors did not influence the amount of released exosomes, indicating that the observed effect is indeed due to inhibition of neuronal endocytosis (Fig. 21 D).

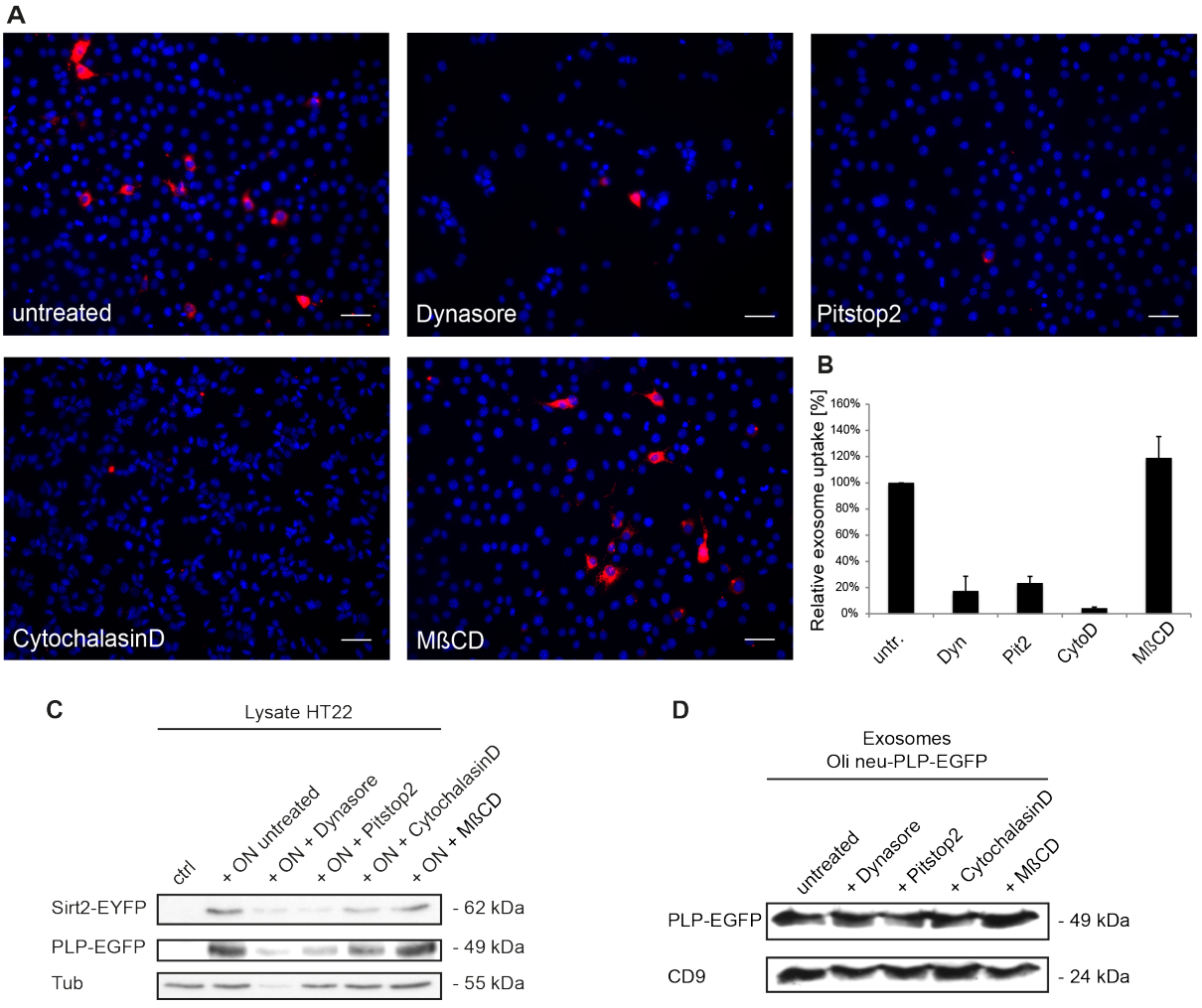


**FIGURE 21: HT22 CELLS INTERNALIZE OLIGODENDROGLIAL EXOSOMES BY ENDOCYTOSIS.** (A-C) HT22 cells were pre-treated with endocytosis inhibitors (Dynasore, 100 µM; Pitstop2, 30 µM; CytochalasinD, 10 µM; Methyl-β-Cyclodextrin (MβCD), 500 µM) for 30 min and subsequently co-cultured in Boyden chambers with Oli-*neu* cells stained with PKH26 (A and B) or ectopically expressing Sirt2-EYFP and PLP-EGFP (C) for 24 h. (A and B) The relative exosome uptake was quantified as the signal-intensity of internalized PKH26-positive exosomes (red) normalized to total cell number (DAPI, blue). Scale bar, 50 µm; n=2; error bars, SEM. (C) Western blot of neuronal lysates after co-culture. (D) Oli-*neu* cells ectopically expressing PLP-EGFP were treated with endocytosis inhibitors (same concentrations as in A-C) and after 24 h exosomes were purified from the supernatants and analyzed by Western blotting for the presence of the exosomal markers PLP-EGFP and CD9.

To test whether similar uptake mechanisms are also responsible for the internalization of oligodendroglial exosomes by primary cortical neurons the same inhibitors as described above were used. Primary cortical neurons pre-treated with Dynasore were co-cultured in Boyden

chambers either with primary oligodendrocytes labeled with PKH67 (Fig. 22 A) or with Oli-*neu* cells ectopically expressing Sirt2-EYFP and PLP-EGFP (Fig. 22 B). Dynasore strongly interfered with exosome-uptake in primary cortical neurons (Fig. 22 A). Moreover, the effect was dependent on the applied doses. While 50 µM Dynasore decreased the amount of internalized exosomes by 37 ± 2%, application of 100 µM Dynasore resulted in a decrease of 64 ± 1.7% (Fig. 22 B). Furthermore, inhibition of clathrin-mediated endocytosis by Pitstop2 and inhibition of actin polymerization with CytochalasinD reduced exosome uptake in primary cortical neurons by 51 ± 9% and 35 ± 15%, respectively (Fig. 22 C). Similar to HT22 cells, Methyl-β-Cyclodextrin (MβCD) did not inhibit exosome uptake by primary cortical neurons (Fig. 22 C).

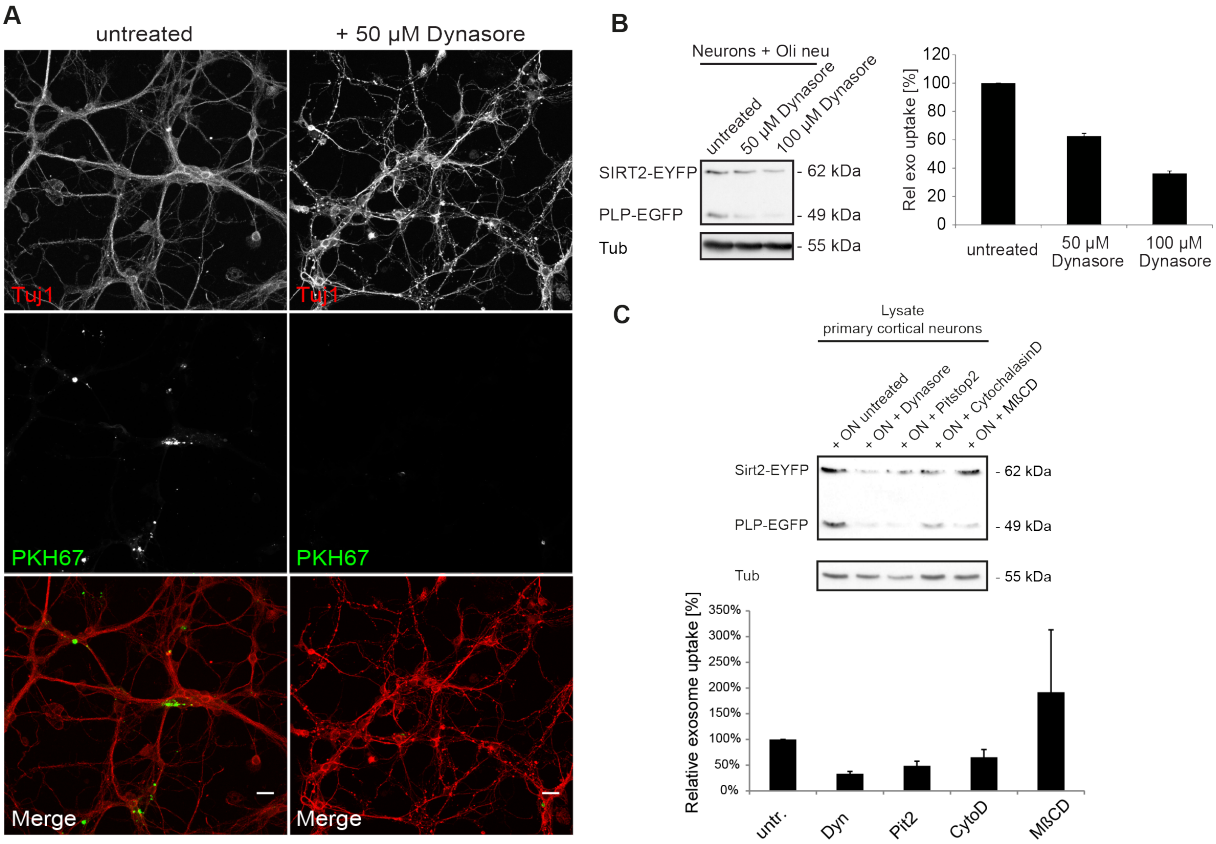


**FIGURE 22: PRIMARY CORTICAL NEURONS INTERNALIZE OLIGODENDROGLIAL EXOSOMES BY ENDOCYTOSIS.** (A) Boyden chamber co-culture of PKH67-labeled pOL (green) with pCN treated or not with 50 µm Dynasore for 24 h. pCN were stained for Tuj1 (red). The maximum projection of a confocal Z-stack is depicted. Scale bar, 20 µm. (B and C) Western blot of pCN lysates after co-culture with Oli-*neu* cells ectopically expressing Sirt2-EYFP and PLP-EGFP. pCN were pre-treated with 50 and 100 µM Dynasore, respectively (B; n=4) or with different endocytosis inhibitors (C; n= 3; Dynasore, 100 µM; Pitstop2, 30 µM; CytochalasinD, 10 µM; Methyl-β-Cyclodextrin (MβCD), 500 µM) for 30 min before co-culture for 24 h. The relative exosome uptake is calculated as the densitometric signal of exosomal Sirt2-EYFP and PLP-EGFP normalized to neuronal tubulin (Tub). Error bars, SEM.

In line with the results obtained from endocytosis inhibitor experiments, expression of the dominant negative dynamin construct DynK44A in HT22 cells markedly reduced the uptake of

PKH26-labeled Oli-*neu*-derived exosomes (Fig. 23 A and B). In the DynK44A construct, the amino acid 44 is mutated from a lysine to an alanine abolishing the functionality of dynamin in endocytosis. The dominant-negative action of this dynamin mutant was validated by uptake inhibition of Alexa568-conjugated transferrin (Fig. 23 A, right panel). Quantification of internalized PKH26-labeled exosomes revealed a robust inhibition of exosome uptake by 79 ± 9% (Fig 23 B). Similar results were obtained after co-culture of HT22 cells expressing DynK44A with Oli-*neu* cells ectopically expressing Sirt2-EYFP and PLP-EGFP. Expression of dominant negative dynamin interferes with the exosome-mediated transfer of Sirt2-EYFP and PLP-EGFP (Fig. 23 C). Taken together, these results indicate that neurons internalize oligodendroglial exosomes by dynamin and clathrin dependent endocytosis involving actin polymerization.

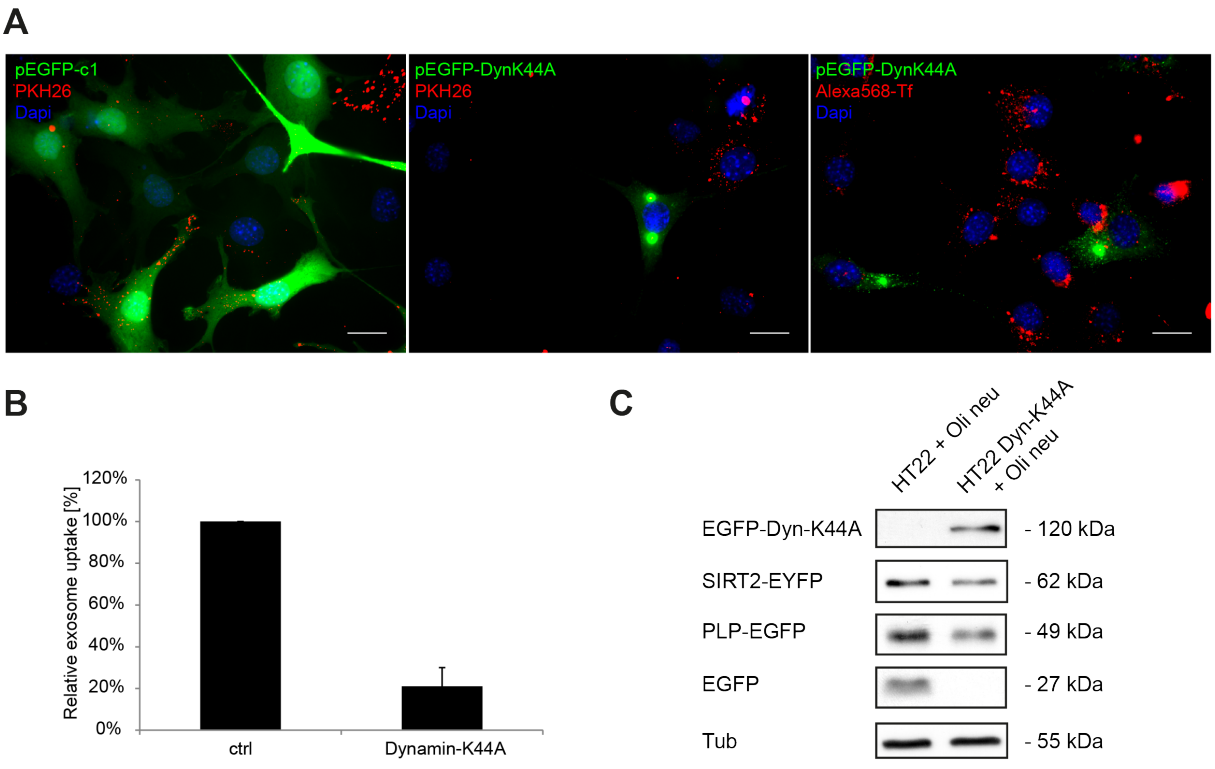


**Figure 23: Oligodendroglial Exosomes are Internalized by Dynamin Dependent Endocytosis.** (A) HT22 cells either expressing dominant negative dynamin (pEGFP-DynK44A; green) or EGFP as control (pEGFP-c1; green) were co-cultured with Oli-*neu* cells stained with PKH26 (exosomes are displayed in red) for 24 h. To visualize the endocytosis blocking function of pEGFP-DynK44A, HT22 cells were incubated with Alexa568-conjugated transferrin (Alexa568-Tf; red). Nuclei were stained with DAPI (blue). Scale bar, 20 µm. (B) Relative exosome uptake was quantified as the amount of internalized PKH26-postive exosomes normalized to total cell number (n=3; Error bars, SEM). (C) HT22 cells expressing pEGFP-DynK44A or pEGFP-c1 were co-cultured with Oli-*neu* cells ectopically expressing Sirt2-EYFP and PLP-EGFP in Boyden chambers for 24 h and subsequently, lysates of the HT22 cells were analyzed by Western blotting using antibodies against GFP and Tubulin (Tub).

## 5.6. FUNCTIONAL RETRIEVAL OF EXOSOMAL CARGO *IN VITRO* AND *IN VIVO*

Since neuronal exosome uptake occurs via clathrin and dynamin dependent endocytosis and internalized exosomes accumulate in late endosomal compartments, exosomal cargo may end up in lysosomes for degradation. Alternatively, exosomes may back-fuse with the endosomal membrane resulting in release of exosomal components, e.g. proteins and RNAs into the cytoplasm. After recovery from the endosomal system, the exosomal cargo may exhibit distinct functions in the target cell. To follow the fate of exosomal components after internalization of oligodendroglial exosomes, we employed the Cre-loxP system. Transfer of Cre recombinase-containing exosomes from oligodendrocytes to neurons and subsequent release of Cre recombinase from the internalized exosomes would lead to reporter gene recombination and reporter expression in the recipient cell. Therefore, primary oligodendrocytes were transduced

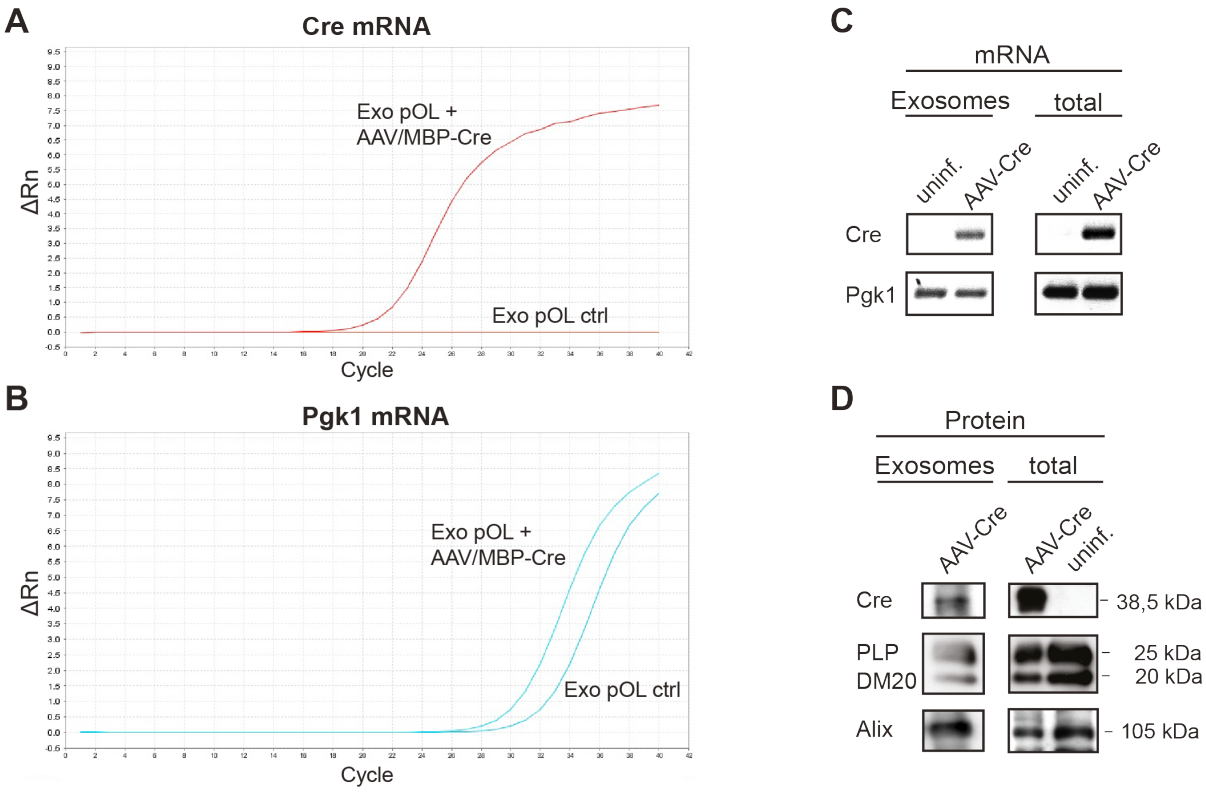


**FIGURE 24: CRE RECOMBINASE RNA AND PROTEIN ARE PRESENT IN OLIGODENDROGLIAL EXOSOMES.** (A-C) qRT-PCR of exosomes derived from pOL transduced with recombinant AAV/MBP-Cre or from uninfected pOL after 7 DIV using primers recognizing Cre recombinase or Pgk1 (as standard). Amplification blots (A and B) and agarose gel (C) are depicted. Rn-value in A and B depicts the fluorescence emission intensity of the reporter dye divided by the fluorescence emission intensity of the passive reference dye. (D) Western blot of exosomes and total lysates from pOL transduced with recombinant AAV/MBP-Cre or not. PLP/DM20 and Alix are used as standards.

with a replication-deficient, recombinant Adeno-associated virus (AAV) expressing Cre recombinase under control of the oligodendrocyte-specific MBP promoter (AAV/MBP-Cre) (von Jonquieres et al., 2013). After 7 days in culture, exosomes were collected and analyzed by qRT-PCR and Western blotting for the presence of Cre mRNA and Cre protein, respectively. Cre mRNA (Fig. 24 A- C) as well as Cre protein (Fig. 24 D) was present in exosomes derived from AAV/MBP-Cre infected primary oligodendrocytes.

To visualize functional retrieval within recipient neurons, primary cortical neurons were infected with a reporter AAV vector encoding humanized renilla GFP (hrGFP) under control of the ubiquitous chicken β-actin (CBA) promoter followed by a floxed transcriptional termination element (AAV/CBA-floxstop-hrGFP). Cre-mediated excision of the floxed zerotrans cassette results in specific expression of the reporter hrGFP (Guggenhuber et al., 2010). Boyden chamber co-culture of primary cortical neurons infected with AAV/CBA-floxstop-hrGFP with primary oligodendrocytes transduced with AAV/MBP-Cre for 2 days results in recombinant, hrGFP-expressing neurons (Fig. 25 B and D). In contrast, reporter neurons co-cultured with uninfected oligodendrocytes did not acquire hrGFP reporter expression (Fig. 25 A and D). Interference with oligodendroglial exosome release by treatment with the neutral sphingomyelinase inhibitor GW4869 (Trajkovic et al., 2008) significantly reduced target neuron recombination (Fig. 25 C and F). Consistently, decreasing exosome secretion by siRNA-mediated knockdown of Rab35 (Hsu et al., 2010) led to a reduced hrGFP reporter expression in target neurons upon co-culture (Fig. 25 E). On the other hand, stimulation of exosome release with glutamate strongly enhanced neuronal reporter expression (Fig. 25 D). To validate that hrGFP reporter expression in neurons is indeed a result of exosome mediated Cre transfer and not due to carried over soluble Cre protein, reporter virus infected primary cortical neurons were incubated with exosome-depleted culture supernatant (by 100 000 x g centrifugation) from AAV/MBP-Cre transduced primary oligodendrocytes. These neurons did not acquire hrGFP reporter expression (Fig. 25 F). To exclude that the observed recombination in neurons is due to a carry over of residual AAV/MBP-Cre viruses, reporter neurons were co-cultured with AAV/MBP-Cre infected Oli-*neu* or HEK cells. These cells do not express MBP promoter-driven Cre recombinase. However, co-culture did not result in neuronal hrGFP expression indicating that no residual AAVs are carried over (Fig. 25 G). Contrary, reporter virus-infected primary cortical neurons co-cultured with Oli-*neu* cells expressing Cre under control of the ubiquitous CBA promoter instead of the MBP promoter acquire reporter hrGFP expression, finally ruling out leakiness of the viral expression system (Fig. 25 H). Taken together, these results demonstrate that the cargo of oligodendroglial exosomes is functionally retrieved by primary cortical neurons *in vitro*.

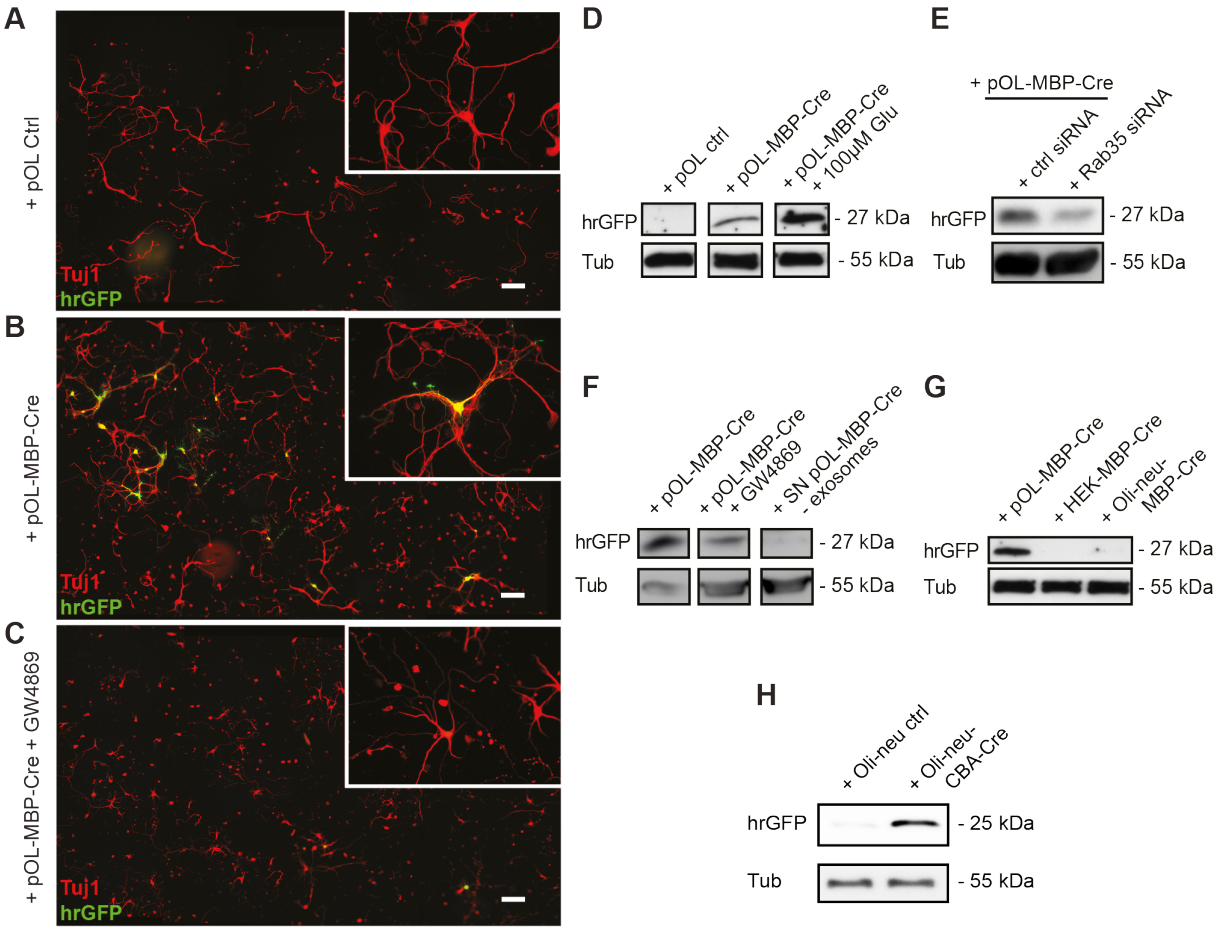


**FIGURE 25: FUNCTIONAL RETRIEVAL OF EXOSOMAL CARGO BY NEURONS *IN VITRO*.** (A-H) Boyden chamber co-culture of pCN transduced with AAV/CBA-floxstop-hrGFP (pCN-floxstop-hrGFP) and pOL transduced with recombinant AAV/MBP-Cre (pOL-MBP-Cre) or Oli-*neu* transfected with pAM/CBA-Cre for 2 d. hrGFP expression indicates exosome mediated Cre-dependent recombination in the target pCN. (A-C) Immunocytochemical staining of pCN co-cultured with uninfected pOL (A), pOL-MBP-Cre (B), or pOL-MBP-Cre treated with 5 µM GW4869 (C). pCN are stained for Tuj1 (red), hrGFP expression is shown in green. Scale bar, 100 µm. (D-H) Western blot analysis of neuronal lysates after co-culture. Reporter gene expression (hrGFP) is depicted. Tubulin (Tub) is used as standard. pCN-floxstop-hrGFP are co-cultured with uninfected pOL, pOL-MBP-Cre, or pOL-MBP-Cre stimulated with 100 µM glutamate (D); with pOL-MBP-Cre transfected with Rab35 or control siRNA (E); with pOL-MBP-Cre treated or not with 5 µM GW4869 (F); with exosome-depleted supernatant from pOL-MBP-Cre (F, right lane); with pOL, Oli-*neu*, or HEK cells transduced with AAV/MBP-Cre (G); or with Oli-*neu* cells transfected with pAM/CBA-Cre or control plasmid (H).

To validate the *in vitro* results *in vivo*, exosomes isolated from AAV/MBP-Cre infected primary oligodendrocytes by differential centrifugation were stereotactically injected into the hippocampus and cerebellum of adult Rosa26-LacZ reporter mice. Exosome uptake followed by retrieval of exosomal Cre recombinase would result in target cell recombination and β-galactosidase expression. Indeed, in the injected hippocampus and cerebellum β-galactosidase positive cells were found after X-Gal staining. The cells of the hippocampus were located within the pyramidal cell layer of the CA3 region and are positive for neuron-specific enolase (NSE; 8

cells per injection; n=5) (Fig. 26 A-D). In the cerebellum only a few positive cells could be found (5 cells per injection; n=5). These cells carry the GABA-$R_{\alpha 6}$ subunit, a marker of cerebellar granule cells (Fig. 26 E and F). As a control, exosomes derived from uninfected primary oligodendrocytes were injected. Neither in these mice nor at the contra-lateral side of injection, β-galactosidase positive cells were found indicating specific target cell recombination after exosomal Cre transfer. The relative low abundance of recombined neurons after injection of Cre bearing exosomes may be due to low spatial expansion of injected exosomes. In summary, these results provide the proof of principle that oligodendroglial exosomes can be internalized by neurons *in vivo* and that their cargo is functionally retrieved.

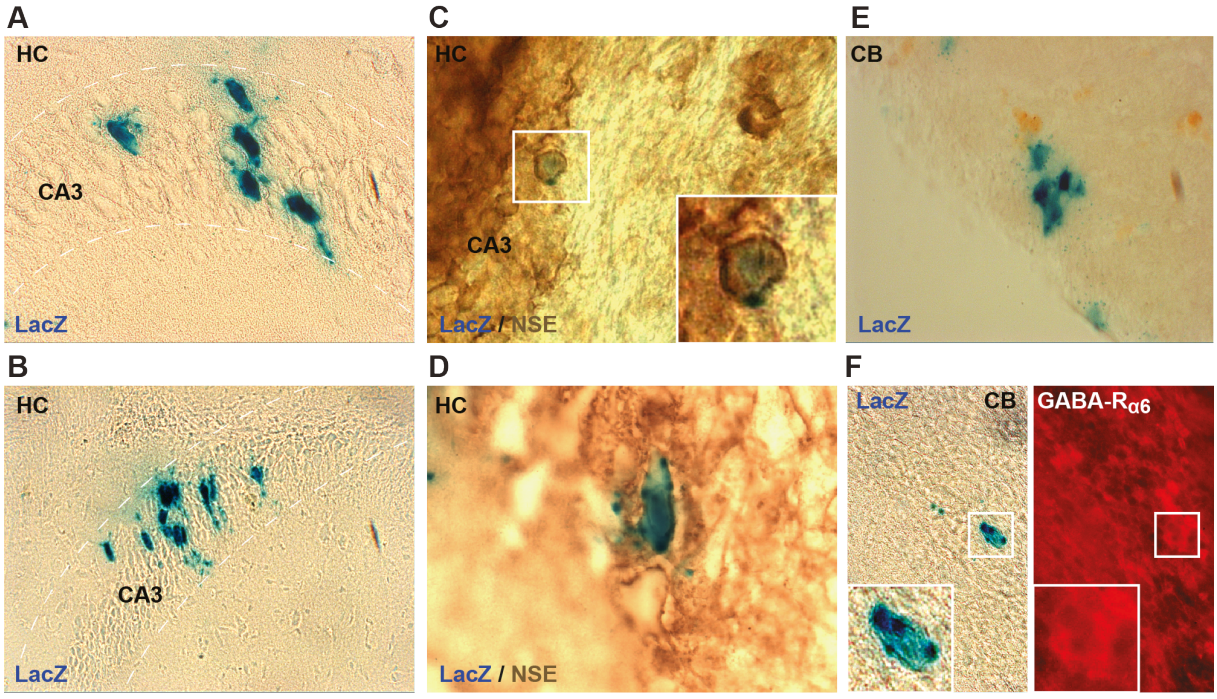


**FIGURE 26: FUNCTIONAL RETRIEVAL OF EXOSOMAL CARGO BY NEURONS *IN VIVO*.** (A-F) Stereotactic injection of exosomes derived from pOL transduced with AAV/MBP-Cre into the hippocampus (HC; A-D) or the cerebellum (E and F) of adult Rosa26-LacZ reporter mice. X-Gal staining marks β-galactosidase positive cells as blue. Neurons were stained for neuron-specific enolase (NSE; C and D) or for GABA-$R_{\alpha 6}$ (F). Mice were analyzed 14 d post injection (n = 5). Stereotactic injections were performed in collaboration with Anja Schneider (Department of Psychiatry and Psychotherapy, University of Göttingen, Germany) and Mikael Simons (Max Planck Institute of Experimental Medicine, Göttingen, Germany).

## 5.7. MOGI-CRE MICE EXHIBIT REPORTER GENE RECOMBINATION IN NEURONS

The previous findings raise the question whether exosome transfer also occurs *in vivo*. Therefore, MOGi-Cre/Rosa26-EGFP and MOGi-Cre/Rosa26-LacZ double transgenic mice were analyzed. The Myelin Oligodendrocyte Glycoprotein (MOG) is widely used as a marker of mature oligodendrocytes and the MOG promoter is specifically active in late stages of oligodendrocyte

development (Cahoy et al., 2008). MOGi-Cre transgenic mice carry Cre recombinase as a knock-in allele under control of the MOG promoter, driving Cre expression exclusively in mature oligodendrocytes (Hovelmeyer et al., 2005; Locatelli et al., 2012). Crossing of MOGi-Cre mice with Rosa26-EGFP (Fig. 27) or Rosa26-LacZ (Fig. 28) reporter mice should solely result in reporter-gene expression in oligodendrocytes. However, besides oligodendrocytes a subset of neurons exhibited reporter gene recombination. The strongest neuronal reporter expression could be detected in cells of the granular layer of the cerebellum (Fig. 27 B and C; Fig. 28 B). In contrast, only individual recombinant neurons were found in the cortex (Fig. 27 D; Fig. 28 A and C), hippocampus (Fig. 27 E and F), and brainstem (Fig. 28 D). Quantification of recombinant neurons (NeuN-labeled cells expressing β-galactosidase) in one MOGi-Cre/Rosa26-LacZ mouse revealed that 17% of the neurons in the cerebellum, 3.8% in the cortex, 1.2% in the hippocampus, and 2.9% in the brainstem were recombinant. Quantification of recombinant neurons in two MOGi-Cre/Rosa26-EGFP mice revealed slightly different numbers. 24% of the neurons in the cerebellum, 0.6% in the cortex, and 0.3% in the hippocampus were recombinant.

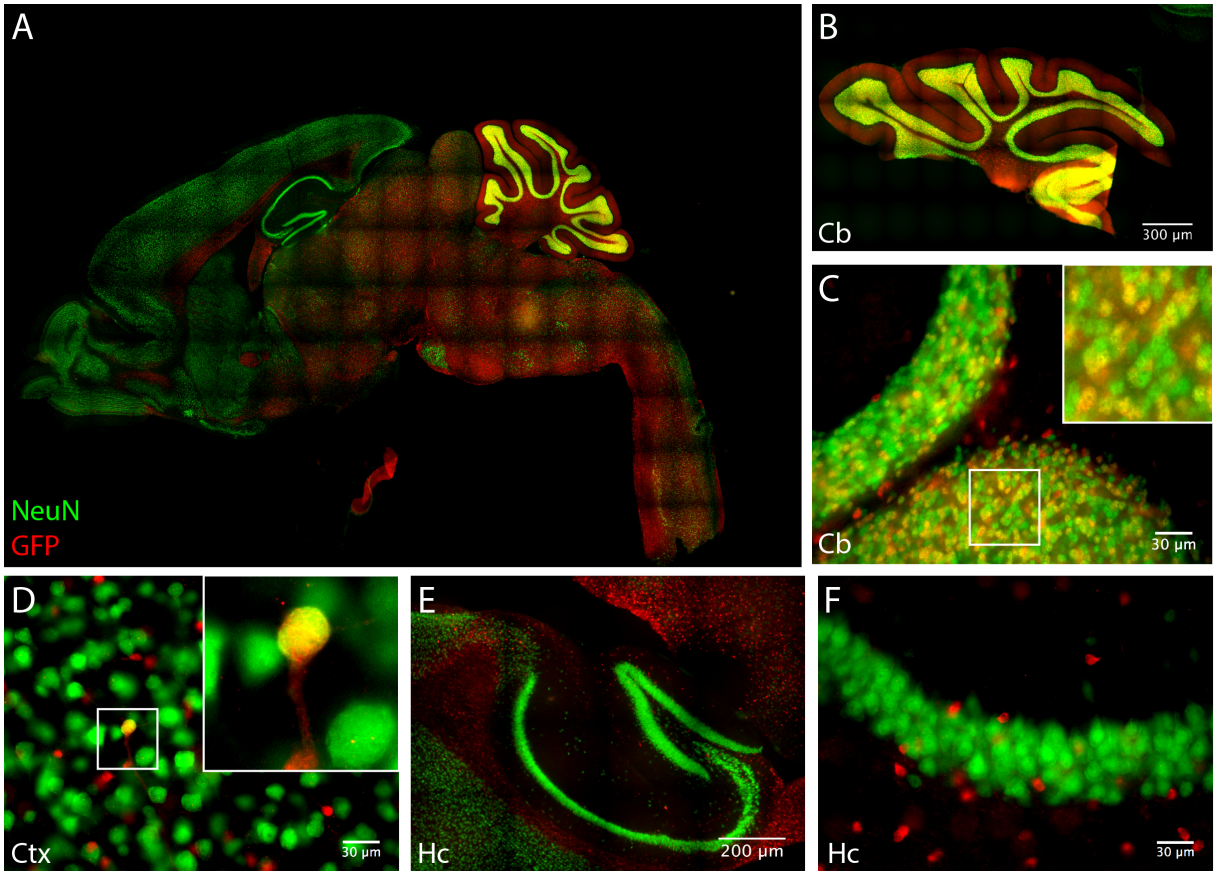


**FIGURE 27: NEURONAL RECOMBINATION IN MOGI-CRE/ROSA26-EGFP MICE.** (A-F) Immunohistochemical staining of brain sections derived from MOGi-Cre/Rosa26-EGFP mice. Recombinant GFP positive cells were stained with antibodies against GFP (red), neurons were labeled with antibodies against NeuN (green). Different brain areas are depicted: whole brain (A), cerebellum (Cb; B and C), cortex (Ctx; D), and hippocampus (Hc; E and F). Scale bar size is depicted in the individual pictures. Crossings were performed in collaboration with Simone Wörtge (Institute for Molecular Medicine, Mainz, Germany).

However, there may be different explanations for the presence of recombinant neurons in adult mice. First, there may be some residual MOG promoter activity in individual neurons or their precursors. To rule out MOG promoter activity in early embryonic progenitor cells, the presence of MOG transcripts at different developmental stages (embryonic day 10 and 14, postnatal day 0 and 7, adult) has been analyzed by qRT-PCR (Fig. 28 E). MOG mRNA was almost undetectable until postnatal day 7 and was then up-regulated, accompanying the appearance of mature oligodendrocytes. The virtual absence of MOG transcripts during early developmental stages makes it unlikely that MOG promoter activity in neuronal precursors is responsible for neuronal recombination in adult mice. The second explanation for reporter gene expression in neurons may be a horizontal transfer of Cre recombinase from oligodendrocytes to neurons possibly by the means of exosomes. Although the presence of recombinant neurons in the analyzed transgenic mice is per se not a proof of exosome-mediated transfer *in vivo*, it is at least consistent with the results obtained from injection experiments with Cre recombinase bearing exosomes.

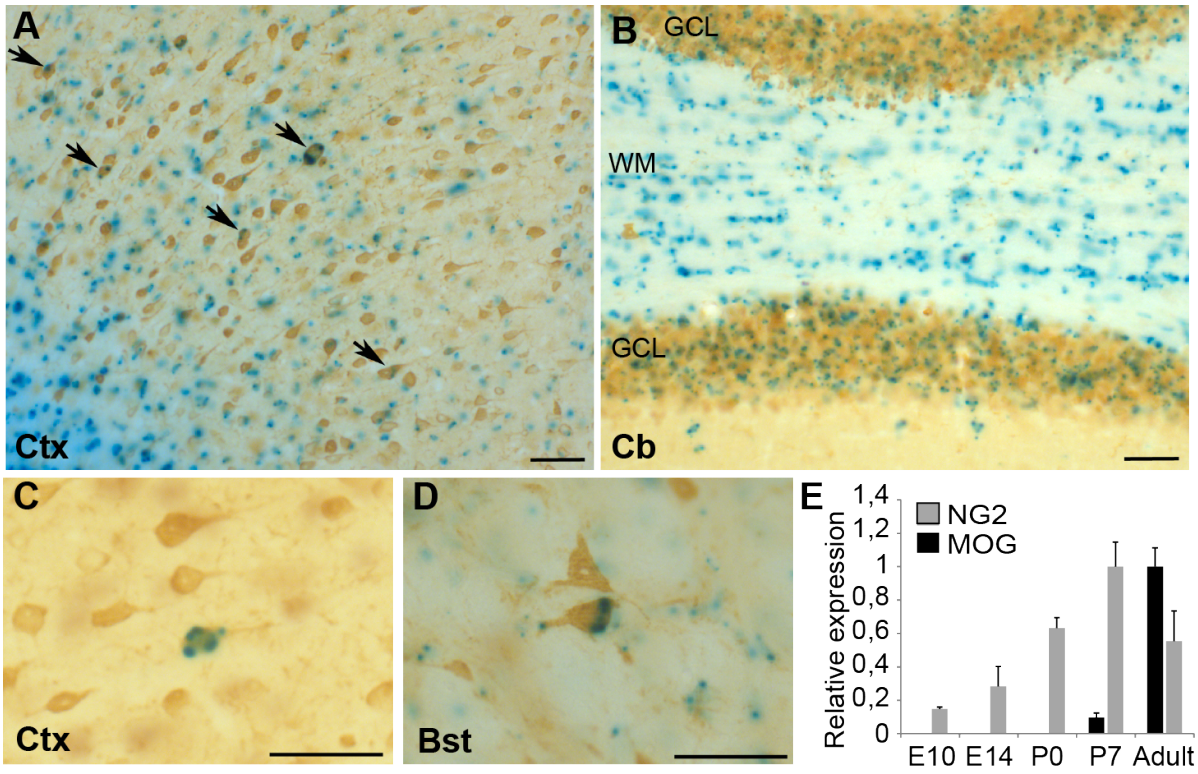


**FIGURE 28: NEURONAL RECOMBINATION IN MOGI-CRE/ROSA26-LACZ MICE.** (A-D) Immunohistochemical staining of brain sections derived from MOGi-Cre/Rosa26-LacZ mice. X-Gal staining marks β-galactosidase positive cells as blue. Neurons were stained with antibodies against NeuN (brown). Different brain areas are depicted: cortex (Ctx; A and C), cerebellum (Cb; B), and brainstem (Bst; D). Scale bar, 50 µm. Crossings were performed by Sandra Goebbels (Max Planck Institute of Experimental Medicine, Göttingen, Germany). (E) qRT-PCR of MOG and NG2 transcript expression in the brains of E10, E14, P0, P7, and adult mice (n=3). The relative expression is depicted (maximal expression was set to 1).

MOG is expressed in mature oligodendrocytes while NG2 is expressed in oligodendroglial progenitor cells. Error bars, SEM.

## 5.8. SOMATODENDRITIC VS. AXONAL UPTAKE OF EXOSOMES

Since exosomes accumulate in late endosomal structures located within the cell body of neurons, we asked whether the uptake occurs at the somatodendritic or axonal compartment of the neuron. To distinguish between somatodendritic and axonal uptake of oligodendroglial exosomes, primary cortical neurons were cultured in microfluidic chambers for 7 d to allow the axons to grow through the microgrooves (channels connecting the two compartments of the device) into the opposite chamber. Exosomes isolated from primary oligodendrocytes by differential centrifugation were either applied to the somatodendritic or the axonal compartment. Uptake of PKH67-labeled exosomes could be visualized at both, the somatodendritic and axonal domain of the neurons (Fig. 29 A). Application of exosomes purified from primary oligodendrocytes transduced with AAV/MBP-Cre to the somatodendritic and axonal compartment of AAV/CBA-floxstop-hrGFP infected primary cortical neurons, likewise resulted in reporter hrGFP expression in target neurons located close to the microgrooves (Fig. 29 B). Quantification of recombined neurons located within an area of 100 µm from the microgrooves, giving all neurons in this area the chance to project their axons into the axonal compartment, did not reveal significant differences between somatodendritic and axonal exosome addition (Fig. 29 C). However, only a small proportion of neurons located within this area acquired reporter gene expression, presumably, because only a subset of neurons located in the quantified area grow their axons through the microgrooves, restricting the number of neurons that are able to come into contact with exosomes. Taken together, these results indicate that neuronal uptake of oligodendroglial exosomes can take place at the somatodendritic as well as the axonal domain of neurons.

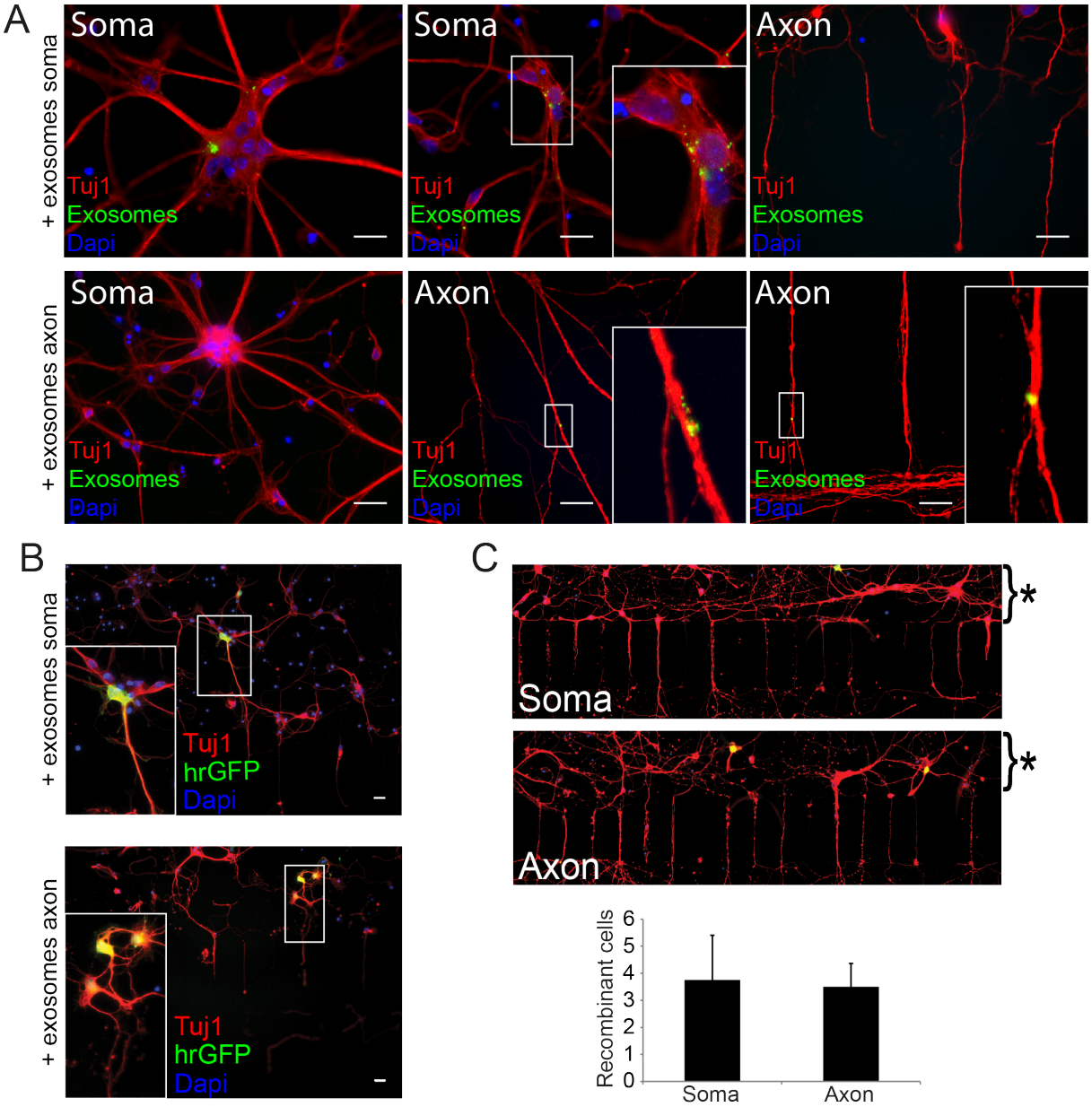


**FIGURE 29: SOMATODENDRITIC VS. AXONAL UPTAKE OF OLIGODENDROGLIAL EXOSOMES.** (A-C) pCN were cultured in microfluidic chambers for 7 d to allow the axons to grow through the microgrooves. Exosomes purified from pOL either stained with PKH67 (green; A) or transduced with AAV/MBP-Cre (B and C) were applied to the somatodendritic or axonal side of the device. In case of Cre bearing exosomes, pCN were infected with AAV/CBA-floxstop-hrGFP reporter virus (B and C). hrGFP expression indicates exosome-mediated Cre-dependent recombination (green; B and C). Neurons were stained with the neuronal marker Tuj1 (red) and nuclei with Dapi (blue). Scale bar, 20 µm. (D) Quantification of recombinant pCN after exosome application either to the somatodendritic (upper panel) or the axonal (lower panel) compartment. Only pCN located in an area of 100 µm above the microgrooves are quantified (marked by the asterisk). Error bars, SEM (n=4).

## 5.9. WILD-TYPE VS. PLP- AND CNP-KO EXOSOME TRANSFER

PLP- and CNP-KO mice develop axonal swellings followed by severe axonal degeneration due to a lack of glial support. Since exosomes may transfer supportive molecules and provide trophic support to neurons, it was highly interesting to investigate whether the exosome transfer in these mouse mutants is impaired. Reporter neurons transduced with AAV/CBA-floxstop-hrGFP were co-cultured for 2 d in Boyden chambers with primary oligodendrocytes infected with AAV/MBP-Cre. Primary cortical neurons were either derived from wild type or from PLP- or CNP-KO mice (KPLP or CNCE). The functional transfer of exosomal cargo to neurons was displayed by the expression of hrGFP in primary cortical neurons (Fig. 30). Intriguingly, co-culture with PLP- and CNP-KO oligodendrocytes resulted in much lower reporter recombination in the target neurons indicating that the transfer of exosomal cargo may be disturbed in these mutants.

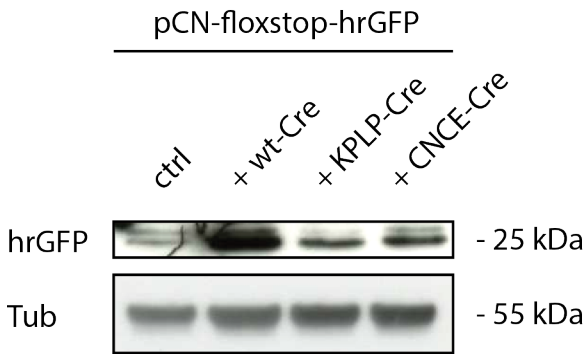


**FIGURE 30: WILD TYPE VS. PLP- AND CNP-KO EXOSOME TRANSFER.** Western blot analysis of lysates from pCN infected with AAV/CBA-floxstop-hrGFP that were co-cultured in Boyden chambers for 2 d with pOL (transduced with AAV/MBP-Cre) derived from wiltype, PLP-KO, or CNP-KO mice. hrGFP reflects the amount of recombination in pCN. Tubulin (Tub) is used as normalization standard.

## 5.10. EXOSOME-DEPENDENT REGULATION OF PROTEINS IN NEURONS

In order to test whether oligodendroglial exosomes have an influence on distinct neuronal proteins, the expression levels of interesting candidates were analyzed after exosome uptake. Oligodendrocytes may provide some supportive and protective proteins to neurons by the means of exosomes. We have already shown that Hsc/Hsp70 is transferred to neurons via exosomes. Another interesting candidate could be catalase, which catalyzes the reaction of hydrogen peroxide to water and oxygen, and therefore, plays an essential role in the protection of cells from oxidative stress. Interestingly, after Boyden chamber co-culture of primary cortical neurons with PKH67-labeled primary oligodendrocytes, catalase expression was increased in

cells that have internalized exosomes (Fig. 31 A). Also in the whole neuronal cell population, the catalase levels were elevated by 22 ± 5% after Boyden chamber co-culture with oligodendrocytes, as demonstrated by Western blotting (Fig. 31 B and C). Successful transfer of oligodendroglial exosomes is displayed by the presence of PLP/DM20 in the neuronal lysate after co-culture (Fig. 31 B).

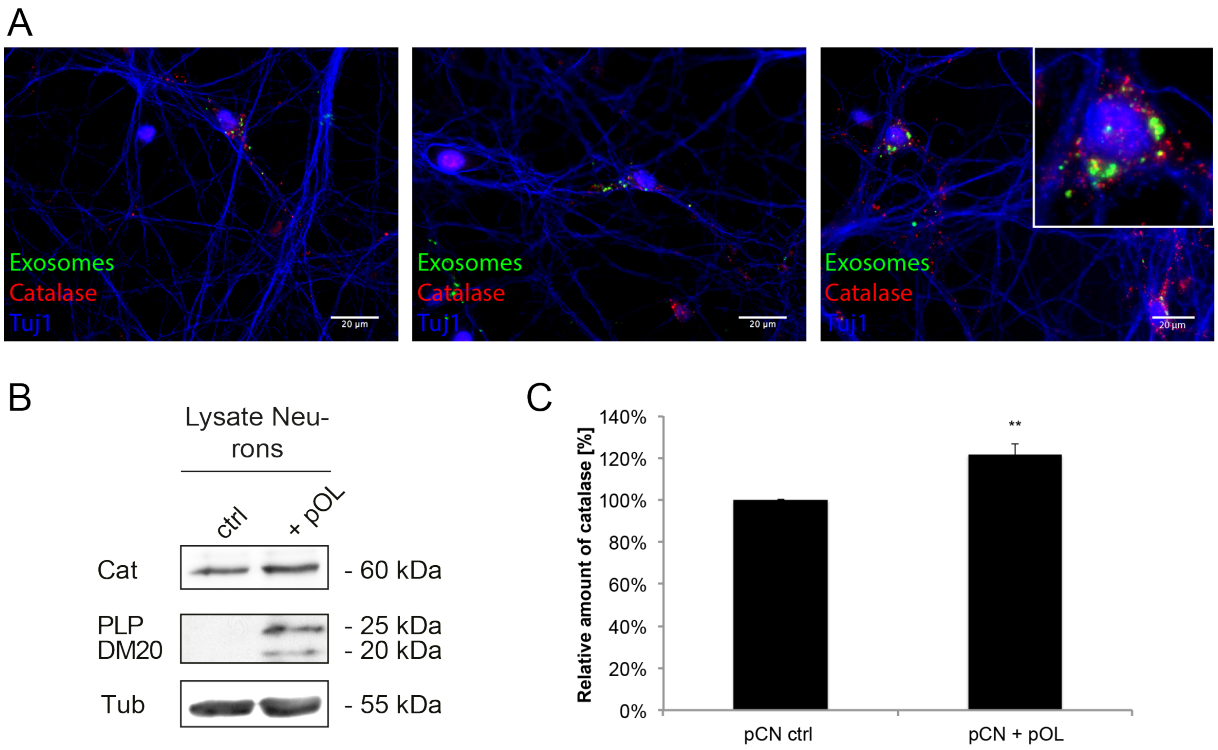


**FIGURE 31: NEURONAL CATALASE EXPRESSION AFTER EXOSOME UPTAKE.** (A) Boyden chamber co-culture of pCN with PKH67-stained pOL for 2 d. PKH67-labeled exosomes are displayed in green, catalase in red, and the neuronal marker Tuj1 in blue. Scale bar, 20 µm. (B and C) Western blot analysis of neuronal lysates after Boyden chamber co-culture with pOL for 2 d. The relative catalase (Cat) expression was measured as the catalase signal normalized to tubulin (Tub) (n=10). PLP/DM20 displays neuronal exosome uptake. Error bars, SEM (** $p<0.01$; Wilcoxon-test).

Besides the supportive role, oligodendroglial exosomes may also influence neuronal development. We found the miRNAs miR-9, miR-17, and miR19a in oligodendroglial exosomes. All three miRNAs were predicted to bind Doublecortin (DCX) (algorithm from www.microRNA.org). DCX is a microtubule-binding protein (Horesh et al., 1999), which is commonly used as a marker for neuronal precursor cells and immature neurons. Therefore, downregulation of DCX accompanies neuronal differentiation. To test whether exosome-mediated transfer of these miRNAs may influence neuronal DCX expression, we applied oligodendroglial exosomes to cultured primary cortical neurons and analyzed neuronal DCX by

Western blotting. Application of exosomes derived from the oligodendrocyte precursor cell line Oli-*neu* to primary cortical neurons (Fig. 32 A and D) or Boyden chamber co-culture of primary cortical neurons with Oli-*neu* cells (Fig. 32 B and D), likewise resulted in a decreased DCX expression in recipient neurons. The Oli-*neu* cells ectopically expressed Sirt2-EYFP and PLP-EGFP, which were used as markers to follow exosome transfer to neurons. Both proteins were detectable in neuronal lysates, indicating successful transfer of exosomes (Fig. 32 A and B). Contrary, co-culture with mature primary oligodendrocytes slightly increased the neuronal DCX expression, even though this effect was not significant (Fig. 32 C and D). Taken together, exosomes derived from oligodendroglial precursors but not from mature oligodendrocytes were able to decrease neuronal DCX expression *in vitro*, eventually transferring a differentiation signal.

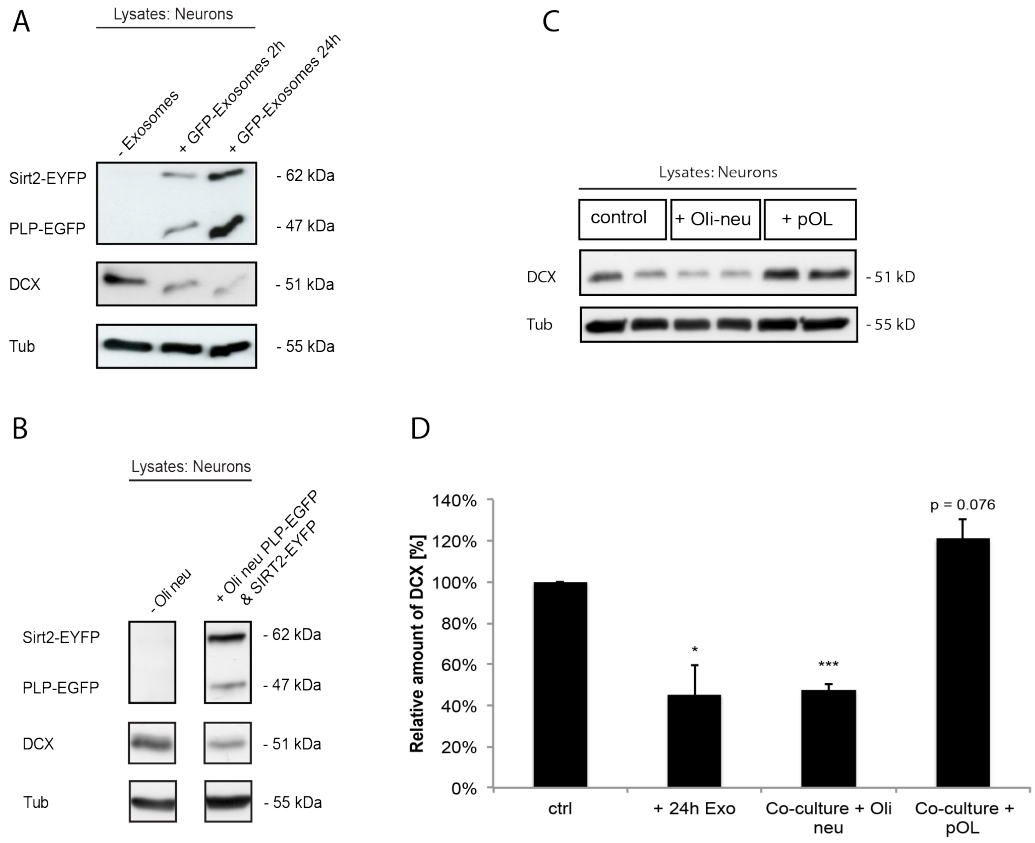


**FIGURE 32: NEURONAL DOUBLECORTIN EXPRESSION AFTER EXOSOME UPTAKE.** (A-D) Western blot analysis of neuronal lysates. The relative Doublecortin (DCX) expression was measured as the DCX signal normalized to Tubulin (Tub) (D). (A) pCN were treated with exosomes purified from Oli-*neu* cells ectopically expressing Sirt2-EYFP and PLP-EGFP for 2 or 24 h (n =6). (B and C) Boyden chamber co-culture of pCN either with Oli-*neu* cells ectopically expressing Sirt-EYFP and PLP-EGFP (B and C; n=4) or with pOL (C; n=6). Error bars, SEM (* $p<0.05$; ** $p<0.01$; *** $p<0.001$; Students t-test).

## 5.11. Influence of Oligodendroglial Exosomes on Neuronal Activity

Previously, it has been shown that microglia-derived microvesicles can influence neuronal electrical activity (Antonucci et al., 2012). To test whether oligodendroglial exosomes also have the potential to alter neuronal activity, multi-electrode arrays (MEA) were performed. Primary cortical neurons were cultured on 6well MEA chips (9 electrodes per well) for 14 d. After this period neurons establish neuronal circuits and are electrically active. 1 h after recording was

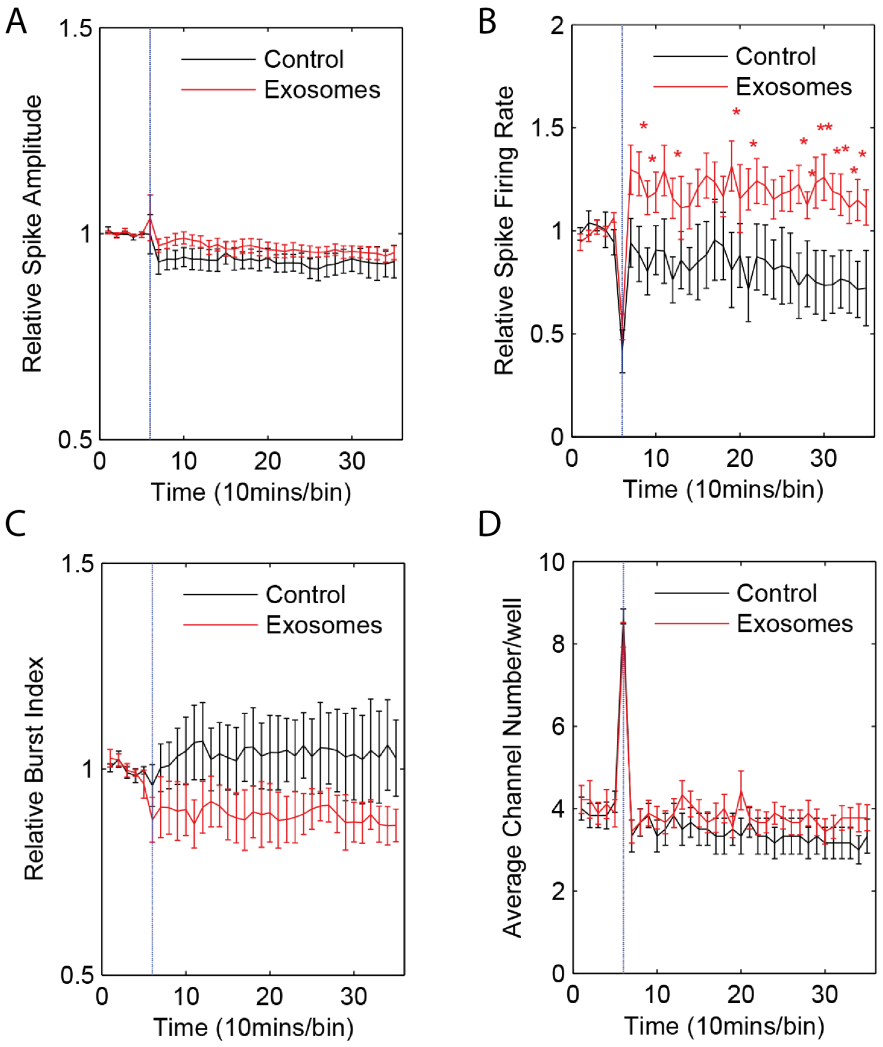


**Figure 33: Influence of oligodendroglial exosomes on neuronal electrical activity.** (A-D) pCN were cultured on multi-electrode arrays for 14 d to allow the cultures to establish neuronal circuits and develop spontaneous electrical activity. After 14 DIV recordings were started and after 1 h of recording pOL exosomes resuspended in neurobasal feeding medium were applied (blue vertical line; n=9). Recording was stopped after 6 h. As a control, feeding medium alone was added (n=6). Relative spike amplitude (A), relative spike firing rate (B), relative burst index (C), and average channel number/well (D) are depicted. Only if 3 or more channels per well were active the results were taken into account. Error bars, SD (* $p<0.05$; Students t-test). Arrays were performed in collaboration with Jyh-Jang Sun and Heiko Luhmann (Institute of Physiology, Johannes Gutenberg-University, Mainz, Germany).

started, exosomes isolated by differential centrifugation from cultured primary oligodendrocytes were diluted in neurobasal feeding medium and applied to the neurons. As control, feeding medium alone was added. After 6 h of recording the experiment was terminated and the relative spike amplitude (Fig. 33 A), firing rate (Fig. 33 B), burst index (Fig. 33 C), and the average channel number per well (Fig. 33 D) were calculated. The results were only taken in account if the average number of active channels (electrodes) was higher than 3 during the recording (Fig. 33 D). While the relative spike amplitude was not changed after application of oligodendroglial exosomes (Fig. 33 A), the relative firing rate increased significantly and immediately (Fig. 33 B). In contrast to the firing rate, the relative burst index decreased slightly after exosome treatment (Fig. 33 C). The relative burst index is a measurement for the synchronism of neuronal circuits, so a lower burst index implies that the cultured neurons fire less synchronized. In summary, neuronal uptake of oligodendroglial exosomes results in an increased number of action potential while the spike amplitude remains unaltered. Concomitantly, the cultured neurons fire less orchestrated, which may be a sign for a rearrangement of neuronal circuits.

## 5.12. Influence of Oligodendroglial Exosomes on Neuronal Gene Expression

Exosomes contain a distinct set of mRNAs and miRNAs. It has been shown previously that mRNA enclosed in exosomes is transferred to recipient cells and subsequently, translated into a functional protein (Valadi et al., 2007). Moreover, exosomal miRNAs are also functionally transferred between cells and can mediate gene knockdown in the target cell (Pegtel et al., 2010). It has been proposed that the RNA transported by the means of exosomes is called “exosomal shuttle RNA” (esRNA) (Valadi et al., 2007). Alternatively, transcription factors transferred via exosomes or signal transduction pathways triggered by exosomes may also have an influence on neuronal transcription. To test whether neuronal gene expression is altered upon exosome uptake, a microarray analysis was performed. Primary cortical neurons were co-cultured in Boyden chambers with primary oligodendrocytes for 2 d. As a control, neurons were cultured in the absence of oligodendrocytes. To ensure most adequate control settings, an insert filled with oligodendrocyte-conditioned, exosome-depleted medium was added to the neurons. So, soluble factors released by primary oligodendrocytes were present except of oligodendroglial exosomes. Subsequently, neuronal mRNA was prepared and differentially expressed genes were evaluated by microarray analysis. A list of the most significant differentially regulated genes can be found below (Table 22).

**TABLE 22: DIFFERENTIALLY REGULATED GENES IN PCN AFTER BOYDEN CHAMBER CO-CULTURE WITH POL.** pCN were co-cultured with pOL for 2d and subsequently, neuronal mRNA was analyzed on Illumina microarray chips. As control, pCN were cultured in the absence of pOL but with an insert filled with pOL-conditioned, exosome-depleted medium. Most significantly regulated genes are depicted (down to a false discovery rate (FDR) of 20%; n=4). The logFC value is the logarithmic representation of the fold change (FC) value. The candidate genes displayed in red were further validated by qRT-PCR. Microarrays were performed in collaboration with Sheena Pinto and Bruno Kyewski (Deutsches Krebsforschungszentrum (DKFZ), Heidelberg, Germany). Data analysis was performed by Jörn Tödling (Institute of Molecular Biology (IMB), Mainz, Germany).

| ID | Symbol | Describtion | logFC | FDR (p-value) |
|---|---|---|---|---|
| ILMN_2737200 | Mbp | myelin basic protein | 0,87 | 1.79e-07 |
| ILMN_1216764 | Ier3 | immediate early response 3 | -0,52 | 1.48e-04 |
| ILMN_1221503 | Ccnd1 | cyclin D1 | -0,52 | 1.48e-04 |
| ILMN_2601471 | Ccnd1 | cyclin D1 | -0,47 | 3.10e-03 |
| ILMN_2836654 | NA | NA | -0,46 | 3.10e-03 |
| ILMN_2929896 | Pbk | PDZ binding kinase | -0,42 | 3.10e-03 |
| ILMN_2955725 | Cort | cortistatin | -0,44 | 3.10e-03 |
| ILMN_1226607 | Cort | cortistatin | -0,42 | 3.10e-03 |
| ILMN_2739843 | Metrn | meteorin, glial cell differentiation regulator | -0,42 | 3.10e-03 |
| ILMN_2795040 | NA | NA | -0,45 | 4.06e-03 |
| ILMN_1219574 | Hist1h2af | histone cluster 1, H2af | -0,46 | 4.11e-03 |
| ILMN_2634520 | Ctnnd2 | catenin (cadherin associated protein), delta 2 | 0,41 | 4.20e-03 |
| ILMN_1236574 | Cenpa | centromere protein A | -0,4 | 4.25e-03 |
| ILMN_1234112 | Tomm70a | translocase of outer mitochondrial membrane 70 homolog A (yeast) | 0,39 | 9.30e-03 |
| ILMN_3112526 | Ldb2 | LIM domain binding 2 | 0,39 | 1.30e-02 |
| ILMN_2754435 | Ldb2 | LIM domain binding 2 | 0,38 | 1.44e-02 |
| ILMN_1220100 | Ywhae | tyrosine 3-monooxygenase/tryptophan 5-monooxygenase activation | 0,38 | 1.93e-02 |
| ILMN_2925923 | Vgf | VGF nerve growth factor inducible | -0,36 | 2.52e-02 |
| ILMN_1225182 | Cdca3 | cell division cycle associated 3 | -0,4 | 2.67e-02 |
| ILMN_2933022 | Plekhb1 | pleckstrin homology domain containing, family B (evectins) member 1 | -0,38 | 2.67e-02 |
| ILMN_2847144 | Hist1h2ak | histone cluster 1, H2ak | -0,42 | 2.86e-02 |
| ILMN_2693895 | Acta2 | actin, alpha 2, smooth muscle, aorta | 0,60 | 2.92e-02 |
| ILMN_3128907 | Cd63 | CD63 antigen | -0,36 | 3.06e-02 |
| ILMN_2617468 | Chac1 | ChaC, cation transport regulator 1 | -0,37 | 3.36e-02 |
| ILMN_2662264 | Bcas1 | breast carcinoma amplified sequence 1 | 0,37 | 4.60e-02 |
| ILMN_2670398 | Eif4ebp1 | eukaryotic translation initiation factor 4E binding protein 1 | -0,35 | 4.64e-02 |
| ILMN_2644008 | Chl1 | cell adhesion molecule with homology to L1CAM | 0,34 | 4.72e-02 |
| ILMN_2652909 | Ddit3 | DNA-damage inducible transcript 3 | -0,35 | 4.87e-02 |
| ILMN_2591440 | Ccrn4l | CCR4 carbon catabolite repression 4-like (S. cerevisiae) | 0,33 | 5.36e-02 |
| ILMN_2627557 | Tbc1d19 | TBC1 domain family, member 19 | 0,34 | 5.75e-02 |
| ILMN_1257987 | Slc7a3 | solute carrier family 7 (cationic amino acid transporter, y+ system), | -0,33 | 6.00e-02 |
| ILMN_1260082 | Asphd1 | aspartate beta-hydroxylase domain containing 1 | -0,34 | 7.02e-02 |
| ILMN_2601884 | Gpcpd1 | glycerophosphocholine phosphodiesterase GDE1 homolog (S. cerevisiae) | 0,32 | 7.11e-02 |
| ILMN_2657844 | Cdk1 | cyclin-dependent kinase 1 | -0,32 | 7.45e-02 |
| ILMN_2662450 | Runx1t1 | runt-related transcription factor 1; translocated to, 1 (cyclin D-related) | 0,32 | 7.74e-02 |
| ILMN_2669699 | NA | NA | 0,34 | 8.55e-02 |
| ILMN_3161626 | Prkag2 | protein kinase, AMP-activated, gamma 2 non-catalytic subunit | 0,31 | 1.06e-01 |
| ILMN_2852957 | Dkk3 | dickkopf homolog 3 (Xenopus laevis) | 0,31 | 1.13e-01 |
| ILMN_2662926 | Egr1 | early growth response 1 | 0,51 | 1.17e-01 |

| | | | | |
|---|---|---|---|---|
| ILMN_1245335 | Neurl1b | neuralized homolog 1b (Drosophila) | 0,33 | 1.17e-01 |
| ILMN_2722938 | Ppp1r15a | protein phosphatase 1, regulatory (inhibitor) subunit 15A | -0,31 | 1.20e-01 |
| ILMN_2693922 | Egfr | epidermal growth factor receptor | -0,31 | 1.21e-01 |
| ILMN_2623216 | Pgrmc1 | progesterone receptor membrane component 1 | 0,31 | 1.21e-01 |
| ILMN_1234072 | Pdlim1 | PDZ and LIM domain 1 (elfin) | -0,32 | 1.23e-01 |
| ILMN_2512541 | Ube2n | ubiquitin-conjugating enzyme E2N | 0,31 | 1.27e-01 |
| ILMN_1224333 | Osbpl11 | oxysterol binding protein-like 11 | 0,33 | 1.27e-01 |
| ILMN_3105417 | Bdnf | brain derived neurotrophic factor | -0,33 | 1.28e-01 |
| ILMN_1216042 | Apoe | apolipoprotein E | -0,33 | 1.32e-01 |
| ILMN_2632712 | Birc5 | baculoviral IAP repeat-containing 5 | -0,32 | 1.41e-01 |
| ILMN_2730329 | Hist1h2ah | histone cluster 1, H2ah | -0,34 | 1.45e-01 |
| ILMN_1228557 | Id2 | inhibitor of DNA binding 2 | 0,32 | 1.65e-01 |
| ILMN_1248830 | Hist1h2an | histone cluster 1, H2an | -0,35 | 1.65e-01 |
| ILMN_2625167 | Eif4g2 | eukaryotic translation initiation factor 4, gamma 2 | 0,32 | 1.72e-01 |
| ILMN_1247066 | Caprin1 | cell cycle associated protein 1 | 0,3 | 1.72e-01 |
| ILMN_1225528 | Trib3 | tribbles homolog 3 (Drosophila) | -0,3 | 1.72e-01 |
| ILMN_2762326 | Kif22 | kinesin family member 22 | -0,33 | 1.72e-01 |
| ILMN_1220409 | Cetn2 | centrin 2 | 0,33 | 1.79e-01 |
| ILMN_1248892 | Tmem184c | transmembrane protein 184C | 0,3 | 1.79e-01 |
| ILMN_2528345 | Zfhx2 | zinc finger homeobox 2 | -0,32 | 1.90e-01 |
| ILMN_2908070 | Gtse1 | G two S phase expressed protein 1 | -0,32 | 1.92e-01 |
| ILMN_2868280 | Dcxr | dicarbonyl L-xylulose reductase | -0,29 | 1.92e-01 |
| ILMN_2719202 | Hist1h2bf | histone cluster 1, H2bf | -0,3 | 1.92e-01 |
| ILMN_1255053 | Plk1 | polo-like kinase 1 | -0,31 | 1.92e-01 |
| ILMN_2647627 | Ppp1cb | protein phosphatase 1, catalytic subunit, beta isoform | 0,31 | 1.93e-01 |
| ILMN_2886828 | Rarb | retinoic acid receptor, beta | -0,3 | 1.96e-01 |
| ILMN_2598420 | Scaf8 | SR-related CTD-associated factor 8 | 0,29 | 1.96e-01 |
| ILMN_2751854 | Ndrg4 | N-myc downstream regulated gene 4 | 0,31 | 1.96e-01 |
| ILMN_1231710 | Crhbp | corticotropin releasing hormone binding protein | -0,3 | 1.98e-01 |

The most promising candidates (highlighted in red) were validated by qRT-PCR in independent biological replicates (Fig. 34). Validation revealed significant different expression of the following genes: Immediate early response 3 (Ier3), cortistatin (Cort), VGF nerve growth factor inducible (Vgf), actin alpha 2 (Acta2), cell adhesion molecule with homology to L1CAM (Chl1), cyclin dependent kinase 1 (Cdk1), and brain derived neurotrophic factor (Bdnf). Moreover, the oligodendrocyte specific transcripts of PLP, CNP, and MBP were detectable in primary cortical neurons after co-culture with primary oligodendrocytes. These mRNAs may be sorted to oligodendroglial exosomes and are therefore transferred to neurons.

To test whether the observed effects can be really attributed to exosomes, oligodendroglial exosomes purified by differential centrifugation were applied to primary cortical neurons and the expression of candidate genes was determined by qRT-PCR (Fig. 35). Comparison of the qRT-PCR results derived from the co-cultured and exosome-treated neurons revealed a

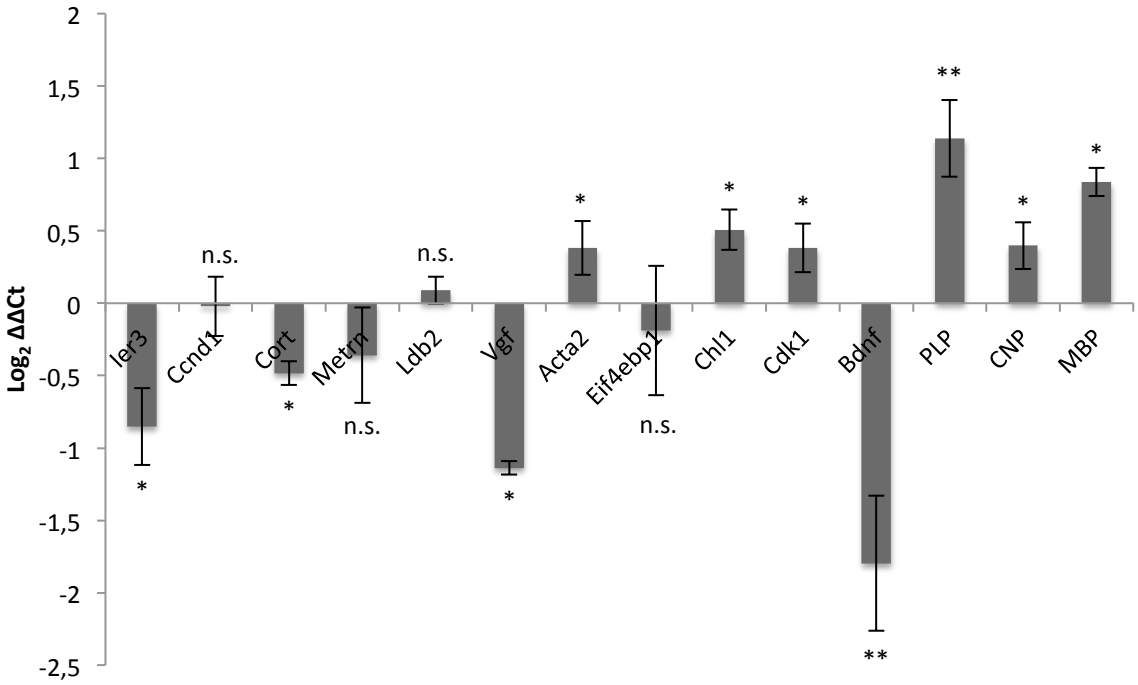


**FIGURE 34: VALIDATION OF CANDIDATE GENES BY QRT-PCR.** Boyden chamber co-culture of pCN with pOL for 2 d. As control, pCN were cultured in the absence of pOL but with an insert filled with pOL-conditioned, exosome-depleted medium. After co-culture, mRNA was prepared from pCN and the corresponding cDNAs were synthesized and analyzed by qRT-PCR using specific TaqMan probes (n=6; BDNF and PLP, n=14). Pgk1 was used as normalization standard. Log2 values of the ΔΔCt values are displayed. Error bars, SEM (n.s., not significant; * $p<0.05$; ** $p<0.01$; Wilcoxon test).

proportion of likewise regulated genes with statistic significance. However, there are also some, yet not significant, trends in gene regulation, e.g. cortistatin, meteorin, and MBP show the same tendency. Ier3, Vgf, and Bdnf are significantly down-regulated, while Plp is significantly up-regulated in both experimental settings, indicating a robust, exosome-mediated effect. The up-regulation of Plp may be due to an exosomal transfer of Plp mRNA. Contrary, the knockdown of Ier3, Vgf, and Bdnf may be accomplished by the transfer of specific miRNAs via oligodendroglial exosomes. Ier3 belongs to the class of immediate early genes (IEGs), which are activated rapidly and transiently in response to various stimuli. IER3 is involved in cell cycle control and apoptosis (Arlt and Schafer, 2011). Interestingly, VGF and BDNF both belong to the class of growth factors. While BDNF is a neurotrophic factor, VGF is a neuropeptide that plays a role in regulation of metabolism, synaptic plasticity and energy homeostasis. Intriguingly, BDNF induces the expression of Vgf (Bozdagi et al., 2008). Therefore, decreased Vgf expression may be a secondary effect of reduced Bdnf expression. The functional relevance of transferred

oligodendroglial esRNA and in particular of the exosome-mediated knockdown of Ier3, Vgf, and Bdnf will be the subject of future studies.

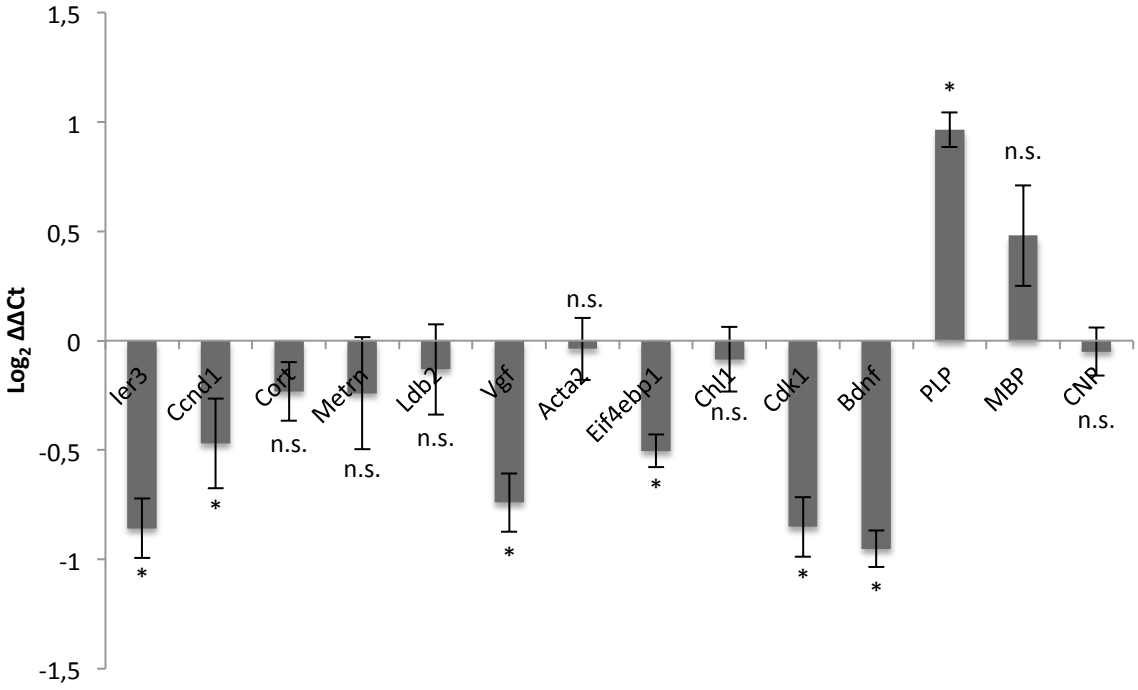


**FIGURE 35: DIFFERENTIALLY REGULATED GENES IN PCN AFTER APPLICATION OF PURIFIED OLIGODENDROGLIAL EXOSOMES.** Exosomes derived from pOL were applied to pCN for 24 h and subsequently, mRNA was prepared from pCN, the corresponding cDNAs were synthesized and analyzed by qRT-PCR using specific TaqMan probes. As control, untreated pCN were used (n=7; BDNF, PLP, MBP, and CNP, n=5). Pgk1 was used as standard. Log2 values of the ΔΔCt values are displayed. Error bars, SEM (n.s., not significant; * $p<0.05$; Wilcoxon test).

# 6. DISCUSSION

The present study provides evidence for a novel mode of communication in the CNS, mediated by the transfer of vesicles between cells. We have shown that bioactive molecules are functionally transferred from oligodendrocytes to neurons. Since the secretion of oligodendroglial exosomes is triggered by neuronal glutamate release (Frühbeis et al., 2013a), this may be part of a feedback loop by which oligodendrocytes support long myelinated axons (Fig. 36). In theory, electrically active neurons release the neurotransmitter glutamate, which can activate oligodendroglial ionotropic glutamate receptors of the NMDA- and AMPA-subtype

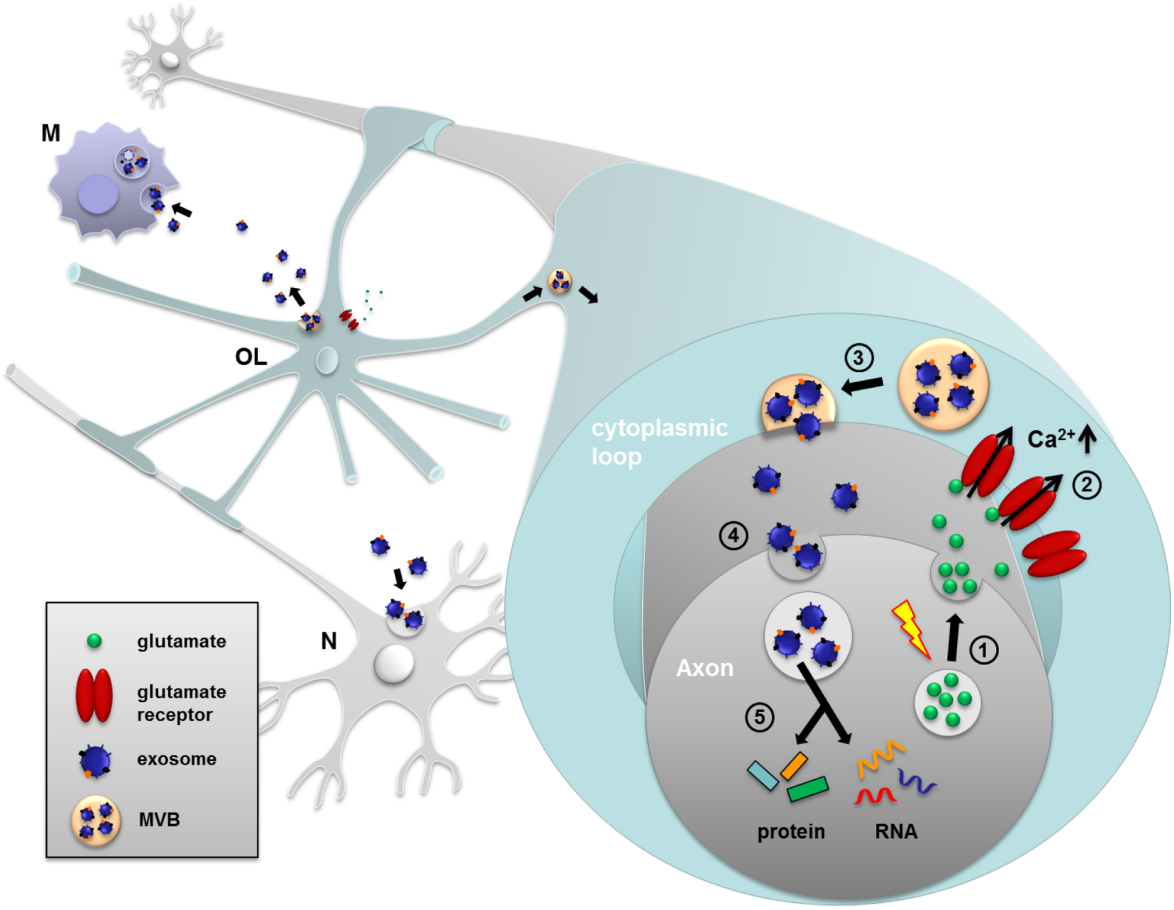


**FIGURE 36: REGULATION OF OLIGODENDROGLIAL EXOSOME RELEASE AND THE ROLE OF EXOSOMES IN RECIPROCAL NEURON-GLIA COMMUNICATION.** Electrically active neurons (N) release glutamate (1), which activates oligodendroglial ionotropic glutamate receptors provoking $Ca^{2+}$ influx into the oligodendrocyte (OL) (2). The rise in intracellular $Ca^{2+}$ forces MVBs to fuse with the plasma membrane resulting in the release of exosomes (3). The exosomes are internalized by neurons (4), resulting in functional retrieval of their cargo (5). Alternatively, oligodendroglial exosomes are internalized by microglia (M), what may lead to cargo degradation.

provoking $Ca^{2+}$ influx into the oligodendrocyte. The rise in intracellular $Ca^{2+}$ forces MVBs to fuse with the plasma membrane resulting in the release of exosomes from oligodendrocytes. In turn, the exosomes are internalized at the axonal or somatodendritic domain of neurons by clathrin- and dynamin-dependent endocytosis, resulting in functional retrieval of their protein and RNA cargo. This concept of an "on demand" support is further strengthened by the *in vivo* finding that MVBs are predominantly located within the non-compact myelin of the adaxonal loop. Fusion of MVBs with the oligodendroglial plasma membrane results in the release of exosomes into the periaxonal space, where they can in turn be internalized by the axon. In addition to the axonal uptake, exosomes are also internalized at the somatodendritic compartment with potentially different functional outcomes. This study does not only provide the proof of principle for the functional transfer of exosomal cargo, but further provides initial evidence that this transfer has functional implications on neuronal development, electrical activity, and gene expression.

## 6.1. NEURONAL UPTAKE OF EXOSOMES

This study shows that oligodendroglial exosomes are mainly internalized by microglia and neurons, while uptake by astrocytes and oligodendrocytes occurs only sporadically. Microglia internalize oligodendroglial exosomes non-selectively by macropinocytosis and the uptake most likely results in degradation of the exosomal cargo without inducing an inflammatory response (Fitzner et al., 2011). In contrast to microglia, neurons selectively internalize oligodendroglial exosomes by endocytosis requiring clathrin, dynamin, and actin polymerization. However, uptake of oligodendroglial exosomes is only detectable in 20% of the cultured neurons. It could either be that the remaining neurons internalize less exosomes and that the uptake is below the detection limit of the used methods, or that only a specific subtype of neurons internalizes oligodendroglial exosomes.

Selective uptake by neurons probably requires specific receptors on the neuronal surface. However, it remains unclear which receptors are responsible for the uptake of oligodendroglial exosomes by neurons. Exosomes can be regarded as a kind of "endogenous viruses" as they share common properties. Both, exosomes and viruses transfer various types of nucleic acids and use evolutionary conserved mechanisms for their biogenesis and release. It has been shown that some viruses enter their target cells after binding to cell surface heparan sulfate proteoglycans (HSPGs) (Shukla and Spear, 2001). A recent study provides evidence that the uptake of cancer cell derived exosomes also depends on the presence of HSPGs on the surface of recipient cells, indicating that endogenous exosomes and exogenous viruses share similar

uptake mechanisms (Christianson et al., 2013). Therefore, it may be possible that HSPGs or other sulfated receptors, e.g. sulfated lipids, glycoproteins, and tyrosine-sulfated proteins represent a conserved mechanism mediating exosome-uptake across different cell types, including neurons. Target cell specificity may also be achieved by exposure of distinct adhesion molecules like integrins and tetraspanins on the surface of exosomes (Rana and Zoller, 2011; Rana et al., 2012). Oligodendroglial exosomes express adhesion molecules like integrins, tetraspanins (CD63 and CD81), and the Ig superfamily member 8 (IGSF8) on their surface (Krämer-Albers et al., 2007), which may be involved in target cell selection and uptake.

After endocytosis, the internalized exosomes accumulate in late endosomal compartments. To become functionally retrieved by the recipient cell, the cargo must be sorted out of the late endosomes to reach the site of action. This may happen by back-fusion of the internalized exosomes with the limiting endosomal membrane resulting in the release of luminal proteins and RNAs into the cytosol of the recipient cell. However, we cannot completely exclude that a proportion of exosomes directly fuses with the plasma membrane of the target cell releasing the exosomal cargo into the cytoplasm. Especially at the axon, direct fusion would have some advantages compared to endocytosis. On the one hand, it might be faster and on the other hand, it would not require the whole endocytosis machinery.

## 6.2. OLIGODENDROGLIAL EXOSOMES IN INTERCELLULAR COMMUNICATION

The concept of exosomes as mediators of intercellular communication has been proven for various cell types outside the CNS (Raposo and Stoorvogel, 2013). Especially in the immune system, a multitude of functions has been ascribed to exosomes, for instance the presentation of antigens and the modulation of immune responses (Thery et al., 2009). In the CNS, the release of exosomes from primary rat cortical neurons is stimulated by glutamatergic synaptic activity involving intracellular $Ca^{2+}$ signaling (Lachenal et al., 2011). Similarly, the release of exosomes from oligodendrocytes is regulated by stimulation of ionotropic glutamate receptors and subsequently, the rise of intracellular $Ca^{2+}$ (Krämer-Albers et al., 2007; Frühbeis et al., 2013a). The neuronal exosomes carry the L1 cell adhesion molecule as well as the GluR2/3 AMPA receptor subunits and may modulate synaptic plasticity (Faure et al., 2006). The only described function of oligodendroglial exosomes so far was the modulation of myelin biogenesis by inhibition of myelin membrane sheath formation (Bakhti et al., 2011). Additionally, it has been demonstrated that microglial cells can internalize exosomes released by oligodendrocytes in an immunologically silent manner (Fitzner et al., 2011). The present study unravels a novel function of oligodendroglial exosomes as vehicles for the transfer of bioactive molecules from

oligodendrocytes to neurons and provides the first *in vitro* and *in vivo* evidence that target cells in the CNS can functionally retrieve exosomal cargo. The studies were performed using the Cre/loxP-system employing Cre-mediated recombination as a reporter. Intriguingly, injection of Cre-containing exosomes into the hippocampus and cerebellum of reporter mice provokes neuronal recombination based on a functional Cre transport. Together with the finding that neuronal recombination also occurs in MOGi-Cre/Rosa26-LacZ and MOGi-Cre/Rosa26-EGFP double transgenic mice, this is the first *in vivo* evidence for functional exosome transfer in the CNS. However, in transgenic mice MOGi-Cre mediated recombination predominantly occurred in granule cells of the cerebellum. Granule cells are very small cells with only 4-5 dendrites located within the granular layer of the cerebellar cortex. The thin and unmeylinated axon of granule cells rises to the upper molecular layer where it branches into two processes forming a parallel fiber. Since the axons are unmeylinated, the frequent recombination is probably not the result of Cre transfer via exosomes released from the adaxonal loop, but may be a consequence of residual MOG promoter activity during development.

Even though the Cre/loxP-system represents an artificial reporter system and may just provide a proof of principle for functional exosome transfer, it opens a new perspective on intercellular communication in the CNS. Exosomes carry a multitude of molecules including proteins, lipids, and nucleic acids that may affect recipient cells. Especially the functional transfer of mRNAs and miRNAs has gained particular attention in recent years (Valadi et al., 2007; Pegtel et al., 2010). Likewise, oligodendroglial exosomes contain mRNAs and miRNAs as well as various proteins with implied functions in metabolism and the relief of cell stress (Table 23) (Krämer-Albers et al., 2007). Among this large group of enzymes, many chaperones (e.g. HSP70, HSP90, and 14-3-3 proteins), metabolic enzymes (e.g. glyceraldehyde 3-phosphate dehydrogenase (GAPDH), pyruvate kinase, and carbonic anhydrase), and enzymes involved in the oxidative stress response (e.g. peroxiredoxin and glutathione S-transferase) can be found. By transporting these enzymes to neurons, oligodendroglial exosomes could essentially contribute to the supportive function of oligodendrocytes.

Recently, we showed that oligodendroglial exosomes have an impact on neuronal survival by protecting neurons from oxidative stress and starvation (Frühbeis et al., 2013a). However, the molecular determinants of this supportive function remained unclear. Interesting candidates are heat shock proteins (HSPs), which are up-regulated in response to heat shock or other cellular stress and are involved in folding and unfolding of other proteins. Their role in neuroprotection is well established and it has been shown previously that they can be supplemented from adjacent glial cells (Tytell, 2005; Brown, 2007). *In vitro* experiments demonstrated that cultured glioma cells release Hsc/Hsp70, which enhanced the neuronal stress tolerance of cultured neuroblastoma cells upon uptake (Guzhova et al., 2001). Moreover, it has been shown in squid

that Hsc/Hsp70 can be transferred from adjacent glial cells to the squid giant axon (Tytell et al., 1986). Interestingly, Hsc/Hsp70 and Hsc/Hsp90 are both present in oligodendroglial exosomes (Table 23) (Krämer-Albers et al., 2007) and Hsc/Hsp70 is transferred via exosomes from

**TABLE 23: EXOSOME-ASSOCIATED ENZYMES.** Exosome-associated enzymes and chaperones identified by proteomics performed with density-gradient purified exosomes isolated from primary oligodendrocytes. Adapted from (Krämer-Albers et al., 2007).

| | Accession | Entry | Description |
|---|---|---|---|
| **Enzymes (Oxidative Stress)** | O08553 | DPYL2_MOUSE | Dihydropyrimidinase related protein 2 |
| | Q62188 | DPYL3_MOUSE | Dihydropyrimidinase related protein 3 |
| | P19157 | GSTP1_MOUSE | Glutathione S transferase P 1 |
| | P35700 | PRDX1_MOUSE | Peroxiredoxin 1 |
| | Q61171 | PRDX2_MOUSE | Peroxiredoxin 2 |
| **Enzymes (Metabolism)** | P05064 | ALDOA_MOUSE | Fructose bisphosphate aldolase A |
| | P00920 | CAH2_MOUSE | Carbonic anhydrase 2 E |
| | Q8BVI4 | DHPR_MOUSE | Dihydropteridine reductase |
| | P17182 | ENOA_MOUSE | Alpha enolase |
| | P16858 | G3P_MOUSE | Glyceraldehyde 3 phosphate dehydrogenase |
| | P13707 | GPDA_MOUSE | Glycerol 3 phosphate dehydrogenase |
| | Q04447 | KCRB_MOUSE | Creatine kinase B type |
| | P52480 | KPYM_MOUSE | Pyruvate kinase isozyme M2 |
| | P14152 | MDHC_MOUSE | Malate dehydrogenase cytoplasmic |
| | P15532 | NDKA_MOUSE | Nucleoside diphosphate kinase A |
| | Q01768 | NDKB_MOUSE | Nucleoside diphosphate kinase B |
| | P09411 | PGK1_MOUSE | Phosphoglycerate kinase 1 |
| | P09041 | PGK2_MOUSE | Phosphoglycerate kinase testis specific |
| | Q8VDQ8 | SIRT2_MOUSE | NAD dependent deacetylase sirtuin 2 |
| | Q93092 | TALDO_MOUSE | Transaldolase |
| | Q01853 | TERA_MOUSE | Transitional endoplasmic reticulum ATPase |
| | P40142 | TKT_MOUSE | Transketolase |
| | P17751 | TPIS_MOUSE | Triosephosphate isomerase |
| | P61089 | UBE2N_MOUSE | Ubiquitin conjugating enzyme E2 |
| **Chaperones** | Q61696 | HS70A_MOUSE | Heat shock 70 kDa protein 1A |
| | P17879 | HS70B_MOUSE | Heat shock 70 kDa protein 1B |
| | P16627 | HS70L_MOUSE | Heat shock 70 kDa protein 1L |
| | P07901 | HS90A_MOUSE | Heat shock protein HSP 90 alpha |
| | P11499 | HS90B_MOUSE | Heat shock protein HSP 90 beta |
| | P17156 | HSP72_MOUSE | Heat shock related 70 kDa protein 2 |
| | P63017 | HSP7C_MOUSE | Heat shock cognate 71 kDa protein |
| | P17742 | PPIA_MOUSE | Peptidyl prolyl cis trans isomerase A |
| | Q9CQV8 | 1433B_MOUSE | 14 3 3 protein beta alpha |
| | P62259 | 1433E_MOUSE | 14 3 3 protein epsilon |
| | P68510 | 1433F_MOUSE | 14 3 3 protein eta |
| | P61982 | 1433G_MOUSE | 14 3 3 protein gamma |
| | P68254 | 1433T_MOUSE | 14 3 3 protein theta |
| | P63101 | 1433Z_MOUSE | 14 3 3 protein zeta delta |

oligodendrocytes to neurons. In addition to oligodendroglial exosomes, Hsc/Hsp70 is also released in association with astroglial exosomes in response to heat or oxidative stress

suggesting a signal-induced delivery of protective factors to neurons by the means of exosomes (Taylor et al., 2007).

Besides Hsc/Hsp70, also catalase is transferred to neurons via exosomes. Since catalase mediates the reaction of hydrogen peroxide to water and oxygen, this may be the molecular basis for the stress protective action of oligodendroglial exosomes.

Also in the PNS, the transfer of glial exosomes seems to be beneficial. Schwann cell-derived exosomes are internalized by axons from dorsal root ganglia *in vitro* and *in vivo* and increase axonal regeneration by inhibiting RhoA GTPase activity in growth cones (Lopez-Verrilli et al., 2013). Additionally, Schwann cell-derived ribosomes are also transferred to axons by vesicular means supplying injured axons locally with components of the protein synthesis machinery (Court et al., 2008; Court et al., 2011).

## 6.3. IMPACT OF EXOSOMES ON NEURONAL DIFFERENTIATION

Uptake of exosomes derived from the oligodendroglial precursor cell line Oli-*neu* but not from mature oligodendrocytes leads to a decreased Doublecortin (DCX) expression in recipient neurons, possibly by the transfer of glial miRNAs. We found the miRNAs miR-9, miR-17, and miR-19a with predicted binding to DCX in oligodendroglial exosomes. It has been shown previously that expression of all three miRNAs is down-regulated during oligodendrocyte maturation (Lau et al., 2008). This is consistent with the finding that transfer of exosomes derived from oligodendroglial precursor cells and not from mature oligodendrocytes decreased neuronal DCX expression.

DCX is a microtubule-stabilizing protein, which is mainly expressed by neuronal precursor cells and immature neurons (Horesh et al., 1999). Down-regulation of DCX is associated with neuronal maturation and differentiation. Oligodendroglial progenitor cells (NG2 cells) are equally distributed all over the adult brain. After CNS injury, induced acutely or through chronic diseases, a glial scar forms by enhanced proliferation and accumulation of glia around the lesion. The glial scar is thought to limit further injury and to promote tissue repair. Besides microglia, astrocytes, and macrophages, also NG2 cells accumulate at the injured site (Hughes et al., 2013). It is tempting to speculate that oligodendroglial precursors are involved in ongoing repair processes and may stimulate axonal regeneration via the secretion of exosomes. Although neurogenesis is very limited in the adult brain, after injury neuronal precursor cells could migrate into the lesioned area and start differentiation once they have sensed an exosomal stimulus. It may also be possible that neuronal precursors that migrate from the subventricular zone (SVZ) to the olfactory bulb along the rostral migratory stream start to differentiate once

they have come into contact with exosomes. Also during development, oligodendroglial exosomes may provide a differentiation signal to neurons, either initiating differentiation of neuronal precursor cells or keeping mature neurons in a differentiated state. However, this is entirely speculative and requires further studies.

## 6.4. Influence of Exosomes on Neuronal Activity

This study indicates that treatment of cultured neurons with oligodendroglial exosomes increases the neuronal electrical activity. Cultured neurons with already established synaptic connections exposed to exosomes generate more action potentials but at the same time fire less synchronized. This may be a sign for the rearrangement of neuronal circuits. Consistently, an excitatory effect has been reported previously for microglia-derived microvesicles, which stimulate spontaneous and evoked excitatory transmission in hippocampal neurons. Neurons exposed to microvesicles show an increase in miniature excitatory postsynaptic current (mEPSC) frequency without changes in mEPSC amplitude (Antonucci et al., 2012). It has been demonstrated that the microvesicles act at the presynaptic site of the excitatory synapse by increasing the release probability of synaptic vesicles through induction of the sphingolipid metabolism in neurons resulting in an increased ceramide and sphingosine production from sphingomyelin (Antonucci et al., 2012). Since oligodendroglial exosomes can also act at the somatodendritic site of the neurons, a similar mechanism may be responsible for the stimulation of neuronal activity by oligodendrocyte-derived exosomes.

## 6.5. Influence of Exosomes on Neuronal Gene Expression

This study provides evidence that treatment of cultured neurons with oligodendroglial exosomes results in differentially regulated genes. This could be a result of transferred exosomal shuttle RNAs or transcription factors. Alternatively, oligodendroglial exosome may initiate signal transductions pathways in the recipient neurons resulting in differentially expressed genes. However, the ability to modify neuronal gene expression by the release of exosomes enables oligodendrocytes to influence surrounding neurons. They could either transfer mRNAs encoding for proteins needed by the neurons, or transfer miRNAs to down-regulate the expression of distinct target genes.

The most significantly regulated genes are Plp, Ier3, Vgf, and Bdnf. Since PLP mRNA can be found in oligodendroglial exosomes, the up-regulation of Plp may be a consequence of transferred Plp mRNA via exosomes. It has been reported previously that mRNA is transferred between mast cells by the means of exosomes and translated into functional proteins within the target cells (Valadi et al., 2007). Knockdown of Ier3, Vgf, and Bdnf may be a result of transferred miRNAs. The transfer of miRNAs and the subsequent knockdown of their target genes have been shown before (Pegtel et al., 2010). Ier3 is an immediate early gene (IEGs) that is induced by a variety of stimuli such as growth factors, cytokines, ionizing radiation, viral infection, and other kinds of cellular stress (Arlt and Schafer, 2011). IER3 plays a complex and contradictory role in apoptosis and cell cycle control depending on the cellular context and the growth conditions (Arlt and Schafer, 2011). For instance, if the cells are grown in unfavorable conditions, IER3 acts pro-apoptotic, while grown in favorable conditions (sufficient serum and growth factors) it may rather be anti-apoptotic and involved in cell-cycle progression. It has been demonstrated that down-regulation of IER3 in HEK-293 cells results in a delayed cell-cycle transition and proliferation (Grobe et al., 2001). Accordingly, knockdown of Ier3 after exosome treatment may accompany the differentiation-promoting effect of oligodendroglial precursor cell-derived exosomes (see sections 5.9 and 6.3).

VGF and BDNF both belong to the class of growth factors. Growth factors in general and BDNF in particular are essential mediators of neuronal development, survival, axonal outgrowth, and synaptic plasticity. BDNF deficient mice show impaired hippocampal-dependent associative memory (Gorski et al., 2003). Moreover, BDNF signaling via its receptor TrkB plays a role in the pathology of depression and, consequently, decreased BDNF levels are found in depressed patients (Shimizu et al., 2003). Interestingly, direct infusion of BDNF into the hippocampus of adult rats increased neurogenesis of hippocampal neurons (Scharfman et al., 2005). BDNF induces the expression of Vgf via the transcription factor cAMP response element-binding protein (CREB) (Bozdagi et al., 2008), so reduced Vgf levels may be a consequence of decreased Bdnf expression. VGF is further processed into distinct polypeptides, which are subsequently released and exhibit a variety of functions, for instance the regulation of hippocampal synaptic plasticity and depressive behavior in rodents (Alder et al., 2003; Thakker-Varia et al., 2007). Moreover, it has been demonstrated that also VGF increases the proliferation rate of hippocampal neurons (Thakker-Varia et al., 2007), so the exosome-mediated down-regulation of Bdnf and Vgf may rather have differentiation-promoting effects. This is consistent with the finding that transfer of Oli-*neu*-derived exosomes reduces the expression of DCX in cultured neurons and may contribute to the differentiation initiating or differentiation preserving effect of oligodendroglial exosomes.

However, the functional relevance of transferred oligodendroglial RNA and in particular the exosome-mediated knockdown of Ier3, Vgf, and Bdnf will be subject of future studies.

## 6.6. OLIGODENDROGLIAL EXOSOMES IN NEURODEGENERATIVE DISEASES

Mice deficient for the myelin protein PLP are used as a model for spastic paraplegia type 2, a neurodegenerative disorder with progressive spasticity and weakness in the lower limbs due to the degeneration of distal parts oft the axons (Edgar and Nave, 2009). Cause of the axonal degenerations are axonal swellings, focal accumulations of axonal organelles and phosphorylated neurofilaments, leading to a breakdown of fast axonal transport. Similar symptoms can be observed in CNP-deficient mice (Lappe-Siefke et al., 2003). Interestingly, the transfer of exosomal cargo appears to be impaired in both mutants. This finding together with the fact that oligodendroglial exosomes contain a variety of metabolic and stress-protective proteins (Table 23), which are transferred from oligodendrocytes to neurons (e.g. Hsc/Hsp70 and catalase), makes it very tempting to speculate that exosome-mediated transfer of bioactive molecules may contribute to the glial support of axons. Recent studies provide evidence that oligodendrocytes directly support axons with energy metabolites like lactate via the monocarboxylate transporter 1 (MCT1) essentially contributing to the maintenance of axons (Fünfschilling et al., 2012; Lee et al., 2012). However, this finding alone does not suffice to explain the phenotype of PLP- and CNP-deficient mice, since the lack of PLP and CNP in these mutants cannot directly be linked to lactate supply. Therefore, the exosome-dependent delivery of RNA and proteins may accompany the transfer of energetic metabolites via MCT1, complementing the energy supply of neurons by delivering metabolizing enzymes. Intriguingly, electrically active neurons themselves can stimulate the secretion of exosomes from oligodendrocytes by the release of glutamate, linking the exosomal transfer to the neuronal energy consumption (Frühbeis et al., 2013a). In this neuron-glia interplay, exosomes could act as on demand supply for long myelinated axons.

However, the exosome-mediated neuron-glia communication may also be involved in pathological processes. It has been demonstrated that exosomes can be hijacked by various pathogens like viruses or pathogenic proteins, which use this physiological transfer route for their spreading. In the CNS, prions, APP as well as several APP cleavage products, SOD, α-synuclein, and phosphorylated tau are released in association with exosomes and have been suggested to be involved in disease progression (Bellingham et al., 2012; Schneider and Simons, 2013).

## 6.7. Oligodendroglial Exosomes – Promising Tools for Clinical Applications

In recent years, exosomes and other extracellular vesicles have emerged as valuable biomarkers as well as therapeutic targets in a variety of diseases. The exosomes released under disease conditions, e.g. during cancer or inflammation differ in composition and quantity from the ones secreted by healthy cells. For instance, exosomes and microvesicles present in the CSF have been suggested as biomarkers for multiple neurodegenerative disorders (Bellingham et al., 2012; Colombo et al., 2012). The amount of microglia derived microvesicles present in the CSF increases under brain inflammatory conditions like experimental autoimmune encephalomyelitis (EAE) or multiple sclerosis (Verderio et al., 2012). It remains to be analyzed whether under similar conditions the amount and composition of oligodendrocyte-derived exosomes and microvesicles is altered in a comparable way. Furthermore, exosomes derived from cells of the CNS are not only present in the CSF. It has been suggested that exosomes are able to pass the blood brain barrier making them promising candidates for the non-invasive diagnosis of brain diseases (Skog et al., 2008).

Recently, exosomes have been used as novel vehicles for gene therapy, successfully overcoming targeting difficulties and unwanted side effects of classical gene delivery vectors. For instance, the targeted delivery of GAPDH and BACE1 siRNA to the brain by systemic injection of exosomes led to knockdown of GAPDH and BACE1 in neurons, oligodendrocytes, and microglia. Not only nucleic acids but also distinct drugs can be delivered to the brain by the means of exosomes. The anti-inflammatory drugs curcumin and JSI124 encapsulated in exosomes were specifically and non-invasively targeted to microglial cells via intranasal application, protecting mice from brain inflammation, progression of EAE, and brain tumor growth (Zhuang et al., 2011). It will be interesting so see whether oligodendroglial exosomes also hold the potential to cross the blood brain barrier and deliver nucleic acids or drugs specifically to neurons and microglia in the brain, or vice versa can be detected as biomarkers of dysmeylinating disorders outside the brain.

## 6.8. Outlook

This study provides the proof of principle of an exosome-based intercellular communication in the brain by which oligodendrocytes may support neurons. Further studies should address the detailed determination of the uptake mechanisms. It has to be shown which receptors and target molecules are involved during the uptake of exosomes and which are responsible for target cell specificity. Interesting candidates could be cell surface heparan sulfate proteoglycans (HSPGs),

which have been reported previously to mediate the uptake of cancer cell derived exosomes (Christianson et al., 2013). Moreover, further studies are needed to show whether all or just a subtype of neurons internalize oligodendroglial exosomes. Therefore, oligodendrocyte-derived exosomes could be applied to distinct neuronal subtypes, for instance cortical or hippocampal neurons, and the uptake could be visualized as described previously in this study.

The most interesting part will be to further unravel the functional implications of the exosome-mediated transfer of bioactive molecules from oligodendrocytes to neurons. Further investigations should determine how horizontal transfer of genetic information can affect the phenotype of target cells and whether the knockdown of Ier3, Bdnf, and Vgf is mediated by exosomal miRNAs. First, the presence of miRNAs with predicted binding sites to these mRNAs should be confirmed in oligodendroglial exosomes by qRT-PCR and second, the use of specific miRNA inhibitors may demonstrate that these miRNAs are indeed responsible for the target gene knockdown within neurons.

Moreover, it will be intriguing to see if oligodendroglial exosomes indeed have the potential to metabolically support neurons and promote their survival. Initial results indicate the potential of oligodendroglial exosomes as protective agents under distinct stress conditions (Frühbeis et al., 2013a). Further studies are needed to unravel the detailed mechanism of this supportive function. Moreover, the molecular determinants of the support have to be identified. Comprehensive screens like proteomics, next generation sequencing, metabolomics, or phosphorylation assays either of the target cells or of the exosomes themselves could shed light on interesting candidates mediating the supportive effect. However, it will be interesting to see whether the therapeutic application of oligodendroglial exosomes in PLP and CNP knockout mice has the potential to ameliorate the symptoms of these mutants. To validate that the supportive effect can indeed be attributed to oligodendroglial exosomes, a conditional knockout that specifically interferes with exosome secretion from oligodendrocytes *in vivo* may be instructive. This could not be achieved so far since all candidates investigated, e.g. Rab35 or Rab27a and -b, could never completely abolish exosome secretion.

Finally, to investigate the potential of oligodendroglial exosomes in clinical applications may provide valuable results. Analysis of CSF or blood samples from patients suffering from multiple sclerosis or leukodystrophies compared to healthy controls may provide new insights for the use of oligodendroglial exosomes as diagnostic markers in these kinds of diseases. Moreover, to test the potential of oligodendroglial exosomes as future gene therapy vectors for the delivery of nucleic acids or drugs to the brain could hold great potential for future applications.

# 7. REFERENCES

Abounit, S. and Zurzolo, C. (2012). "Wiring through tunneling nanotubes--from electrical signals to organelle transfer." J Cell Sci **125**(Pt 5): 1089-1098.

Al-Nedawi, K., Meehan, B. and Rak, J. (2009). "Microvesicles: messengers and mediators of tumor progression." Cell Cycle **8**(13): 2014-2018.

Alder, J., Thakker-Varia, S., Bangasser, D. A., Kuroiwa, M., Plummer, M. R., Shors, T. J. and Black, I. B. (2003). "Brain-derived neurotrophic factor-induced gene expression reveals novel actions of VGF in hippocampal synaptic plasticity." J Neurosci **23**(34): 10800-10808.

Allen, N. J. and Barres, B. A. (2009). "Neuroscience: Glia - more than just brain glue." Nature **457**(7230): 675-677.

Alvarez-Erviti, L., Seow, Y., Yin, H., Betts, C., Lakhal, S. and Wood, M. J. (2011). "Delivery of siRNA to the mouse brain by systemic injection of targeted exosomes." Nature biotechnology **29**(4): 341-345.

Antonucci, F., Turola, E., Riganti, L., Caleo, M., Gabrielli, M., Perrotta, C., Novellino, L., Clementi, E., Giussani, P., Viani, P., Matteoli, M. and Verderio, C. (2012). "Microvesicles released from microglia stimulate synaptic activity via enhanced sphingolipid metabolism." EMBO J **31**(5): 1231-1240.

Arlt, A. and Schafer, H. (2011). "Role of the immediate early response 3 (IER3) gene in cellular stress response, inflammation and tumorigenesis." Eur J Cell Biol **90**(6-7): 545-552.

Bakhti, M., Winter, C. and Simons, M. (2011). "Inhibition of myelin membrane sheath formation by oligodendrocyte-derived exosome-like vesicles." J Biol Chem **286**(1): 787-796.

Basso, M., Pozzi, S., Tortarolo, M., Fiordaliso, F., Bisighini, C., Pasetto, L., Spaltro, G., Lidonnici, D., Gensano, F., Battaglia, E., Bendotti, C. and Bonetto, V. (2013). "Mutant copper-zinc superoxide dismutase (SOD1) induces protein secretion pathway alterations and exosome release in astrocytes: implications for disease spreading and motor neuron pathology in amyotrophic lateral sclerosis." J Biol Chem **288**(22): 15699-15711.

Bellingham, S. A., Guo, B. B., Coleman, B. M. and Hill, A. F. (2012). "Exosomes: vehicles for the transfer of toxic proteins associated with neurodegenerative diseases?" Front Physiol **3**: 124.

Bergersen, L., Rafiki, A. and Ottersen, O. P. (2002). "Immunogold cytochemistry identifies specialized membrane domains for monocarboxylate transport in the central nervous system." Neurochem Res **27**(1-2): 89-96.

Bernimoulin, M., Waters, E. K., Foy, M., Steele, B. M., Sullivan, M., Falet, H., Walsh, M. T., Barteneva, N., Geng, J. G., Hartwig, J. H., Maguire, P. B. and Wagner, D. D. (2009). "Differential stimulation of monocytic cells results in distinct populations of microparticles." J Thromb Haemost **7**(6): 1019-1028.

Bianco, F., Perrotta, C., Novellino, L., Francolini, M., Riganti, L., Menna, E., Saglietti, L., Schuchman, E. H., Furlan, R., Clementi, E., Matteoli, M. and Verderio, C. (2009). "Acid sphingomyelinase activity triggers microparticle release from glial cells." EMBO J **28**(8): 1043-1054.

Bianco, F., Pravettoni, E., Colombo, A., Schenk, U., Moller, T., Matteoli, M. and Verderio, C. (2005). "Astrocyte-derived ATP induces vesicle shedding and IL-1 beta release from microglia." J Immunol **174**(11): 7268-7277.

Bozdagi, O., Rich, E., Tronel, S., Sadahiro, M., Patterson, K., Shapiro, M. L., Alberini, C. M., Huntley, G. W. and Salton, S. R. (2008). "The neurotrophin-inducible gene Vgf regulates hippocampal function and behavior through a brain-derived neurotrophic factor-dependent mechanism." J Neurosci **28**(39): 9857-9869.

Brown, I. R. (2007). "Heat shock proteins and protection of the nervous system." Ann N Y Acad Sci **1113**: 147-158.

Cahoy, J. D., Emery, B., Kaushal, A., Foo, L. C., Zamanian, J. L., Christopherson, K. S., Xing, Y., Lubischer, J. L., Krieg, P. A., Krupenko, S. A., Thompson, W. J. and Barres, B. A. (2008). "A transcriptome database for astrocytes, neurons, and oligodendrocytes: a new resource for understanding brain development and function." J Neurosci **28**(1): 264-278.

Ceruti, S., Colombo, L., Magni, G., Vigano, F., Boccazzi, M., Deli, M. A., Sperlagh, B., Abbracchio, M. P. and Kittel, A. (2011). "Oxygen-glucose deprivation increases the enzymatic activity and the microvesicle-mediated release of ectonucleotidases in the cells composing the blood-brain barrier." Neurochem Int **59**(2): 259-271.

Chen, S., Rio, C., Ji, R. R., Dikkes, P., Coggeshall, R. E., Woolf, C. J. and Corfas, G. (2003). "Disruption of ErbB receptor signaling in adult non-myelinating Schwann cells causes progressive sensory loss." Nat Neurosci **6**(11): 1186-1193.

Chieregatti, E. and Meldolesi, J. (2005). "Regulated exocytosis: new organelles for non-secretory purposes." Nat Rev Mol Cell Biol **6**(2): 181-187.

Chivet, M., Hemming, F., Pernet-Gallay, K., Fraboulet, S. and Sadoul, R. (2012). "Emerging role of neuronal exosomes in the central nervous system." Front Physiol **3**: 145.

Chivet, M., Javalet, C., Hemming, F., Pernet-Gallay, K., Laulagnier, K., Fraboulet, S. and Sadoul, R. (2013). "Exosomes as a novel way of interneuronal communication." Biochem Soc Trans **41**(1): 241-244.

Christianson, H. C., Svensson, K. J., van Kuppevelt, T. H., Li, J. P. and Belting, M. (2013). "Cancer cell exosomes depend on cell-surface heparan sulfate proteoglycans for their internalization and functional activity." Proc Natl Acad Sci U S A.

Cocucci, E., Racchetti, G. and Meldolesi, J. (2009). "Shedding microvesicles: artefacts no more." Trends Cell Biol **19**(2): 43-51.

Colombo, E., Borgiani, B., Verderio, C. and Furlan, R. (2012). "Microvesicles: novel biomarkers for neurological disorders." Front Physiol **3**: 63.

Conde-Vancells, J., Rodriguez-Suarez, E., Embade, N., Gil, D., Matthiesen, R., Valle, M., Elortza, F., Lu, S. C., Mato, J. M. and Falcon-Perez, J. M. (2008). "Characterization and comprehensive proteome profiling of exosomes secreted by hepatocytes." J Proteome Res **7**(12): 5157-5166.

Court, F. A., Hendriks, W. T., MacGillavry, H. D., Alvarez, J. and van Minnen, J. (2008). "Schwann cell to axon transfer of ribosomes: toward a novel understanding of the role of glia in the nervous system." J Neurosci **28**(43): 11024-11029.

Court, F. A., Midha, R., Cisterna, B. A., Grochmal, J., Shakhbazau, A., Hendriks, W. T. and Van Minnen, J. (2011). "Morphological evidence for a transport of ribosomes from Schwann cells to regenerating axons." Glia **59**(10): 1529-1539.

Del Conde, I., Shrimpton, C. N., Thiagarajan, P. and Lopez, J. A. (2005). "Tissue-factor-bearing microvesicles arise from lipid rafts and fuse with activated platelets to initiate coagulation." Blood **106**(5): 1604-1611.

Denzer, K., van Eijk, M., Kleijmeer, M. J., Jakobson, E., de Groot, C. and Geuze, H. J. (2000). "Follicular dendritic cells carry MHC class II-expressing microvesicles at their surface." J Immunol **165**(3): 1259-1265.

During, M. J., Young, D., Baer, K., Lawlor, P. and Klugmann, M. (2003). "Development and optimization of adeno-associated virus vector transfer into the central nervous system." Methods in molecular medicine **76**: 221-236.

Edgar, J. M., McLaughlin, M., Werner, H. B., McCulloch, M. C., Barrie, J. A., Brown, A., Faichney, A. B., Snaidero, N., Nave, K. A. and Griffiths, I. R. (2009). "Early ultrastructural defects of axons and axon-glia junctions in mice lacking expression of Cnp1." Glia **57**(16): 1815-1824.

Edgar, J. M., McLaughlin, M., Yool, D., Zhang, S. C., Fowler, J. H., Montague, P., Barrie, J. A., McCulloch, M. C., Duncan, I. D., Garbern, J., Nave, K. A. and Griffiths, I. R. (2004). "Oligodendroglial modulation of fast axonal transport in a mouse model of hereditary spastic paraplegia." J Cell Biol **166**(1): 121-131.

Edgar, J. M. and Nave, K. A. (2009). "The role of CNS glia in preserving axon function." Curr Opin Neurobiol **19**(5): 498-504.

Escudier, B., Dorval, T., Chaput, N., Andre, F., Caby, M. P., Novault, S., Flament, C., Leboulaire, C., Borg, C., Amigorena, S., Boccaccio, C., Bonnerot, C., Dhellin, O., Movassagh, M., Piperno, S., Robert, C., Serra, V., Valente, N., Le Pecq, J. B., Spatz, A., Lantz, O., Tursz, T., Angevin, E. and Zitvogel, L. (2005). "Vaccination of metastatic melanoma patients with autologous dendritic cell (DC) derived-exosomes: results of thefirst phase I clinical trial." J Transl Med **3**(1): 10.

Faure, J., Lachenal, G., Court, M., Hirrlinger, J., Chatellard-Causse, C., Blot, B., Grange, J., Schoehn, G., Goldberg, Y., Boyer, V., Kirchhoff, F., Raposo, G., Garin, J. and Sadoul, R. (2006). "Exosomes are released by cultured cortical neurones." Mol Cell Neurosci **31**(4): 642-648.

Fevrier, B. and Raposo, G. (2004). "Exosomes: endosomal-derived vesicles shipping extracellular messages." Curr Opin Cell Biol **16**(4): 415-421.

Fevrier, B., Vilette, D., Archer, F., Loew, D., Faigle, W., Vidal, M., Laude, H. and Raposo, G. (2004). "Cells release prions in association with exosomes." Proc Natl Acad Sci U S A **101**(26): 9683-9688.

Fitzner, D., Schnaars, M., van Rossum, D., Krishnamoorthy, G., Dibaj, P., Bakhti, M., Regen, T., Hanisch, U. K. and Simons, M. (2011). "Selective transfer of exosomes from oligodendrocytes to microglia by macropinocytosis." J Cell Sci **124**(Pt 3): 447-458.

Frühbeis, C., Fröhlich, D. and Krämer-Albers, E. M. (2012). "Emerging roles of exosomes in neuron-glia communication." Front Physiol **3**: 119.

Frühbeis, C., Fröhlich, D., Kuo, W. P., Amphornrat, J., Thilemann, S., Saab, A. S., Kirchhoff, F., Möbius, W., Goebbels, S., Nave, K. A., Schneider, A., Simons, M., Klugmann, M., Trotter, J. and

Krämer-Albers, E. M. (2013a). "Neurotransmitter-triggered transfer of exosomes mediates oligodendrocyte-neuron communication." PLoS Biol **11**(7): e1001604.

Frühbeis, C., Fröhlich, D., Kuo, W. P. and Krämer-Albers, E. M. (2013b). "Extracellular vesicles as mediators of neuron-glia communication." Front Cell Neurosci **7**: 182.

Fünfschilling, U., Supplie, L. M., Mahad, D., Boretius, S., Saab, A. S., Edgar, J., Brinkmann, B. G., Kassmann, C. M., Tzvetanova, I. D., Mobius, W., Diaz, F., Meijer, D., Suter, U., Hamprecht, B., Sereda, M. W., Moraes, C. T., Frahm, J., Goebbels, S. and Nave, K. A. (2012). "Glycolytic oligodendrocytes maintain myelin and long-term axonal integrity." Nature **485**(7399): 517-521.

Futter, C. E., Pearse, A., Hewlett, L. J. and Hopkins, C. R. (1996). "Multivesicular endosomes containing internalized EGF-EGF receptor complexes mature and then fuse directly with lysosomes." J Cell Biol **132**(6): 1011-1023.

Gan, X. and Gould, S. J. (2011). "Identification of an inhibitory budding signal that blocks the release of HIV particles and exosome/microvesicle proteins." Mol Biol Cell **22**(6): 817-830.

Gerdes, H. H. and Carvalho, R. N. (2008). "Intercellular transfer mediated by tunneling nanotubes." Curr Opin Cell Biol **20**(4): 470-475.

Ghosh, A., Manrique-Hoyos, N., Voigt, A., Schulz, J. B., Kreutzfeldt, M., Merkler, D. and Simons, M. (2011). "Targeted ablation of oligodendrocytes triggers axonal damage." PLoS One **6**(7): e22735.

Gorski, J. A., Balogh, S. A., Wehner, J. M. and Jones, K. R. (2003). "Learning deficits in forebrain-restricted brain-derived neurotrophic factor mutant mice." Neuroscience **121**(2): 341-354.

Gould, S. J., Booth, A. M. and Hildreth, J. E. (2003). "The Trojan exosome hypothesis." Proc Natl Acad Sci U S A **100**(19): 10592-10597.

Gousset, K., Schiff, E., Langevin, C., Marijanovic, Z., Caputo, A., Browman, D. T., Chenouard, N., de Chaumont, F., Martino, A., Enninga, J., Olivo-Marin, J. C., Mannel, D. and Zurzolo, C. (2009). "Prions hijack tunnelling nanotubes for intercellular spread." Nat Cell Biol **11**(3): 328-336.

Gravel, M., Robert, F., Kottis, V., Gallouzi, I. E., Pelletier, J. and Braun, P. E. (2009). "2',3'-Cyclic nucleotide 3'-phosphodiesterase: a novel RNA-binding protein that inhibits protein synthesis." J Neurosci Res **87**(5): 1069-1079.

Griffiths, I., Klugmann, M., Anderson, T., Yool, D., Thomson, C., Schwab, M. H., Schneider, A., Zimmermann, F., McCulloch, M., Nadon, N. and Nave, K. A. (1998). "Axonal swellings and degeneration in mice lacking the major proteolipid of myelin." Science **280**(5369): 1610-1613.

Grobe, O., Arlt, A., Ungefroren, H., Krupp, G., Folsch, U. R., Schmidt, W. E. and Schafer, H. (2001). "Functional disruption of IEX-1 expression by concatemeric hammerhead ribozymes alters growth properties of 293 cells." FEBS Lett **494**(3): 196-200.

Gross, J. C., Chaudhary, V., Bartscherer, K. and Boutros, M. (2012). "Active Wnt proteins are secreted on exosomes." Nat Cell Biol **14**(10): 1036-1045.

Guescini, M., Genedani, S., Stocchi, V. and Agnati, L. F. (2010). "Astrocytes and Glioblastoma cells release exosomes carrying mtDNA." J Neural Transm **117**(1): 1-4.

Guggenhuber, S., Monory, K., Lutz, B. and Klugmann, M. (2010). "AAV vector-mediated overexpression of CB1 cannabinoid receptor in pyramidal neurons of the hippocampus protects against seizure-induced excitoxicity." PLoS One **5**(12): e15707.

Gurke, S., Barroso, J. F. and Gerdes, H. H. (2008). "The art of cellular communication: tunneling nanotubes bridge the divide." Histochem Cell Biol **129**(5): 539-550.

Guzhova, I., Kislyakova, K., Moskaliova, O., Fridlanskaya, I., Tytell, M., Cheetham, M. and Margulis, B. (2001). "In vitro studies show that Hsp70 can be released by glia and that exogenous Hsp70 can enhance neuronal stress tolerance." Brain Res **914**(1-2): 66-73.

Hajrasouliha, A. R., Jiang, G., Lu, Q., Lu, H., Kaplan, H. J., Zhang, H. G. and Shao, H. (2013). "Exosomes from retinal astrocytes contain anti-angiogenic components that inhibit laser-induced choroidal neovascularization." J Biol Chem.

Hanisch, U. K. and Kettenmann, H. (2007). "Microglia: active sensor and versatile effector cells in the normal and pathologic brain." Nat Neurosci **10**(11): 1387-1394.

Hauck, B., Chen, L. and Xiao, W. (2003). "Generation and characterization of chimeric recombinant AAV vectors." Molecular therapy : the journal of the American Society of Gene Therapy **7**(3): 419-425.

Hooper, C., Sainz-Fuertes, R., Lynham, S., Hye, A., Killick, R., Warley, A., Bolondi, C., Pocock, J. and Lovestone, S. (2012). "Wnt3a induces exosome secretion from primary cultured rat microglia." BMC Neurosci **13**: 144.

Horesh, D., Sapir, T., Francis, F., Wolf, S. G., Caspi, M., Elbaum, M., Chelly, J. and Reiner, O. (1999). "Doublecortin, a stabilizer of microtubules." Hum Mol Genet **8**(9): 1599-1610.

Hovelmeyer, N., Hao, Z., Kranidioti, K., Kassiotis, G., Buch, T., Frommer, F., von Hoch, L., Kramer, D., Minichiello, L., Kollias, G., Lassmann, H. and Waisman, A. (2005). "Apoptosis of oligodendrocytes via Fas and TNF-R1 is a key event in the induction of experimental autoimmune encephalomyelitis." J Immunol **175**(9): 5875-5884.

Hsu, C., Morohashi, Y., Yoshimura, S., Manrique-Hoyos, N., Jung, S., Lauterbach, M. A., Bakhti, M., Gronborg, M., Mobius, W., Rhee, J., Barr, F. A. and Simons, M. (2010). "Regulation of exosome secretion by Rab35 and its GTPase-activating proteins TBC1D10A-C." J Cell Biol **189**(2): 223-232.

Hu, G., Yao, H., Chaudhuri, A. D., Duan, M., Yelamanchili, S. V., Wen, H., Cheney, P. D., Fox, H. S. and Buch, S. (2012). "Exosome-mediated shuttling of microRNA-29 regulates HIV Tat and morphine-mediated neuronal dysfunction." Cell Death Dis **3**: e381.

Hughes, E. G., Kang, S. H., Fukaya, M. and Bergles, D. E. (2013). "Oligodendrocyte progenitors balance growth with self-repulsion to achieve homeostasis in the adult brain." Nat Neurosci **16**(6): 668-676.

Hurley, J. H. (2008). "ESCRT complexes and the biogenesis of multivesicular bodies." Curr Opin Cell Biol **20**(1): 4-11.

Irion, U. and St Johnston, D. (2007). "bicoid RNA localization requires specific binding of an endosomal sorting complex." Nature **445**(7127): 554-558.

Johnstone, R. M. (2006). "Exosomes biological significance: A concise review." Blood Cells Mol Dis **36**(2): 315-321.

Johnstone, R. M., Mathew, A., Mason, A. B. and Teng, K. (1991). "Exosome formation during maturation of mammalian and avian reticulocytes: evidence that exosome release is a major route for externalization of obsolete membrane proteins." J Cell Physiol **147**(1): 27-36.

Jung, M., Kramer, E., Grzenkowski, M., Tang, K., Blakemore, W., Aguzzi, A., Khazaie, K., Chlichlia, K., von Blankenfeld, G., Kettenmann, H. and et al. (1995). "Lines of murine oligodendroglial precursor cells immortalized by an activated neu tyrosine kinase show distinct degrees of interaction with axons in vitro and in vivo." The European journal of neuroscience **7**(6): 1245-1265.

Karadottir, R. and Attwell, D. (2007). "Neurotransmitter receptors in the life and death of oligodendrocytes." Neuroscience **145**(4): 1426-1438.

Kassmann, C. M., Lappe-Siefke, C., Baes, M., Brugger, B., Mildner, A., Werner, H. B., Natt, O., Michaelis, T., Prinz, M., Frahm, J. and Nave, K. A. (2007). "Axonal loss and neuroinflammation caused by peroxisome-deficient oligodendrocytes." Nat Genet **39**(8): 969-976.

Kassmann, C. M., Quintes, S., Rietdorf, J., Mobius, W., Sereda, M. W., Nientiedt, T., Saher, G., Baes, M. and Nave, K. A. (2011). "A role for myelin-associated peroxisomes in maintaining paranodal loops and axonal integrity." FEBS Lett **585**(14): 2205-2211.

Klugmann, M., Symes, C. W., Leichtlein, C. B., Klaussner, B. K., Dunning, J., Fong, D., Young, D. and During, M. J. (2005). "AAV-mediated hippocampal expression of short and long Homer 1 proteins differentially affect cognition and seizure activity in adult rats." Molecular and cellular neurosciences **28**(2): 347-360.

Korkut, C., Ataman, B., Ramachandran, P., Ashley, J., Barria, R., Gherbesi, N. and Budnik, V. (2009). "Trans-synaptic transmission of vesicular Wnt signals through Evi/Wntless." Cell **139**(2): 393-404.

Korkut, C., Li, Y., Koles, K., Brewer, C., Ashley, J., Yoshihara, M. and Budnik, V. (2013). "Regulation of postsynaptic retrograde signaling by presynaptic exosome release." Neuron **77**(6): 1039-1046.

Krämer-Albers, E. M., Bretz, N., Tenzer, S., Winterstein, C., Möbius, W., Berger, H., Nave, K. A., Schild, H. and Trotter, J. (2007). "Oligodendrocytes secrete exosomes containing major myelin and stress-protective proteins: Trophic support for axons?" Proteomics Clin Appl **1**(11): 1446-1461.

Krämer-Albers, E. M. and Frühbeis, C. (2013). "Delivery on call: Exosomes as "Care packages" from glia cells for stressed neurons." Neuroforum **04/2013**: 146-152.

Kumar, P., Wu, H., McBride, J. L., Jung, K. E., Kim, M. H., Davidson, B. L., Lee, S. K., Shankar, P. and Manjunath, N. (2007). "Transvascular delivery of small interfering RNA to the central nervous system." Nature **448**(7149): 39-43.

Lachenal, G., Pernet-Gallay, K., Chivet, M., Hemming, F. J., Belly, A., Bodon, G., Blot, B., Haase, G., Goldberg, Y. and Sadoul, R. (2011). "Release of exosomes from differentiated neurons and its regulation by synaptic glutamatergic activity." Mol Cell Neurosci **46**(2): 409-418.

Lappe-Siefke, C., Goebbels, S., Gravel, M., Nicksch, E., Lee, J., Braun, P. E., Griffiths, I. R. and Nave, K. A. (2003). "Disruption of Cnp1 uncouples oligodendroglial functions in axonal support and myelination." Nat Genet **33**(3): 366-374.

Lau, P., Verrier, J. D., Nielsen, J. A., Johnson, K. R., Notterpek, L. and Hudson, L. D. (2008). "Identification of dynamically regulated microRNA and mRNA networks in developing oligodendrocytes." J Neurosci **28**(45): 11720-11730.

Le Pecq, J. B. (2005). "Dexosomes as a therapeutic cancer vaccine: from bench to bedside." Blood Cells Mol Dis **35**(2): 129-135.

Lee, J., Gravel, M., Zhang, R., Thibault, P. and Braun, P. E. (2005). "Process outgrowth in oligodendrocytes is mediated by CNP, a novel microtubule assembly myelin protein." J Cell Biol **170**(4): 661-673.

Lee, Y., Morrison, B. M., Li, Y., Lengacher, S., Farah, M. H., Hoffman, P. N., Liu, Y., Tsingalia, A., Jin, L., Zhang, P. W., Pellerin, L., Magistretti, P. J. and Rothstein, J. D. (2012). "Oligodendroglia metabolically support axons and contribute to neurodegeneration." Nature **487**(7408): 443-448.

Liu, J., Li, L. and Suo, W. Z. (2009). "HT22 hippocampal neuronal cell line possesses functional cholinergic properties." Life sciences **84**(9-10): 267-271.

Locatelli, G., Wortge, S., Buch, T., Ingold, B., Frommer, F., Sobottka, B., Kruger, M., Karram, K., Buhlmann, C., Bechmann, I., Heppner, F. L., Waisman, A. and Becher, B. (2012). "Primary oligodendrocyte death does not elicit anti-CNS immunity." Nat Neurosci **15**(4): 543-550.

Lopez-Verrilli, M. A. and Court, F. A. (2012). "Transfer of vesicles from schwann cells to axons: a novel mechanism of communication in the peripheral nervous system." Front Physiol **3**: 205.

Lopez-Verrilli, M. A., Picou, F. and Court, F. A. (2013). "Schwann cell-derived exosomes enhance axonal regeneration in the peripheral nervous system." Glia.

Macia, E., Ehrlich, M., Massol, R., Boucrot, E., Brunner, C. and Kirchhausen, T. (2006). "Dynasore, a cell-permeable inhibitor of dynamin." Dev Cell **10**(6): 839-850.

Madduri, S. and Gander, B. (2010). "Schwann cell delivery of neurotrophic factors for peripheral nerve regeneration." J Peripher Nerv Syst **15**(2): 93-103.

Marzo, L., Gousset, K. and Zurzolo, C. (2012). "Multifaceted roles of tunneling nanotubes in intercellular communication." Front Physiol **3**: 72.

Mathivanan, S., Ji, H. and Simpson, R. J. (2010). "Exosomes: extracellular organelles important in intercellular communication." J Proteomics **73**(10): 1907-1920.

Morrison, B. M., Lee, Y. and Rothstein, J. D. (2013). "Oligodendroglia metabolically support axons and maintain structural integrity." Trends Cell Biol.

Morse, M. A., Garst, J., Osada, T., Khan, S., Hobeika, A., Clay, T. M., Valente, N., Shreeniwas, R., Sutton, M. A., Delcayre, A., Hsu, D. H., Le Pecq, J. B. and Lyerly, H. K. (2005). "A phase I study of dexosome immunotherapy in patients with advanced non-small cell lung cancer." J Transl Med **3**(1): 9.

Muralidharan-Chari, V., Clancy, J., Plou, C., Romao, M., Chavrier, P., Raposo, G. and D'Souza-Schorey, C. (2009). "ARF6-regulated shedding of tumor cell-derived plasma membrane microvesicles." Curr Biol **19**(22): 1875-1885.

Nave, K. A. (2010a). "Myelination and support of axonal integrity by glia." Nature **468**(7321): 244-252.

Nave, K. A. (2010b). "Myelination and the trophic support of long axons." Nat Rev Neurosci **11**(4): 275-283.

Nguyen, D. G., Booth, A., Gould, S. J. and Hildreth, J. E. (2003). "Evidence that HIV budding in primary macrophages occurs through the exosome release pathway." J Biol Chem **278**(52): 52347-52354.

Oluich, L. J., Stratton, J. A., Xing, Y. L., Ng, S. W., Cate, H. S., Sah, P., Windels, F., Kilpatrick, T. J. and Merson, T. D. (2012). "Targeted ablation of oligodendrocytes induces axonal pathology independent of overt demyelination." J Neurosci **32**(24): 8317-8330.

Onfelt, B., Nedvetzki, S., Yanagi, K. and Davis, D. M. (2004). "Cutting edge: Membrane nanotubes connect immune cells." J Immunol **173**(3): 1511-1513.

Ostrowski, M., Carmo, N. B., Krumeich, S., Fanget, I., Raposo, G., Savina, A., Moita, C. F., Schauer, K., Hume, A. N., Freitas, R. P., Goud, B., Benaroch, P., Hacohen, N., Fukuda, M., Desnos, C., Seabra, M. C., Darchen, F., Amigorena, S., Moita, L. F. and Thery, C. (2010). "Rab27a and Rab27b control different steps of the exosome secretion pathway." Nat Cell Biol **12**(1): 19-30; sup pp 11-13.

Pegtel, D. M., Cosmopoulos, K., Thorley-Lawson, D. A., van Eijndhoven, M. A., Hopmans, E. S., Lindenberg, J. L., de Gruijl, T. D., Wurdinger, T. and Middeldorp, J. M. (2010). "Functional delivery of viral miRNAs via exosomes." Proc Natl Acad Sci U S A **107**(14): 6328-6333.

Pizzirani, C., Ferrari, D., Chiozzi, P., Adinolfi, E., Sandona, D., Savaglio, E. and Di Virgilio, F. (2007). "Stimulation of P2 receptors causes release of IL-1beta-loaded microvesicles from human dendritic cells." Blood **109**(9): 3856-3864.

Potolicchio, I., Carven, G. J., Xu, X., Stipp, C., Riese, R. J., Stern, L. J. and Santambrogio, L. (2005). "Proteomic analysis of microglia-derived exosomes: metabolic role of the aminopeptidase CD13 in neuropeptide catabolism." J Immunol **175**(4): 2237-2243.

Prada, I., Furlan, R., Matteoli, M. and Verderio, C. (2013). "Classical and unconventional pathways of vesicular release in microglia." Glia **61**(7): 1003-1017.

Proia, P., Schiera, G., Mineo, M., Ingrassia, A. M., Santoro, G., Savettieri, G. and Di Liegro, I. (2008). "Astrocytes shed extracellular vesicles that contain fibroblast growth factor-2 and vascular endothelial growth factor." Int J Mol Med **21**(1): 63-67.

Rafiki, A., Boulland, J. L., Halestrap, A. P., Ottersen, O. P. and Bergersen, L. (2003). "Highly differential expression of the monocarboxylate transporters MCT2 and MCT4 in the developing rat brain." Neuroscience **122**(3): 677-688.

Rak, J. (2010). "Microparticles in cancer." Semin Thromb Hemost **36**(8): 888-906.

Rana, S., Yue, S., Stadel, D. and Zoller, M. (2012). "Toward tailored exosomes: the exosomal tetraspanin web contributes to target cell selection." Int J Biochem Cell Biol **44**(9): 1574-1584.

Rana, S. and Zoller, M. (2011). "Exosome target cell selection and the importance of exosomal tetraspanins: a hypothesis." Biochem Soc Trans **39**(2): 559-562.

Ransohoff, R. M. and Cardona, A. E. (2010). "The myeloid cells of the central nervous system parenchyma." Nature **468**(7321): 253-262.

Raposo, G., Nijman, H. W., Stoorvogel, W., Liejendekker, R., Harding, C. V., Melief, C. J. and Geuze, H. J. (1996). "B lymphocytes secrete antigen-presenting vesicles." J Exp Med **183**(3): 1161-1172.

Raposo, G. and Stoorvogel, W. (2013). "Extracellular vesicles: exosomes, microvesicles, and friends." J Cell Biol **200**(4): 373-383.

Rosenbluth, J., Nave, K. A., Mierzwa, A. and Schiff, R. (2006). "Subtle myelin defects in PLP-null mice." Glia **54**(3): 172-182.

Rustom, A., Saffrich, R., Markovic, I., Walther, P. and Gerdes, H. H. (2004). "Nanotubular highways for intercellular organelle transport." Science **303**(5660): 1007-1010.

Sambrook, J. and Russell, D. (2001). "Molecular Cloning - A Laboratory Manual." Cold Spring Harbor Laboratory Press, New York, USA.

Savina, A., Fader, C. M., Damiani, M. T. and Colombo, M. I. (2005). "Rab11 promotes docking and fusion of multivesicular bodies in a calcium-dependent manner." Traffic **6**(2): 131-143.

Savina, A., Furlan, M., Vidal, M. and Colombo, M. I. (2003). "Exosome release is regulated by a calcium-dependent mechanism in K562 cells." J Biol Chem **278**(22): 20083-20090.

Scharfman, H., Goodman, J., Macleod, A., Phani, S., Antonelli, C. and Croll, S. (2005). "Increased neurogenesis and the ectopic granule cells after intrahippocampal BDNF infusion in adult rats." Exp Neurol **192**(2): 348-356.

Schneider, A. and Simons, M. (2013). "Exosomes: vesicular carriers for intercellular communication in neurodegenerative disorders." Cell Tissue Res **352**(1): 33-47.

Shimizu, E., Hashimoto, K., Okamura, N., Koike, K., Komatsu, N., Kumakiri, C., Nakazato, M., Watanabe, H., Shinoda, N., Okada, S. and Iyo, M. (2003). "Alterations of serum levels of brain-derived neurotrophic factor (BDNF) in depressed patients with or without antidepressants." Biol Psychiatry **54**(1): 70-75.

Shukla, D. and Spear, P. G. (2001). "Herpesviruses and heparan sulfate: an intimate relationship in aid of viral entry." J Clin Invest **108**(4): 503-510.

Simons, M. and Raposo, G. (2009). "Exosomes--vesicular carriers for intercellular communication." Curr Opin Cell Biol **21**(4): 575-581.

Skog, J., Wurdinger, T., van Rijn, S., Meijer, D. H., Gainche, L., Sena-Esteves, M., Curry, W. T., Jr., Carter, B. S., Krichevsky, A. M. and Breakefield, X. O. (2008). "Glioblastoma microvesicles transport RNA and proteins that promote tumour growth and provide diagnostic biomarkers." Nat Cell Biol **10**(12): 1470-1476.

Subra, C., Laulagnier, K., Perret, B. and Record, M. (2007). "Exosome lipidomics unravels lipid sorting at the level of multivesicular bodies." Biochimie **89**(2): 205-212.

Tamboli, I. Y., Barth, E., Christian, L., Siepmann, M., Kumar, S., Singh, S., Tolksdorf, K., Heneka, M. T., Lutjohann, D., Wunderlich, P. and Walter, J. (2010). "Statins promote the degradation of extracellular amyloid {beta}-peptide by microglia via stimulation of exosome-associated insulin-degrading enzyme (IDE) secretion." J Biol Chem **285**(48): 37405-37414.

Taylor, A. R., Robinson, M. B., Gifondorwa, D. J., Tytell, M. and Milligan, C. E. (2007). "Regulation of heat shock protein 70 release in astrocytes: role of signaling kinases." Dev Neurobiol **67**(13): 1815-1829.

Thakker-Varia, S., Krol, J. J., Nettleton, J., Bilimoria, P. M., Bangasser, D. A., Shors, T. J., Black, I. B. and Alder, J. (2007). "The neuropeptide VGF produces antidepressant-like behavioral effects and enhances proliferation in the hippocampus." J Neurosci **27**(45): 12156-12167.

Thery, C., Amigorena, S., Raposo, G. and Clayton, A. (2006). "Isolation and characterization of exosomes from cell culture supernatants and biological fluids." Curr Protoc Cell Biol **Chapter 3**: Unit 3 22.

Thery, C., Duban, L., Segura, E., Veron, P., Lantz, O. and Amigorena, S. (2002). "Indirect activation of naive CD4+ T cells by dendritic cell-derived exosomes." Nat Immunol **3**(12): 1156-1162.

Thery, C., Ostrowski, M. and Segura, E. (2009). "Membrane vesicles as conveyors of immune responses." Nat Rev Immunol **9**(8): 581-593.

Trajkovic, K., Hsu, C., Chiantia, S., Rajendran, L., Wenzel, D., Wieland, F., Schwille, P., Brugger, B. and Simons, M. (2008). "Ceramide triggers budding of exosome vesicles into multivesicular endosomes." Science **319**(5867): 1244-1247.

Trapp, B. D., Peterson, J., Ransohoff, R. M., Rudick, R., Mork, S. and Bo, L. (1998). "Axonal transection in the lesions of multiple sclerosis." N Engl J Med **338**(5): 278-285.

Tremblay, R. G., Sikorska, M., Sandhu, J. K., Lanthier, P., Ribecco-Lutkiewicz, M. and Bani-Yaghoub, M. (2010). "Differentiation of mouse Neuro 2A cells into dopamine neurons." Journal of neuroscience methods **186**(1): 60-67.

Trotter, J., Karram, K. and Nishiyama, A. (2010). "NG2 cells: Properties, progeny and origin." Brain Res Rev **63**(1-2): 72-82.

Trotter, J. and Schachner, M. (1989). "Cells positive for the O4 surface antigen isolated by cell sorting are able to differentiate into astrocytes or oligodendrocytes." Brain research. Developmental brain research **46**(1): 115-122.

Turola, E., Furlan, R., Bianco, F., Matteoli, M. and Verderio, C. (2012). "Microglial microvesicle secretion and intercellular signaling." Front Physiol **3**: 149.

Twiss, J. L. and Fainzilber, M. (2009). "Ribosomes in axons--scrounging from the neighbors?" Trends Cell Biol **19**(5): 236-243.

Tytell, M. (2005). "Release of heat shock proteins (Hsps) and the effects of extracellular Hsps on neural cells and tissues." Int J Hyperthermia **21**(5): 445-455.

Tytell, M., Greenberg, S. G. and Lasek, R. J. (1986). "Heat shock-like protein is transferred from glia to axon." Brain Res **363**(1): 161-164.

Valadi, H., Ekstrom, K., Bossios, A., Sjostrand, M., Lee, J. J. and Lotvall, J. O. (2007). "Exosome-mediated transfer of mRNAs and microRNAs is a novel mechanism of genetic exchange between cells." Nat Cell Biol **9**(6): 654-659.

Verderio, C., Muzio, L., Turola, E., Bergami, A., Novellino, L., Ruffini, F., Riganti, L., Corradini, I., Francolini, M., Garzetti, L., Maiorino, C., Servida, F., Vercelli, A., Rocca, M., Dalla Libera, D., Martinelli, V., Comi, G., Martino, G., Matteoli, M. and Furlan, R. (2012). "Myeloid microvesicles are a marker and therapeutic target for neuroinflammation." Ann Neurol **72**(4): 610-624.

Viaud, S., Thery, C., Ploix, S., Tursz, T., Lapierre, V., Lantz, O., Zitvogel, L. and Chaput, N. (2010). "Dendritic cell-derived exosomes for cancer immunotherapy: what's next?" Cancer Res **70**(4): 1281-1285.

Volterra, A. and Meldolesi, J. (2005). "Astrocytes, from brain glue to communication elements: the revolution continues." Nat Rev Neurosci **6**(8): 626-640.

Von Bartheld, C. S. and Altick, A. L. (2011). "Multivesicular bodies in neurons: distribution, protein content, and trafficking functions." Prog Neurobiol **93**(3): 313-340.

von Jonquieres, G., Mersmann, N., Klugmann, C. B., Harasta, A. E., Lutz, B., Teahan, O., Housley, G. D., Fröhlich, D., Kramer-Albers, E. M. and Klugmann, M. (2013). "Glial promoter selectivity following AAV-delivery to the immature brain." PLoS One **8**(6): e65646.

von Kleist, L., Stahlschmidt, W., Bulut, H., Gromova, K., Puchkov, D., Robertson, M. J., MacGregor, K. A., Tomilin, N., Pechstein, A., Chau, N., Chircop, M., Sakoff, J., von Kries, J. P., Saenger, W., Krausslich, H. G., Shupliakov, O., Robinson, P. J., McCluskey, A. and Haucke, V. (2011). "Role of the clathrin terminal domain in regulating coated pit dynamics revealed by small molecule inhibition." Cell **146**(3): 471-484.

Wang, G., Dinkins, M., He, Q., Zhu, G., Poirier, C., Campbell, A., Mayer-Proschel, M. and Bieberich, E. (2012). "Astrocytes secrete exosomes enriched with proapoptotic ceramide and prostate apoptosis response 4 (PAR-4): potential mechanism of apoptosis induction in Alzheimer disease (AD)." J Biol Chem **287**(25): 21384-21395.

Wang, S., Cesca, F., Loers, G., Schweizer, M., Buck, F., Benfenati, F., Schachner, M. and Kleene, R. (2011a). "Synapsin I is an oligomannose-carrying glycoprotein, acts as an oligomannose-binding lectin, and promotes neurite outgrowth and neuronal survival when released via glia-derived exosomes." J Neurosci **31**(20): 7275-7290.

Wang, Y., Cui, J., Sun, X. and Zhang, Y. (2011b). "Tunneling-nanotube development in astrocytes depends on p53 activation." Cell Death Differ **18**(4): 732-742.

Zerial, M. and McBride, H. (2001). "Rab proteins as membrane organizers." Nat Rev Mol Cell Biol **2**(2): 107-117.

Zhang, H. G. and Grizzle, W. E. (2011). "Exosomes and cancer: a newly described pathway of immune suppression." Clin Cancer Res **17**(5): 959-964.

Zhu, D., Tan, K. S., Zhang, X., Sun, A. Y., Sun, G. Y. and Lee, J. C. (2005). "Hydrogen peroxide alters membrane and cytoskeleton properties and increases intercellular connections in astrocytes." J Cell Sci **118**(Pt 16): 3695-3703.

Zhuang, X., Xiang, X., Grizzle, W., Sun, D., Zhang, S., Axtell, R. C., Ju, S., Mu, J., Zhang, L., Steinman, L., Miller, D. and Zhang, H. G. (2011). "Treatment of brain inflammatory diseases by delivering exosome encapsulated anti-inflammatory drugs from the nasal region to the brain." Mol Ther **19**(10): 1769-1779.

Zitvogel, L., Regnault, A., Lozier, A., Wolfers, J., Flament, C., Tenza, D., Ricciardi-Castagnoli, P., Raposo, G. and Amigorena, S. (1998). "Eradication of established murine tumors using a novel cell-free vaccine: dendritic cell-derived exosomes." Nat Med **4**(5): 594-600.

# 8. APPENDIX

## 8.1. LIST OF ABBREVIATIONS

| | |
|---|---|
| Alix | **AL**G-2-**i**nteracting protein **X** |
| ALS | **A**myotrophic **l**ateral **s**clerosis |
| AMPA | α-**A**mino-3-hydroxy-5-**m**ethyl-4-isoxazole**p**ropionic **a**cid |
| AMPAR | **AMPA R**eceptor |
| APC | **A**ntigen **p**resenting **c**ell |
| APP | **A**myloid **p**recursor **p**rotein |
| ATP | **A**denosine **t**ri**p**hosphate |
| BBB | **B**lood-**b**rain **b**arrier |
| Bdnf | **B**rain-**d**erived **n**eurotrophic **f**actor |
| bGHpA | **B**ovine **g**rowth **h**ormone **p**oly**a**denylation signal |
| CREB | **c**AMP **r**esponse **e**lement-**b**inding protein |
| CNS | **C**entral **n**ervous **s**ystem |
| CNP | 2',3'-**c**yclic **n**ucleotide 3'-**p**hosphodiesterase |
| COX | **C**ytochrome c **ox**idase |
| CSF | **C**erebro**s**pinal **f**luid |
| DCX | **D**ouble**c**ortin |
| DEX | **Dex**osomes |
| DIV | **D**ays ***i**n **v**itro* |
| DNA | **D**eoxyribo**n**ucleic **a**cid |
| EAE | **E**xperimental **a**utoimmune **e**ncephalomyelitis |
| EGFP | **E**nhanced **g**reen **f**luorescent **p**rotein |
| ESCRT | **E**ndosomal **S**orting **C**omplex **R**equired for **T**ransport |
| esRNA | **e**xosomal **s**huttle **RNA** |
| EV | **E**xtracellular **v**esicle |
| Evi | **Ev**enness **i**nterrupted |
| floxed | **F**lanked by **lox**P sites |
| GABA | **γ**-**a**mino**b**utyric **a**cid |
| GFAP | **G**lial **f**ibrillary **a**cidic **p**rotein |
| HIV | **H**uman **i**mmunodeficiency **v**irus |
| HSP | **H**eat **s**hock **p**rotein |

| | |
|---|---|
| IDE | **I**nsulin-**d**egrading **e**nzyme |
| IEG | **I**mmediate **e**arly **g**ene |
| IER3 | **I**mmediate **e**arly **r**esponse 3 |
| ILV | **I**ntraluminal **v**esicle |
| ITR | **I**nverted **t**erminal **r**epeats |
| KO | **K**nock**o**ut |
| loxP | **L**ocus **o**f crossover [**X**] in **P**1 |
| LPS | **L**ipo**p**oly**s**accharide |
| MAG | **M**yelin-**a**ssociated **g**lycoprotein |
| MBP | **M**yelin **b**asic **p**rotein |
| MCT | **M**ono**c**arboxylate **t**ransporter |
| MHC | **M**ajor **h**istocompatibility **c**omplex |
| miRNA | **M**icro **r**ibo**n**ucleic **a**cid |
| MOG | **M**yelin **o**ligodendrocyte **g**lycoprotein |
| mRNA | **M**essenger **r**ibo**n**ucleic **a**cid |
| MS | **M**ultiple **s**clerosis |
| MV | **M**icro**v**esicle |
| MVB | **M**ulti**v**esicular **b**ody |
| MVE | **M**ulti**v**esicular **e**ndosome |
| NMDA | ***N*-M**ethyl-**D**-**a**spartate |
| NMDAR | **NMDA r**eceptor |
| NMJ | **N**euro**m**uscular **j**unction |
| NSCLC | **N**on-**s**mall **c**ell **l**ung **c**arcinoma |
| NSE | **N**euron **s**pecific **e**nolase |
| NTDPases | **N**ucleoside **t**riphosphate **d**i**p**hosphohydrol**ases** |
| OPC | **O**ligodendroglial **p**recursor **c**ell |
| PAR4 | **P**rostate **a**poptosis **r**esponse 4 |
| pCN | **P**rimary **c**ortical **n**eurons |
| PLP | **P**roteo**l**ipid **p**rotein |
| PNS | **P**eripheral **n**ervous **s**ystem |
| pOL | **P**rimary **ol**igodendrocytes |
| PrP | **Pr**ion **p**rotein |
| PS | **P**hosphatidyl**s**erine |
| RNA | **R**ibo**n**ucleic **a**cid |
| SC | **S**chwann **c**ell |
| SOD | **S**uper**o**xide **d**ismutase |

| | |
|---|---|
| SVZ | **S**ub**v**entricular **z**one |
| Tat | **T**rans-**a**ctivator of **t**ranscription |
| TNT | **T**unneling **n**ano**t**ube |
| WPRE | **W**oodchuck hepatitis virus (WHP) **p**osttranscriptional **r**egulatory **e**lement |

## 8.2. LIST OF FIGURES

## 8.3. LIST OF TABLES

# 9. PUBLICATIONS

Frühbeis, C*, **Fröhlich, D***, Kuo, WP, Amphornrat, J, Thilemann, S, Saab, AS, Kirchhoff, F, Möbius, W, Goebbels, S, Nave, KA, Schneider, A, Simons, M, Klugmann, M, Trotter, J and Krämer-Albers, EM (2013). "Neurotransmitter-triggered transfer of exosomes mediates oligodendrocyte-neuron communication." PLoS Biol **11**(7): e1001604.
* both authors contributed equally to this work

> Reciprocal interactions between neurons and oligodendrocytes are not only crucial for myelination, but also for long-term survival of axons. Degeneration of axons occurs in several human myelin diseases, however the molecular mechanisms of axon-glia communication maintaining axon integrity are poorly understood. Here, we describe the signal-mediated transfer of exosomes from oligodendrocytes to neurons. These endosome-derived vesicles are secreted by oligodendrocytes and carry specific protein and RNA cargo. We show that activity-dependent release of the neurotransmitter glutamate triggers oligodendroglial exosome secretion mediated by Ca(2+) entry through oligodendroglial NMDA and AMPA receptors. In turn, neurons internalize the released exosomes by endocytosis. Injection of oligodendroglia-derived exosomes into the mouse brain results in functional retrieval of exosome cargo in neurons. Supply of cultured neurons with oligodendroglial exosomes improves neuronal viability under conditions of cell stress. These findings indicate that oligodendroglial exosomes participate in a novel mode of bidirectional neuron-glia communication contributing to neuronal integrity.

Frühbeis, C, **Fröhlich, D** and Krämer-Albers, EM (2012). "Emerging roles of exosomes in neuron-glia communication." Front Physiol **3**: 119.

> Brain function depends on coordinated interactions between neurons and glial cells. Recent evidence indicates that these cells release endosome-derived microvesicles termed exosomes, which are 50-100 nm in size and carry specific protein and RNA cargo. Exosomes can interact with neighboring cells raising the concept that exosomes may mediate signaling between brain cells and facilitate the delivery of bioactive molecules. Oligodendrocytes myelinate axons and furthermore maintain axonal integrity by an yet uncharacterized pathway of trophic support. Here, we highlight the role of exosomes in nervous system cell communication with particular focus on exosomes released by oligodendrocytes and their potential implications in axon-glia interaction and myelin disease, such as multiple sclerosis. These secreted vesicles may contribute to eliminate overproduced myelin membrane or to transfer antigens facilitating immune surveillance of the brain. Furthermore, there is emerging evidence that exosomes participate in axon-glia communication.

Frühbeis, C, **Fröhlich, D**, Kuo, WP and Krämer-Albers, EM (2013). "Extracellular vesicles as mediators of neuron-glia communication." Front Cell Neurosci **7**: 182.

In the nervous system, glia cells maintain homeostasis, synthesize myelin, provide metabolic support, and participate in immune defense. The communication between glia and neurons is essential to synchronize these diverse functions with brain activity. Evidence is accumulating that secreted extracellular vesicles (EVs), such as exosomes and shedding microvesicles, are key players in intercellular signaling. The cells of the nervous system secrete EVs, which potentially carry protein and RNA cargo from one cell to another. After delivery, the cargo has the ability to modify the target cell phenotype. Here, we review the recent advances in understanding the role of EV secretion by astrocytes, microglia, and oligodendrocytes in the central nervous system. Current work has demonstrated that oligodendrocytes transfer exosomes to neurons as a result of neurotransmitter signaling suggesting that these vesicles may mediate glial support of neurons.

von Jonquieres, G, Mersmann, N, Klugmann, CB, Harasta, AE, Lutz, B, Teahan, O, Housley, GD, **Fröhlich, D**, Kramer-Albers, EM and Klugmann, M (2013). "Glial promoter selectivity following AAV-delivery to the immature brain." PloS one **8**(6): e65646.

Recombinant adeno-associated virus (AAV) vectors are versatile tools for gene transfer to the central nervous system (CNS) and proof-of-concept studies in adult rodents have shown that the use of cell type-specific promoters is sufficient to target AAV-mediated transgene expression to glia. However, neurological disorders caused by glial pathology usually have an early onset. Therefore, modelling and treatment of these conditions require expanding the concept of targeted glial transgene expression by promoter selectivity for gene delivery to the immature CNS. Here, we have investigated the AAV-mediated green fluorescent protein (GFP) expression driven by the myelin basic protein (MBP) or glial fibrillary acidic protein (GFAP) promoters in the developing mouse brain. Generally, the extent of transgene expression after infusion at immature stages was widespread and higher than in adults. The GFAP promoter-driven GFP expression was found to be highly specific for astrocytes following vector infusion to the brain of neonates and adults. In contrast, the selectivity of the MBP promoter for oligodendrocytes was poor following neonatal AAV delivery, but excellent after vector injection at postnatal day 10. To extend these findings obtained in naive mice to a disease model, we performed P10 infusions of AAV-MBP-GFP in aspartoacylase (ASPA)-deficient mouse mutants presenting with early onset oligodendrocyte pathology. Spread of GFP expression and selectivity for oligodendrocytes in ASPA-mutants was comparable with our observations in normal animals. Our data suggest that direct AAV infusion to the developing postnatal brain, utilising cellular promoters, results in targeted and long-term transgene expression in glia. This approach will be relevant for disease modelling and gene therapy for the treatment of glial pathology.

# 11. CURRICULUM VITAE


## Dominik Fröhlich

Zanggasse 30, 55116 Mainz, Germany
Tel.: +49 179 9085009 E-Mail: dominik.froehlich@uni-mainz.de
*20.07.1982 in Heidelberg, Germany


**Working Place**

Molecular Cell Biology — 06/09 – present
Johannes Gutenberg University
Bentzelweg 3
55128 Mainz
Germany
Tel: +49 6131 3924149

**Education**

Degree:

Diplom-Biologist, equivalent to Master of Science in Biology

Ph.D. Thesis — 06/09 – 12/13

Molecular Cell Biology, Johannes Gutenberg University, Mainz (D)
Title: Oligodendroglial Exosomes in Glia to Neuron Signaling

Diploma in Biology

Grade: 1.0 with distinction
Subjects: Genetics, Zoology, Pharmacology, Biochemical Psychiatry
Johannes Gutenberg University, Mainz (D)

Study abroad — 07/07 – 12/07

Nelson Mandela Metropolitan University, Port Elizabeth (SA)

Study of Biology — 10/03 – 04/09

Johannes Gutenberg University, Mainz (D)

Military Service — 04/02 – 12/02

5. Schweres Pionierbataillon, Speyer (D)

Abitur (Qualification for University Admission) — 08/93 – 03/02

Gymnasium am Kaiserdom (Secondary School), Speyer (D)

Primary School — 08/89 – 06/93

Zeppelin Grundschule, Speyer (D)

**Work Experience**

Research Assistant — 04/13 – present

Johannes Gutenberg University, Mainz (D)

Research Assistant — 04/12 – 03/13

Clinical Center of the Johannes Gutenberg University, Mainz (D)

Research Assistant 06/09 – 04/10

Johannes Gutenberg University, Mainz (D)

Research Assistant 05/09 – 06/09

Clinical Center of the Johannes Gutenberg University, Mainz (D)

Internship in Business Management 03/03 – 06/03

Actris AG, Mannheim (D)

## Teaching Experience

Internship Supervisor 04/12 – 03/13

Practical Course: "Physiologie für Studierende der Medizin und Zahnmedizin"
Clinical Center of the Johannes Gutenberg University, Mainz (D)

Tutor 01/05 – 04/09

Practical Course: "Zoologische Anfängerübung"
Johannes Gutenberg University, Mainz (D)

## Publications

Frühbeis C*, **Fröhlich D***, Kuo WP, Amphornrat J, Thilemann S, Saab AS, Kirchhoff F, Möbius W, Goebbels S, Nave KA, Schneider A, Simons M, Klugmann M, Trotter J, Krämer-Albers EM (2013) Neurotransmitter-triggered transfer of exosomes mediates oligodendrocyte-neuron communication. *PLoS Biol* **11:** e1001604
* both authors contributed equally to this work

Frühbeis, C, **Fröhlich, D**, Kuo, WP and Krämer-Albers, EM (2013). "Extracellular vesicles as mediators of neuron-glia communication." Front Cell Neurosci **7**: 182.

von Jonquieres G, Mersmann N, Klugmann CB, Harasta AE, Lutz B, Teahan O, Housley GD, **Fröhlich D**, Kramer-Albers EM, Klugmann M (2013) Glial Promoter Selectivity following AAV-Delivery to the Immature Brain. *PLoS One* **8:** e65646

Frühbeis C, **Fröhlich D**, Krämer-Albers EM (2012) Emerging roles of exosomes in neuron-glia communication. *Front Physiol* **3:** 119

## Presentations and Posters

Oligodendroglial Exosomes: Trophic Support for Neurons
Dominik Fröhlich, Wen Ping Kuo, Carsten Frühbeis, Wiebke Möbius, Anja Schneider, Matthias Klugmann, Christoph Zehendner, Heiko Luhmann, Jacqueline Trotter and Eva-Maria Krämer-Albers; **DGZ Meeting, Heidelberg, 2013**

Oligodendroglial Exosomes: Trophic Support for Neurons
Dominik Fröhlich, Wen Ping Kuo, Carsten Frühbeis, Wiebke Möbius, Anja Schneider, Matthias Klugmann, Christoph Zehendner, Heiko Luhmann, Jacqueline Trotter and Eva-Maria Krämer-Albers; **Myelin Netzwerk e.V. Tagung, Kassel, 2013**

Oligodendroglial Exosomes: Trophic Support for Neurons
Dominik Fröhlich, Wen Ping Kuo, Carsten Frühbeis, Wiebke Möbius, Anja Schneider, Matthias Klugmann, Christoph Zehendner, Heiko Luhmann, Jacqueline Trotter and Eva-Maria Krämer-Albers**; RMN² Meeting, Oberwesel, 2012**

Crosstalk between neurons and glia involving exosomes as vesicular carriers of RNA and proteins
Dominik Fröhlich, Carsten Frühbeis, Jesa Amphornrat, Sebastian Thilemann, Aiman Saab, Frank Kirchhoff, Wiebke Möbius, Klaus-Armin Nave, Anja Schneider, Mikael Simons, Matthias Klugmann, Jacqueline Trotter and Eva-Maria Krämer-Albers**; ISEV Meeting, Göteborg, 2012**

Oligodendroglial Exosomes in Glia to Neuron Signaling
Dominik Fröhlich, Jesa Amphornrat, Carsten Frühbeis, Jacqueline Trotter and Eva-Maria Krämer-Albers; **IAK Meeting, Mainz, 2011**

Oligodendroglial Exosomes in Glia to Neuron Signaling
Dominik Fröhlich, Jesa Amphornrat, Carsten Frühbeis, Jacqueline Trotter and Eva-Maria Krämer-Albers; **ISEV Meeting, Paris, 2011**

Neurotransmitter signaling triggers transfer of exosomes from oligodendrocytes to neurons Carsten Frühbeis, Dominik Fröhlich, Jesa Amphornrat, Sebastian Thilemann, Aiman Saab, Frank Kirchhoff, Wiebke Möbius, Jacqueline Trotter and Eva-Maria Krämer-Albers; **RMN² Meeting, Oberwesel, 2010**

Oligodendroglial Exosomes: Transfer of Trophic Substances Modulating the Neuronal Cytoskeleton
Dominik Fröhlich, Jesa Amphornrat, Carsten Frühbeis, Wiebke Möbius, Jacqueline Trotter; **IAK Meeting, Mainz, 2009**

## Stipends and Awards

Fellowship — 11/10 – 07/13
Neuro Graduate School
Johannes Gutenberg University, Mainz (D)

Ph.D. Fellowship — 05/10 – 04/12
Stipendienstiftung Rheinland-Pfalz (D)

Student Fellowship — 10/08 – 03/09
Stipendienstiftung Rheinland-Pfalz (D)

Poster Prize
RMN² Meeting, Oberwesel, 2010

## Languages

German, English, French, Latin

## Computer Skills

Microsoft Office, Adobe Photoshop, Adobe Illustrator, ImageJ

## Hobbies

Hockey, Tennis, Travelling, Surfing, Snowboarding, Mountainbiking

# 12. EIDESSTATTLICHE ERKLÄRUNG

Hiermit erkläre ich, Dominik Fröhlich, geboren am 20.07.1982 in Heidelberg, dass ich meine Dissertation selbstständig und nur unter Verwendung der angegebenen Hilfsmittel angefertigt habe. Ich habe keinen anderen Promotionsversuch unternommen.

| | |
|---|---|
| Ort, Datum | (Dominik Fröhlich) |